

OCD CASE NOS. 14784 AND 14785

IPANM Petition to amend Title 19, Chapter 15,  
part 17 (The PIT Rule)

May 14 - 18, 2012

**IPANM exhibit 11**  
**HELP Engineering Manual**  
- One Hundred Twenty Six (126) pages -

**THE HYDROLOGIC EVALUATION OF LANDFILL  
PERFORMANCE (HELP) MODEL**

***ENGINEERING DOCUMENTATION FOR VERSION 3***

by

Paul R. Schroeder, Tamsen S. Dozier, Paul A. Zappi,  
Bruce M. McEnroe, John W. Sjoström and R. Lee Peyton  
Environmental Laboratory  
U.S. Army Corps of Engineers  
Waterways Experiment Station  
Vicksburg, MS 39180-6199

Interagency Agreement No. DW21931425

Project Officer

Robert E. Landreth  
Waste Minimization, Destruction and Disposal Research Division  
Risk Reduction Engineering Laboratory  
Cincinnati, Ohio 45268

RISK REDUCTION ENGINEERING LABORATORY  
OFFICE OF RESEARCH AND DEVELOPMENT  
U.S. ENVIRONMENTAL PROTECTION AGENCY  
CINCINNATI, OHIO 45268

## DISCLAIMER

The information in this document has been funded wholly or in part by the United States Environmental Protection Agency under Interagency Agreement No. DW21931425 to the U.S. Army Engineer Waterways Experiment Station (WES). It has been subjected to WES peer and administrative review, and it has been approved for publication as an EPA document. Mention of trade names or commercial products does not constitute endorsement or recommendation for use.

## FOREWORD

Today's rapidly developing and changing technologies and industrial products and practices frequently carry with them the increased generation of materials that, if improperly dealt with, can threaten both public health and the environment. Abandoned waste sites and accidental releases of toxic and hazardous substances to the environment also have important environmental and public health implications. The Risk Reduction Engineering Laboratory assists in providing an authoritative and defensible engineering basis for assessing and solving these problems. Its products support the policies, programs and regulations of the Environmental Protection Agency, the permitting and other responsibilities of State and local governments, and the needs of both large and small businesses in handling their wastes responsibly and economically.

This report presents engineering documentation of the Hydrologic Evaluation of Landfill Performance (HELP) model and its user interface. The HELP program is a quasi-two-dimensional hydrologic model for conducting water balance analyses of landfills, cover systems, and other solid waste containment facilities. The model accepts weather, soil and design data and uses solution techniques that account for the effects of surface storage, snowmelt, runoff, infiltration, evapotranspiration, vegetative growth, soil moisture storage, lateral subsurface drainage, leachate recirculation, unsaturated vertical drainage, and leakage through soil, geomembrane or composite liners. Landfill systems including various combinations of vegetation, cover soils, waste cells, lateral drain layers, low permeability barrier soils, and synthetic geomembrane liners may be modeled. The model facilitates rapid estimation of the amounts of runoff, evapotranspiration, drainage, leachate collection and liner leakage that may be expected to result from the operation of a wide variety of landfill designs. The primary purpose of the model is to assist in the comparison of design alternatives. The model is a tool for both designers and permit writers.

E. Timothy Oppelt, Director  
Risk Reduction Engineering Laboratory

## ABSTRACT

The Hydrologic Evaluation of Landfill Performance (HELP) computer program is a quasi-two-dimensional hydrologic model of water movement across, into, through and out of landfills. The model accepts weather, soil and design data and uses solution techniques that account for the effects of surface storage, snowmelt, runoff, infiltration, evapotranspiration, vegetative growth, soil moisture storage, lateral subsurface drainage, leachate recirculation, unsaturated vertical drainage, and leakage through soil, geomembrane or composite liners. Landfill systems including various combinations of vegetation, cover soils, waste cells, lateral drain layers, low permeability barrier soils, and synthetic geomembrane liners may be modeled. The program was developed to conduct water balance analyses of landfills, cover systems, and solid waste disposal and containment facilities. As such, the model facilitates rapid estimation of the amounts of runoff, evapotranspiration, drainage, leachate collection, and liner leakage that may be expected to result from the operation of a wide variety of landfill designs. The primary purpose of the model is to assist in the comparison of design alternatives as judged by their water balances. The model, applicable to open, partially closed, and fully closed sites, is a tool for both designers and permit writers.

This report documents the solution methods and process descriptions used in Version 3 of the HELP model. Program documentation including program options, system and operating requirements, file structures, program structure and variable descriptions are provided in a separate report. Section 1 provides basic program identification. Section 2 provides a narrative description of the simulation model. Section 3 presents data generation algorithms and default values used in Version 3. Section 4 describes the method of solution and hydrologic process algorithms. Section 5 lists the assumptions and limitations of the HELP model.

The user interface or input facility is written in the Quick Basic environment of Microsoft Basic Professional Development System Version 7.1 and runs under DOS 2.1 or higher on IBM-PC and compatible computers. The HELP program uses an interactive and a user-friendly input facility designed to provide the user with as much assistance as possible in preparing data to run the model. The program provides weather and soil data file management, default data sources, interactive layer editing, on-line help, and data verification and accepts weather data from the most commonly used sources with several different formats.

HELP Version 3 represents a significant advancement over the input techniques of Version 2. Users of the HELP model should find HELP Version 3 easy to use and should be able to use it for many purposes, such as preparing and editing landfill profiles and weather data. Version 3 facilitates use of metric units, international applications, and designs with geosynthetic materials.

This report should be cited as follows:

Schroeder, P. R., Dozier, T.S., Zappi, P. A., McEnroe, B. M., Sjostrom, J. W., and Peyton, R. L. (1994). "The Hydrologic Evaluation of Landfill Performance (HELP) Model: Engineering Documentation for Version 3," EPA/600/R-94/168b, September 1994, U.S. Environmental Protection Agency Office of Research and Development, Washington, DC.

This report was submitted in partial fulfillment of Interagency Agreement Number DW21931425 between the U.S. Environmental Protection Agency and the U.S. Army Engineer Waterways Experiment Station, Vicksburg, MS. This report covers a period from November 1988 to August 1994 and work was completed as of August 1994.

## CONTENTS

	<u>Page</u>
DISCLAIMER .....	ii
FOREWORD .....	iii
ABSTRACT .....	iv
FIGURES .....	viii
TABLES .....	ix
ACKNOWLEDGMENTS .....	x
1. PROGRAM IDENTIFICATION .....	1
2. NARRATIVE DESCRIPTION .....	3
3. DATA GENERATION AND DEFAULT VALUES .....	9
3.1 Overview .....	9
3.2 Synthetic Weather Generation .....	9
3.3 Moisture Retention and Hydraulic Conductivity Parameters .....	12
3.3.1 Moisture Retention Parameters .....	12
3.3.2 Unsaturated Hydraulic Conductivity .....	13
3.3.3 Saturated Hydraulic Conductivity for Vegetated Materials .....	15
3.4 Evaporation Coefficient .....	16
3.5 Default Soil and Waste Characteristics .....	17
3.5.1 Default Soil Characteristics .....	17
3.5.2 Default Waste Characteristics .....	21
3.5.3 Default Geosynthetic Material Characteristics .....	25
3.6 Soil Moisture Initialization .....	25
3.7 Default Leaf Area Indices and Evaporative Zone Depths .....	26
4. METHOD OF SOLUTION .....	29
4.1 Overview .....	29
4.2 Runoff .....	30
4.2.1 Adjustment of Curve Number for Soil Moisture .....	34
4.2.2 Computation of Default Curve Numbers .....	36
4.2.3 Adjustment of Curve Number for Surface Slope .....	37
4.2.4 Adjustment of Curve Number for Frozen Soil .....	39
4.2.5 Summary of Daily Runoff Computation .....	39
4.3 Prediction of Frozen Soil Conditions .....	40

4.4	Snow Accumulation and Melt . . . . .	41
4.4.1	Nonrain Snowmelt . . . . .	42
4.4.2	Rain-on-Snow Melt Condition . . . . .	43
4.4.3	Snowmelt Summary . . . . .	45
4.5	Interception . . . . .	47
4.6	Potential Evapotranspiration . . . . .	48
4.7	Surface Evaporation . . . . .	51
4.7.1	No Snow Cover . . . . .	51
4.7.2	Snow Cover Present . . . . .	52
4.7.3	Remaining Evaporative Demand . . . . .	54
4.8	Infiltration . . . . .	55
4.9	Soil Water Evaporation . . . . .	55
4.10	Plant Transpiration . . . . .	59
4.11	Evapotranspiration . . . . .	60
4.12	Vegetative Growth . . . . .	62
4.13	Subsurface Water Routing . . . . .	68
4.14	Vertical Drainage . . . . .	71
4.15	Soil Liner Percolation . . . . .	73
4.16	Geomembrane Liner Leakage . . . . .	74
4.16.1	Vapor Diffusion Through Intact Geomembranes . . . . .	75
4.16.2	Leakage Through Holes in Geomembranes . . . . .	76
4.17	Geomembrane and Soil Liner Design Cases . . . . .	93
4.18	Lateral Drainage . . . . .	98
4.19	Lateral Drainage Recirculation . . . . .	103
4.20	Subsurface Inflow . . . . .	104
4.21	Linkage of Subsurface Flow Processes . . . . .	104
5.	ASSUMPTIONS AND LIMITATIONS . . . . .	106
5.1	Methods of Solution . . . . .	106
5.2	Limits of Application . . . . .	109
	REFERENCES . . . . .	111

## FIGURES

<u>No.</u>		<u>Page</u>
1	Schematic Profile View of a Typical Hazardous Waste Landfill .....	6
2	Relation Among Moisture Retention Parameters and Soil Texture Class .....	13
3	Geographic Distribution of Maximum Leaf Area Index .....	26
4	Geographic Distribution of Minimum Evaporative Depth .....	27
5	Geographic Distribution of Maximum Evaporative Depth .....	27
6	Relation Between Runoff, Precipitation, and Retention .....	31
7	SCS Rainfall-Runoff Relation Normalized on Retention Parameter S .....	33
8	Relation Between SCS Curve Number and Default Soil Texture Number for Various Levels of Vegetation .....	37
9	Leakage with Interfacial Flow Below Flawed Geomembrane .....	84
10	Leakage with Interfacial Flow Above Flawed Geomembrane .....	84
11	Geomembrane Liner Design Case 1 .....	94
12	Geomembrane Liner Design Case 2 .....	95
13	Geomembrane Liner Design Case 3 .....	95
14	Geomembrane Liner Design Case 4 .....	96
15	Geomembrane Liner Design Case 5 .....	98
16	Geomembrane Liner Design Case 6 .....	99
17	Lateral Drainage Definition Sketch .....	100

## TABLES

<u>No.</u>		<u>Page</u>
1	Default Low Density Soil Characteristics .....	19
2	Moderate and High Density Default Soils .....	21
3	Default Soil Texture Abbreviations .....	22
4	Default Waste Characteristics .....	23
5	Saturated Hydraulic Conductivity of Wastes .....	24
6	Default Geosynthetic Material Characteristics .....	25
7	Constants for Use in Equation 32 .....	38
8	Geomembrane Diffusivity Properties .....	77
9	Needle-Punched, Non-Woven Geotextile Properties .....	79

## ACKNOWLEDGMENTS

The support of the project by the Waste Minimization, Destruction and Disposal Research Division, Risk Reduction Engineering Laboratory, U.S. Environmental Protection Agency, Cincinnati, OH and the Headquarters, U.S. Army Corps of Engineers, Washington, DC, through Interagency Agreement No. DW21931425 is appreciated. In particular, the authors wish to thank the U.S. EPA Project Officer, Mr. Robert Landreth, for his long standing support.

This document was prepared at the U.S. Army Corps of Engineers Waterways Experiment Station. The final versions of this document and the HELP program were prepared by Dr. Paul R. Schroeder. Dr. Paul R. Schroeder directed the development of the HELP model and assembled the simulation code. Ms. Tamsen S. Dozier revised, tested and documented the evapotranspiration, snowmelt and frozen soil processes. Mr. Paul A. Zappi revised, assembled and documented the geomembrane leakage processes and the default soil descriptions. Dr. Bruce M. McEnroe revised, tested and documented the lateral drainage process for Version 2, which was finalized in this version. Mr. John W. Sjostrom assembled, tested and documented the synthetic weather generator and the vegetative growth process for Version 2, which was finalized in this version. Dr. R. Lee Peyton developed, revised, tested and documented the slope and soil moisture effects on runoff and curve number. Dr. Paul R. Schroeder developed, tested and documented the remaining processes and the output. Ms. Cheryl Lloyd assisted in the final preparation of the report. The figures used in the report were prepared by Messrs. Christopher Chao, Jimmy Farrell, and Shawn Boelman.

The documentation report and simulation model were reviewed by Dr. Jim Ascough, USDA-ARS-NPA, and Dr. Ragui F. Wilson-Fahmy, Geosynthetic Research Institute, Drexel University. This report has not been subjected to the EPA review and, therefore, the contents do not necessarily reflect the views of the Agency, and no official endorsement should be inferred.

## SECTION 1

### PROGRAM IDENTIFICATION

**PROGRAM TITLE:** Hydrologic Evaluation of Landfill Performance (HELP) Model

**WRITERS:** Paul R. Schroeder, Tamsen S. Dozier, John W. Sjostrom and Bruce M. McEnroe

**ORGANIZATION:** U.S. Army Corps of Engineers, Waterways Experiment Station (WES)

**DATE:** September 1994

**UPDATE:** None Version No.: 3.00

**SOURCE LANGUAGE:** The simulation code is written in ANSI FORTRAN 77 using Ryan-McFarland Fortran Version 2.44 with assembly language and Spindrift Library extensions for Ryan-McFarland Fortran to perform system calls, and screen operations. The user interface is written in BASIC using Microsoft Basic Professional Development System Version 7.1. Several of the user interface support routines are written in ANSI FORTRAN 77 using Ryan-McFarland Fortran Version 2.44, including the synthetic weather generator and the ASCII data import utilities.

**HARDWARE:** The model was written to run on IBM-compatible personal computers under the DOS environment. The program requires an IBM-compatible 8088, 80286, 80386 or 80486-based CPU (preferably 80386 or 80486) with an 8087, 80287, 80387 or 80486 math co-processor. The computer system must have a monitor (preferably color EGA or better), a 3.5- or 5.25-inch floppy disk drive (preferably 3.5-inch double-sided, high-density), a hard disk drive with 6 MB of available storage, and 400k bytes or more of available low level RAM. A printer is needed if a hard copy is desired.

**AVAILABILITY:** The source code and executable code for IBM-compatible personal computers are available from the National Technical Information Service (NTIS). Limited distribution immediately following the initial distribution will be available from the USEPA Risk Reduction Engineering Laboratory, the USEPA Center for Environmental Research Information and the USAE Waterways Experiment Station.

**ABSTRACT:** The Hydrologic Evaluation of Landfill Performance (HELP) computer program is a quasi-two-dimensional hydrologic model of water movement across, into, through and out of landfills. The model accepts weather, soil and design data and uses solution techniques that account for surface storage, snowmelt, runoff, infiltration, vegetative growth, evapotranspiration, soil moisture storage, lateral subsurface drainage, leachate recirculation, unsaturated vertical drainage, and leakage through soil, geomembrane or composite liners. Landfill systems including combinations of vegetation, cover soils, waste cells, lateral drain layers, barrier soils, and synthetic geomembrane liners may be modeled. The program was developed to conduct water balance analyses of landfills, cover systems, and solid waste disposal facilities. As such, the model facilitates rapid estimation of the amounts of runoff, evapotranspiration, drainage, leachate collection, and liner leakage that may be expected to result from the operation of a wide variety of landfill designs. The primary purpose of the model is to assist in the comparison of design alternatives as judged by their water balances. The model, applicable to open, partially closed, and fully closed sites, is a tool for both designers and permit writers.

The HELP model uses many process descriptions that were previously developed, reported in the literature, and used in other hydrologic models. The optional synthetic weather generator is the WGEN model of the U.S. Department of Agriculture (USDA) Agricultural Research Service (ARS) (Richardson and Wright, 1984). Runoff modeling is based on the USDA Soil Conservation Service (SCS) curve number method presented in Section 4 of the National Engineering Handbook (USDA, SCS, 1985). Potential evapotranspiration is modeled by a modified Penman method (Penman, 1963). Evaporation from soil is modeled in the manner developed by Ritchie (1972) and used in various ARS models including the Simulator for Water Resources in Rural Basins (SWRRB) (Arnold et al., 1989) and the Chemicals, Runoff, and Erosion from Agricultural Management System (CREAMS) (Knisel, 1980). Plant transpiration is computed by the Ritchie's (1972) method used in SWRRB and CREAMS. The vegetative growth model was extracted from the SWRRB model. Evaporation of interception, snow and surface water is based on an energy balance. Interception is modeled by the method proposed by Horton (1919). Snowmelt modeling is based on the SNOW-17 routine of the National Weather Service River Forecast System (NWSRFS) Snow Accumulation and Ablation Model (Anderson, 1973). The frozen soil submodel is based on a routine used in the CREAMS model (Knisel et al., 1985). Vertical drainage is modeled by Darcy's (1856) law using the Campbell (1974) equation for unsaturated hydraulic conductivity based on the Brooks-Corey (1964) relationship. Saturated lateral drainage is modeled by an analytical approximation to the steady-state solution of the Boussinesq equation employing the Dupuit-Forchheimer (Forchheimer, 1930) assumptions. Leakage through geomembranes is modeled by a series of equations based on the compilations by Giroud et al. (1989, 1992). The processes are linked together in a sequential order starting at the surface with a surface water balance; then evapotranspiration from the soil profile; and finally drainage and water routing, starting at the surface with infiltration and then proceeding downward through the landfill profile to the bottom. The solution procedure is applied repetitively for each day as it simulates the water routing throughout the simulation period.

## SECTION 2

### NARRATIVE DESCRIPTION

The HELP program, Versions 1, 2 and 3, was developed by the U.S. Army Engineer Waterways Experiment Station (WES), Vicksburg, MS, for the U.S. Environmental Protection Agency (EPA), Risk Reduction Engineering Laboratory, Cincinnati, OH, in response to needs in the Resource Conservation and Recovery Act (RCRA) and the Comprehensive Environmental Response, Compensation and Liability Act (CERCLA, better known as Superfund) as identified by the EPA Office of Solid Waste, Washington, DC. The primary purpose of the model is to assist in the comparison of landfill design alternatives as judged by their water balances.

The Hydrologic Evaluation of Landfill Performance (HELP) model was developed to help hazardous waste landfill designers and regulators evaluate the hydrologic performance of proposed landfill designs. The model accepts weather, soil and design data and uses solution techniques that account for the effects of surface storage, snowmelt, runoff, infiltration, evapotranspiration, vegetative growth, soil moisture storage, lateral subsurface drainage, leachate recirculation, unsaturated vertical drainage, and leakage through soil, geomembrane or composite liners. Landfill systems including various combinations of vegetation, cover soils, waste cells, lateral drain layers, low permeability barrier soils, and synthetic geomembrane liners may be modeled. Results are expressed as daily, monthly, annual and long-term average water budgets.

The HELP model is a quasi-two-dimensional, deterministic, water-routing model for determining water balances. The model was adapted from the HSSWDS (Hydrologic Simulation Model for Estimating Percolation at Solid Waste Disposal Sites) model of the U.S. Environmental Protection Agency (Perrier and Gibson, 1980; Schroeder and Gibson, 1982), and various models of the U.S. Agricultural Research Service (ARS), including the CREAMS (Chemical Runoff and Erosion from Agricultural Management Systems) model (Knisel, 1980), the SWRRB (Simulator for Water Resources in Rural Basins) model (Arnold et al., 1989), the SNOW-17 routine of the National Weather Service River Forecast System (NWSRFS) Snow Accumulation and Ablation Model (Anderson, 1973), and the WGEN synthetic weather generator (Richardson and Wright, 1984).

HELP Version 1 (Schroeder et al., 1984a and 1984b) represented a major advance beyond the HSSWDS program (Perrier and Gibson, 1980; Schroeder and Gibson, 1982), which was also developed at WES. The HSSWDS model simulated only the cover system, did not model lateral flow through drainage layers, and handled vertical drainage only in a rudimentary manner. The infiltration, percolation and evapotranspiration routines were almost identical to those used in the Chemicals, Runoff, and Erosion from Agricultural Management Systems (CREAMS) model, which was developed by Knisel (1980) for the U.S. Department of Agriculture (USDA). The runoff and infiltration routines relied heavily on the Hydrology Section of the National Engineering Handbook

(USDA, Soil Conservation Service, 1985). Version 1 of the HELP model incorporated a lateral subsurface drainage model and improved unsaturated drainage and liner leakage models into the HSSWDS model. In addition, the HELP model provided simulation of the entire landfill including leachate collection and liner systems.

Version 1 of the HELP program was tested extensively using both field and laboratory data. HELP Version 1 simulation results were compared to field data for 20 landfill cells from seven sites (Schroeder and Peyton, 1987a). The lateral drainage component of HELP Version 1 was tested against experimental results from two large-scale physical models of landfill liner/drain systems (Schroeder and Peyton, 1987b). The results of these tests provided motivation for some of the improvements incorporated into HELP Version 2.

Version 2 (Schroeder et al., 1988a and 1988b) presented a great enhancement of the capabilities of the HELP model. The WGEN synthetic weather generator developed by the USDA Agricultural Research Service (ARS) (Richardson and Wright, 1984) was added to the model to yield daily values of precipitation, temperature and solar radiation. This replaced the use of normal mean monthly temperature and solar radiation values and improved the modeling of snow and evapotranspiration. Also, a vegetative growth model from the Simulator for Water Resources in Rural Basins (SWRRB) model developed by the ARS (Arnold et al., 1989) was merged into the HELP model to calculate daily leaf area indices. Modeling of unsaturated hydraulic conductivity and flow and lateral drainage computations were improved. Default soil data were improved, and the model permitted use of more layers and initialization of soil moisture content.

In Version 3, the HELP model has been greatly enhanced beyond Version 2. The number of layers that can be modeled has been increased. The default soil/material texture list has been expanded to contain additional waste materials, geomembranes, geosynthetic drainage nets and compacted soils. The model also permits the use of a user-built library of soil textures. Computations of leachate recirculation and groundwater drainage into the landfill have been added. Moreover, HELP Version 3 accounts for leakage through geomembranes due to manufacturing defects (pinholes) and installation defects (punctures, tears and seaming flaws) and by vapor diffusion through the liner based on the equations compiled by Giroud et al. (1989, 1992). The estimation of runoff from the surface of the landfill has been improved to account for large landfill surface slopes and slope lengths. The snowmelt model has been replaced with an energy-based model; the Priestly-Taylor potential evapotranspiration model has been replaced with a Penman method, incorporating wind and humidity effects as well as long wave radiation losses (heat loss at night). A frozen soil model has been added to improve infiltration and runoff predictions in cold regions. The unsaturated vertical drainage model has also been improved to aid in storage computations. Input and editing have been further simplified with interactive, full-screen, menu-driven input techniques.

The HELP model requires daily climatologic data, soil characteristics, and design specifications to perform the analysis. Daily rainfall data may be input by the user,

generated stochastically, or taken from the model's historical data base. The model contains parameters for generating synthetic precipitation for 139 U.S. cities. The historical data base contains five years of daily precipitation data for 102 U.S. cities. Daily temperature and solar radiation data are generated stochastically or may be input by the user. Necessary soil data include porosity, field capacity, wilting point, saturated hydraulic conductivity, and Soil Conservation Service (SCS) runoff curve number for antecedent moisture condition II. The model contains default soil characteristics for 42 material types for use when measurements or site-specific estimates are not available. Design specifications include such things as the slope and maximum drainage distance for lateral drainage layers, layer thicknesses, leachate recirculation procedure, surface cover characteristics and information on any geomembranes.

Figure 1 is a definition sketch for a somewhat typical closed hazardous waste landfill profile. The top portion of the profile (layers 1 through 4) is the cap or cover. The bottom portion of the landfill is a double liner system (layers 6 through 11), in this case composed of a geomembrane liner and a composite liner. Immediately above the bottom composite liner is a leakage detection drainage layer to collect leakage from the primary liner, in this case, a geomembrane. Above the primary liner are a geosynthetic drainage net and a sand layer that serve as drainage layers for leachate collection. The drain layers composed of sand are typically at least 1-ft thick and have suitably spaced perforated or open joint drain pipe embedded below the surface of the liner. The leachate collection drainage layer serves to collect any leachate that may percolate through the waste layers. In this case where the liner is solely a geomembrane, a drainage net may be used to rapidly drain leachate from the liner, avoiding a significant buildup of head and limiting leakage. The liners are sloped to prevent ponding by encouraging leachate to flow toward the drains. The net effects are that very little leachate should leak through the primary liner and virtually no migration of leachate through the bottom composite liner to the natural formations below. Taken as a whole, the drainage layers, geomembrane liners, and barrier soil liners may be referred to as the leachate collection and removal system (drain/liner system) and more specifically a double liner system.

Figure 1 shows eleven layers--four in the cover or cap, one as the waste layers, three in the primary leachate collection and removal system (drain/liner system) and three in the secondary leachate collection and removal system (leakage detection). These eleven layers comprise three subprofiles or modeling units. A subprofile consists of all layers between (and including) the landfill surface and the bottom of the top liner system, between the bottom of one liner system and the bottom of the next lower liner system, or between the bottom of the lowest liner system and the bottom of the lowest soil layer modeled. In the sketch, the top subprofile contains the cover layers, the middle subprofile contains the waste, drain and liner system for leachate collection, and the bottom subprofile contains the drain and liner system for leakage detection. Six subprofiles in a single landfill profile may be simulated by the model.

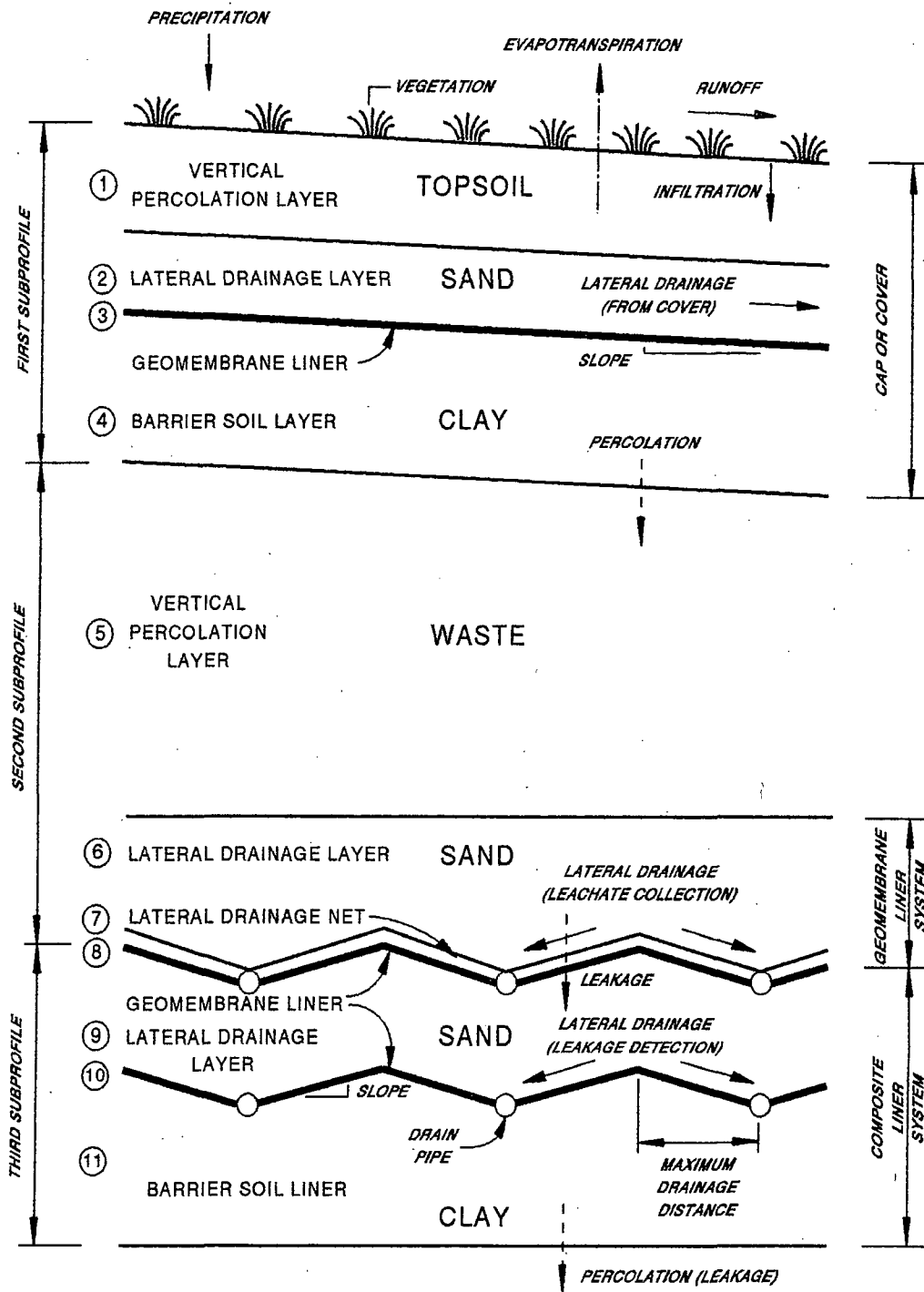


Figure 1. Schematic Profile View of a Typical Hazardous Waste Landfill

The layers in the landfill are typed by the hydraulic function that they perform. Four types of layers are available: vertical percolation layers, lateral drainage layers, barrier soil liners and geomembrane liners. These layer types are illustrated in Figure 1. The topsoil and waste layers are generally vertical percolation layers. Sand layers above liners are typically lateral drainage layers; compacted clay layers are typically barrier soil liners. Geomembranes are typed as geomembrane liners. Composite liners are modeled as two layers. Geotextiles are not considered as layers unless they perform a unique hydraulic function.

Flow in a vertical percolation layer (e.g., layers 1 and 5 in Figure 1) is either downward due to gravity drainage or extracted by evapotranspiration. Unsaturated vertical drainage is assumed to occur by gravity drainage whenever the soil moisture is greater than the field capacity (greater than the wilting point for soils in the evaporative zone) or when the soil suction of the layer below the vertical percolation layer is greater than the soil suction in the vertical percolation layer. The rate of gravity drainage (percolation) in a vertical percolation layer is assumed to be a function of the soil moisture storage and largely independent of conditions in adjacent layers. The rate can be restricted when the layer below is saturated and drains slower than the vertical percolation layer. Layers, whose primary hydraulic function is to provide storage of moisture and detention of drainage, should normally be designated as vertical percolation layers. Waste layers and layers designed to support vegetation should be designated as vertical percolation layers, unless the layers provide lateral drainage to collection systems.

Lateral drainage layers (e.g., layers 2, 6, 7 and 9 in Figure 1) are layers that promote lateral drainage to collection systems at or below the surface of liner systems. Vertical drainage in a lateral drainage layer is modeled in the same manner as for a vertical percolation layer, but saturated lateral drainage is allowed. The saturated hydraulic conductivity of a lateral drainage layer generally should be greater than  $1 \times 10^{-3}$  cm/sec for significant lateral drainage to occur. A lateral drainage layer may be underlain by only a liner or another lateral drainage layer. The slope of the bottom of the layer may vary from 0 to 40 percent.

Barrier soil liners (e.g., layers 4 and 11 in Figure 1) are intended to restrict vertical flow. These layers should have hydraulic conductivities substantially lower than those of the other types of layers, typically below  $1 \times 10^{-6}$  cm/sec. The program allows only downward flow in barrier soil liners. Thus, any water moving into a liner will eventually percolate through it. The leakage (percolation) rate depends upon the depth of water-saturated soil (head) above the base of the layer, the thickness of the liner and the saturated hydraulic conductivity of the barrier soil. Leakage occurs whenever the moisture content of the layer above the liner is greater than the field capacity of the layer. The program assumes that barrier soil liner is permanently saturated and that its properties do not change with time.

Geomembrane liners (e.g., layers 3, 8 and 10 in Figure 1) are layers of nearly

impermeable material that restricts significant leakage to small areas around defects. Leakage (percolation) is computed to be the result from three sources: vapor diffusion, manufacturing flaws (pinholes) and installation defects (punctures, cracks, tears and bad seams). Leakage by vapor diffusion is computed to occur across the entire area of the liner as a function of the head on the surface of the liner, the thickness of the geomembrane and its vapor diffusivity. Leakage through pinholes and installation defects is computed in two steps. First, the area of soil or material contributing to leakage is computed as a function of head on the liner, size of hole and the saturated hydraulic conductivity of the soils or materials adjacent to the geomembrane liner. Second, the rate of leakage in the wetted area is computed as a function of the head, thickness of soil and membrane and the saturated hydraulic conductivity of the soils or materials adjacent to the geomembrane liner.

## SECTION 3

### DATA GENERATION AND DEFAULT VALUES

#### 3.1 OVERVIEW

The HELP model requires general climate data for computing potential evapotranspiration; daily climatologic data; soil characteristics; and design specifications to perform the analysis. The required general climate data include growing season, average annual wind speed, average quarterly relative humidities, normal mean monthly temperatures, maximum leaf area index, evaporative zone depth and latitude. Default values for these parameters were compiled or developed from the "Climates of the States" (Ruffner, 1985) and "Climatic Atlas of the United States" (National Oceanic and Atmospheric Administration, 1974) for 183 U.S. cities. Daily climatologic (weather) data requirements include precipitation, mean temperature and total global solar radiation. Daily rainfall data may be input by the user, generated stochastically, or taken from the model's historical data base. The model contains parameters for generating synthetic precipitation for 139 U.S. cities. The historical data base contains five years of daily precipitation data for 102 U.S. cities. Daily temperature and solar radiation data are generated stochastically or may be input by the user.

Necessary soil data include porosity, field capacity, wilting point, saturated hydraulic conductivity, initial moisture storage, and Soil Conservation Service (SCS) runoff curve number for antecedent moisture condition II. The model contains default soil characteristics for 42 material types for use when measurements or site-specific estimates are not available. The porosity, field capacity, wilting point and saturated hydraulic conductivity are used to estimate the soil water evaporation coefficient and Brooks-Corey soil moisture retention parameters. Design specifications include such items as the slope and maximum drainage distance for lateral drainage layers; layer thicknesses; layer description; area; leachate recirculation procedure; subsurface inflows; surface characteristics; and geomembrane characteristics.

#### 3.2 SYNTHETIC WEATHER GENERATION

The HELP program incorporates a routine for generating daily values of precipitation, mean temperature, and solar radiation. This routine was developed by the USDA Agricultural Research Service (Richardson and Wright, 1984) based on a procedure described by Richardson (1981). The HELP user has the option of generating synthetic daily precipitation data rather than using default or user-specified historical data. Similarly, the HELP user has the option of generating synthetic daily mean temperature and solar radiation data rather than using user-specified historical data. The generating routine is designed to preserve the dependence in time, the correlation between variables and the seasonal characteristics in actual weather data at the specified location.

Coefficients for weather generation are available for up to 183 cities in the United States.

Daily precipitation is generated using a Markov chain-two parameter gamma distribution model. A first-order Markov chain model is used to generate the occurrence of wet or dry days. In this model, the probability of rain on a given day is conditioned on the wet or dry status of the previous day. A wet day is defined as a day with 0.01 inch of rain or more. The model requires two transition probabilities:  $P_i(W/W)$ , the probability of a wet day on day  $i$  given a wet day on day  $i-1$ ; and  $P_i(W/D)$ , the probability of a wet day on day  $i$  given a dry day on day  $i-1$ .

When a wet day occurs, the two-parameter gamma distribution function, which describes the distribution of daily rainfall amounts, is used to generate the precipitation amount. The density function of the two-parameter gamma distribution is given by

$$f(p) = \frac{p^{\alpha-1} e^{-p/\beta}}{\beta^\alpha \Gamma(\alpha)} \quad (1)$$

where

$f(p)$  = density function

$p$  = the probability

$\alpha$  and  $\beta$  = distribution parameters

$\Gamma$  = the gamma function of  $\alpha$

$e$  = the base of natural logarithms

The values of  $P(W/W)$ ,  $P(W/D)$ ,  $\alpha$  and  $\beta$  vary continuously during the year for most locations. The precipitation generating routine uses monthly values of the four parameters. The HELP program contains these monthly values for 139 locations in the United States. These values were computed by the Agricultural Research Service from 20 years (1951-1970) of daily precipitation data for each location.

Daily values of maximum temperature, minimum temperature and solar radiation are generated using the equation

$$t_i(j) = m_i(j) [\chi_i(j) \cdot c_i(j) + 1] \quad (2)$$

where

$t_i(j)$  = daily value of maximum temperature ( $j=1$ ), minimum temperature ( $j=2$ ), or solar radiation ( $j=3$ )

- $m_i(j)$  = mean value on day i  
 $c_i(j)$  = coefficient of variation on day i  
 $\chi_i(j)$  = stochastically generated residual element for day i

The seasonal change in the means and coefficients of variation is described by the harmonic equation

$$u_i = \bar{u} + C \cos \left[ \frac{2\pi}{365} (i - T) \right] \quad (3)$$

where

- $u_i$  = value of  $m_i(j)$  or  $c_i(j)$  on day i  
 $\bar{u}$  = mean value of  $u_i$   
 $C$  = amplitude of the harmonic  
 $T$  = position of the harmonic in days

The Agricultural Research Service computed values of these parameters for the three variables on wet and dry days from 20 years of weather data at 31 locations. The HELP model contains values of these parameters for 184 cities. These values were taken from contour maps prepared by Richardson and Wright (1984).

The residual elements for Equation 2 are generated using a procedure that preserves important serial correlations and cross-correlations. The generating equation is

$$\chi_i(j) = (A \cdot \chi_{i-1}(j)) + (B \cdot \epsilon_i(j)) \quad (4)$$

where

- $\chi_i(j)$  = 3 x 1 matrix for day i whose elements are residuals of maximum temperature (j=1), minimum temperature (J=2), and solar radiation (J=3)  
 $\epsilon_{i(j)}$  = 3 x 1 matrix of independent random components for item j  
*A and B* = 3 x 3 matrices whose elements are defined such that the new sequences have the desired serial correlation and cross-correlation coefficients

Richardson (1981) computed values of the relevant correlation coefficients from 20 years of weather data at 31 locations. The seasonal and spatial variation in these

correlation coefficients were found to be negligible. The elements of the A and B matrices are therefore treated as constants.

### 3.3 MOISTURE RETENTION AND HYDRAULIC CONDUCTIVITY PARAMETERS

The HELP program requires values for the total porosity, field capacity, wilting point, and saturated hydraulic conductivity of each layer that is not a liner. Saturated hydraulic conductivity is required for all liners. Values for these parameters can be specified by the user or selected from a list of default values provided in the HELP program. The values are used to compute moisture storage, unsaturated vertical drainage, head on liners and soil water evaporation.

#### 3.3.1 Moisture Retention Parameters

Relative moisture retention or storage used in the HELP model differs from the water contents typically used by engineers. The soil water storage or content used in the HELP model is on a per volume basis ( $\theta$ ), volume of water ( $V_w$ ) per total (bulk--soil, water and air) soil volume ( $V_t = V_s + V_w + V_a$ ), which is characteristic of practice in agronomy and soil physics. Engineers more commonly express moisture content on a per mass basis ( $w$ ), mass of water ( $M_w$ ) per mass of soil ( $M_s$ ). The two can be related to each other by knowing the dry bulk density ( $\rho_{db}$ ) and water density ( $\rho_w$ ), the dry bulk specific gravity ( $\Gamma_{db}$ ) of the soil (ratio of dry bulk density to water density), ( $\theta = w \cdot \Gamma_{db}$ ), or the wet bulk density ( $\rho_{wb}$ ), wet bulk specific gravity ( $\Gamma_{wb}$ ) of the soil (ratio of wet bulk density to water density), ( $\theta = [w \cdot \Gamma_{wb}] / [1 + w]$ ).

Total porosity is an effective value, defined as the volumetric water content (volume of water per total volume) when the pores contributing to change in moisture storage are at saturation. Total porosity can be used to describe the volume of active pore space present in soil or waste layers. Field capacity is the volumetric water content at a soil water suction of 0.33 bars or remaining after a prolonged period of gravity drainage without additional water supply. Wilting point is the volumetric water content at a suction of 15 bars or the lowest volumetric water content that can be achieved by plant transpiration (See Section 4.1.1). These moisture retention parameters are used to define moisture storage and relative unsaturated hydraulic conductivity.

The HELP program requires that the wilting point be greater than zero but less than the field capacity. The field capacity must be greater than the wilting point and less than the porosity. Total porosity must be greater than the field capacity but less than 1. The general relation among moisture retention parameters and soil texture class is shown in Figure 2.

The HELP user can specify the initial volumetric water contents of all non-liner layers. Soil liners are assumed to remain saturated at all times. If initial water contents

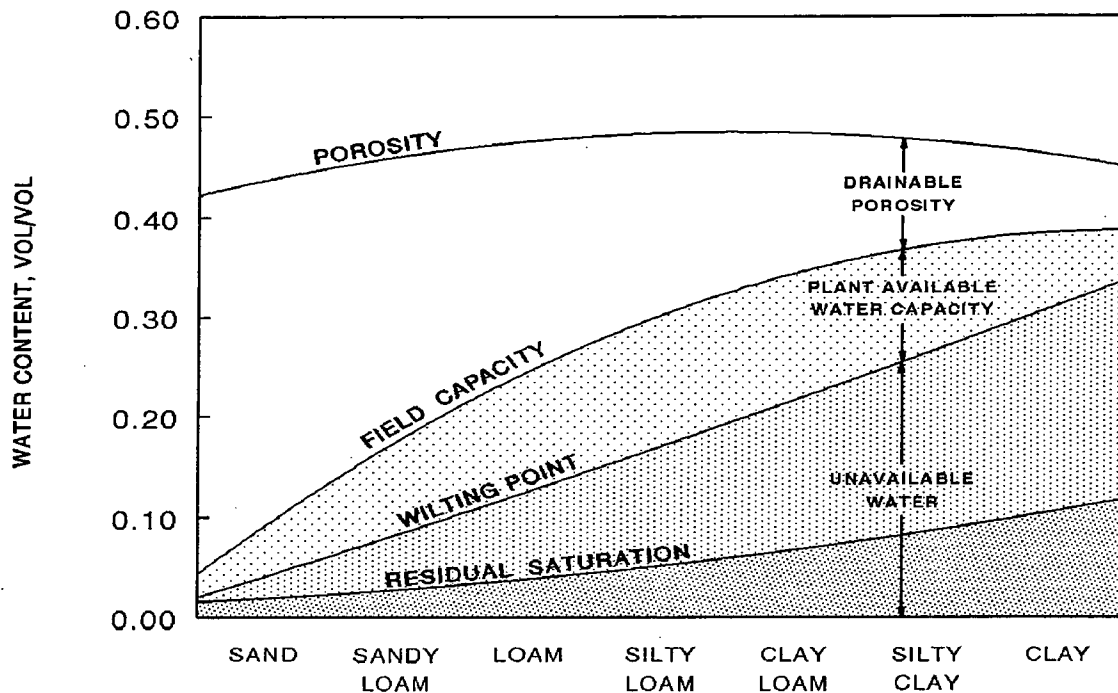


Figure 2. Relation Among Moisture Retention Parameters and Soil Texture Class

are not specified, the program assumes values near the steady-state values (allowing no long-term change in moisture storage) and runs a year of simulation to initialize the moisture contents closer to steady state. The soil water contents at the end of this year are substituted as the initial values for the simulation period. The program then runs the complete simulation, starting again from the beginning of the first year of data. The results of the volumetric water content initialization period are not reported in the output.

### 3.3.2 Unsaturated Hydraulic Conductivity

Darcy's constant of proportionality governing flow through porous media is known quantitatively as hydraulic conductivity or coefficient of permeability and qualitatively as permeability. Hydraulic conductivity is a function of media properties, such as particle size, void ratio, composition, fabric, degree of saturation, and the kinematic viscosity of the fluid moving through the media. The HELP program uses the saturated and unsaturated hydraulic conductivities of soil and waste layers to compute vertical drainage, lateral drainage and soil liner percolation. The vapor diffusivity for geomembranes is specified as a saturated hydraulic conductivity to compute leakage through geomembranes by vapor diffusion.

### ***Saturated Hydraulic Conductivity***

Saturated hydraulic conductivity is used to describe flow through porous media where the void spaces are filled with a wetting fluid (e.g., water). The saturated hydraulic conductivity of each layer is specified in the input. Equations for estimating the hydraulic conductivity for soils and other materials are presented in Appendix A of the HELP Program Version 3 User's Guide.

### ***Unsaturated Hydraulic Conductivity***

Unsaturated hydraulic conductivity is used to describe flow through a layer when the void spaces are filled with both wetting and non-wetting fluid (e.g., water and air). The HELP program computes the unsaturated hydraulic conductivity of each soil and waste layer using the following equation, reported by Campbell (1974):

$$K_u = K_s \left[ \frac{\theta - \theta_r}{\phi - \theta_r} \right]^{3 + \left(\frac{2}{\lambda}\right)} \quad (5)$$

where

- $K_u$  = unsaturated hydraulic conductivity, cm/sec
- $K_s$  = saturated hydraulic conductivity, cm/sec
- $\theta$  = actual volumetric water content, vol/vol
- $\theta_r$  = residual volumetric water content, vol/vol
- $\phi$  = total porosity, vol/vol
- $\lambda$  = pore-size distribution index, dimensionless

Residual volumetric water content is the amount of water remaining in a layer under infinite capillary suction. The HELP program uses the following regression equation, developed using mean soil texture values from Rawls et al. (1982), to calculate the residual volumetric water content:

$$\theta_r = \begin{cases} 0.014 + 0.25 WP & \text{for } WP \geq 0.04 \\ 0.6 WP & \text{for } WP < 0.04 \end{cases} \quad (6)$$

where

- $WP$  = volumetric wilting point, vol/vol

The residual volumetric water content and pore-size distribution index are constants in the Brooks-Corey equation relating volumetric water content to matrix potential (capillary pressure and adsorptive forces) (Brooks and Corey, 1964):

$$\frac{\theta - \theta_r}{\phi - \theta_r} = \left( \frac{\psi_b}{\psi} \right)^\lambda \quad (7)$$

where

$\psi$  = capillary pressure, bars

$\psi_b$  = bubbling pressure, bars

Bubbling pressure is a function of the maximum pore size forming a continuous network of flow channels within the medium (Brooks and Corey, 1964). Brakensiek et al. (1981) reported that Equation 7 provided a reasonably accurate representation of water retention and matrix potential relationships for tensions greater than 50 cm or 0.05 bars (unsaturated conditions).

The HELP program solves Equation 7 for two different capillary pressures simultaneously to determine the bubbling pressure and pore-size distribution index of volumetric moisture content for use in Equation 7. The total porosity is known from the input data. The capillary pressure-volumetric moisture content relationship is known at two points from the input of field capacity and wilting point. Therefore, the field capacity is inserted in Equation 7 as the volumetric moisture content and 0.33 bar is inserted as the capillary pressure to yield one equation. Similarly, the wilting point and 15 bar are inserted in Equation 7 to yield a second equation. Having two equations and two unknowns (bubbling pressure and pore-size distribution index), the two equations are solved simultaneously to yield the unknowns. This process is repeated for each layer to obtain the parameters for computing moisture retention and unsaturated drainage.

### 3.3.3 Saturated Hydraulic Conductivity for Vegetated Materials

The HELP program adjusts the saturated hydraulic conductivities of soils and waste layers in the top half of the evaporative zone whenever those soil characteristics were selected from the default list of soil textures. This adjustment, developed for the model from changes in runoff characteristics and minimum infiltration rates as function of vegetation, is made to account for channeling due to root penetration. These adjustments for vegetation are not made for user-specified soil characteristics; they are made only for default soil textures, which assumed that the soil layer is unvegetated and free of continuous root channels that provide preferential drainage paths. The HELP program calculates the vegetated saturated hydraulic conductivity as follows:

$$(K_s)_v = (1.0 + 0.5966 LAI + 0.132659 LAI^2 + 0.1123454 LAI^3 - 0.04777627 LAI^4 + 0.004325035 LAI^5) (K_s)_{uv} \quad (8)$$

where

$(K_s)_v$  = saturated hydraulic conductivity of vegetated material in top half of evaporative zone, cm/sec

$LAI$  = leaf area index, dimensionless (described in Section 4.11)

$(K_s)_{uv}$  = saturated hydraulic conductivity of unvegetated material in top half of evaporative zone, cm/sec

### 3.4 EVAPORATION COEFFICIENT

The evaporation coefficient indicates the ease with which water can be drawn upward through the soil or waste layer by evaporation. Using laboratory soil data Ritchie (1972) indicated that the evaporation coefficient (in mm/day<sup>0.5</sup>) can be related to the unsaturated hydraulic conductivity at 0.1 bar capillary pressure (calculated using Equations 5 and 7). The HELP program uses the following form of Ritchie's equation to compute the evaporation coefficient:

$$CON = \begin{cases} 3.30 & (K_u)_{0.1 \text{ bar}} \leq 0.05 \text{ cm/day} \\ 2.44 + 17.19 (K_u)_{0.1 \text{ bar}} & 0.05 \text{ cm/day} < (K_u)_{0.1 \text{ bar}} < 0.178 \text{ cm/day} \\ 5.50 & (K_u)_{0.1 \text{ bar}} \geq 0.178 \text{ cm/day} \end{cases} \quad (9)$$

where

$CON$  = evaporation coefficient, mm/day<sup>0.5</sup>

$(K_u)_{0.1 \text{ bar}}$  = unsaturated hydraulic conductivity at 0.1 bar capillary pressure, cm/sec

The HELP program imposes upper and lower limits on the evaporation coefficient so as not to yield a capillary flux outside of the range for soils reported by Knisel (1980). If the calculated value of the evaporation coefficient is less than 3.30, then it is set equal to 3.30, and if the evaporation coefficient is greater than 5.50, then it is set equal to 5.50. The user cannot enter the evaporation coefficient independently.

Since Equation 9 was developed for soil materials, the HELP program imposes

additional checks on the evaporation coefficient based on the relative field capacity and saturated hydraulic conductivity of each soil and waste layer. Relative field capacity is calculated using the following equation:

$$FC_{rel} = \frac{FC - \theta_r}{\phi - \theta_r} \quad (10)$$

where

$FC_{rel}$  = relative field capacity, dimensionless

$FC$  = field capacity, vol/vol

If the relative field capacity is less than 0.20 (typical of sand), then the evaporation coefficient is set equal to 3.30. Additionally, if the saturated hydraulic conductivity is less than  $5 \times 10^{-6}$  cm/sec (the range of compacted clay), the evaporation coefficient is set equal to 3.30.

### 3.5 DEFAULT SOIL AND WASTE CHARACTERISTICS

The total density of soil and waste layers can be defined as the mass of solid and water particles per unit volume of the media. The total density of these layers is dependent on the density of the solid particles, the volume of pore space, and the amount of water in each layer. As previously discussed, total porosity can be used to describe the volume of pore space in a soil or waste layer. Therefore, total porosity can be used to indicate the density of soil and waste layers.

The density of soil and waste layers can be increased by compaction, static loading, and/or dewatering of soil and waste layers. Compaction increases density through the application of mechanical energy. Static loading increases density by the application of the weight of additional soil, barrier, or waste layers. Dewatering increases density by removing pore water and/or reducing the pore pressures in the layer. Dewatering can be accomplished by installing horizontal and/or vertical drains, trenches, water wells, and/or the application of electrical currents. The HELP program provides default values for the total porosity, field capacity, wilting point, and saturated hydraulic conductivity of numerous soil and waste materials as well as geosynthetic materials.

#### 3.5.1 Default Soil Characteristics

Information on default soil moisture retention values for low, moderate, and high-density soil layers is provided in the following sections. High-density soil layers are also described as soil liners. Application of the default soil properties should be limited to

planning level studies and are not intended to replace design level laboratory and field testing programs.

### ***Low-Density Soil Layers***

Rawls et al. (1982) reported mean values for total porosity, residual volumetric water content, bubbling pressure, and pore-size distribution index, for the major US Department of Agriculture (USDA) soil texture classes. These values were compiled from 1,323 soils with about 5,350 horizons (or layers) from 32 states. The geometric mean of the bubbling pressure and pore-size distribution index and the arithmetic mean of total porosity and residual volumetric water content for each soil texture class were substituted into Equation 7 to calculate the field capacity (volumetric water content at a capillary pressure of 1/3 bar) and wilting point (volumetric water content at a capillary pressure of 15 bars) of each soil texture class. Rawls et al. (1982) also reported saturated hydraulic conductivity values for each major USDA uncompact soil texture class. These values were derived from the results of numerous experiments and compared with similar data sets. Default characteristics for the coarse and fine sands (Co and F) were developed by interpolating between Rawls' data.

Freeze and Cherry (1979) reported that typical unconsolidated clay total porosities range from 0.40 to 0.70. Rawls' sandy clay, silty clay, and clay had total porosities of 0.43, 0.48, and 0.47, respectively. Therefore, Rawls' loam and clay soils data are considered to represent conditions typical of minimal densification efforts or low-density soils. Default characteristics for Rawls et al. (1982) low-density soil layers are summarized in Table 1. The USDA soil textures reported in Table 1 were converted to Unified Soil Classification System (USCS) soil textures using a soil classification triangle provided in McAneny et al. (1985). Applicable USDA and USCS soil texture abbreviations are provided in Table 3.

### ***Moderate-Density Soil Layers***

Rawls et al. (1982) presented the following form of Brutsaert's (1967) saturated hydraulic conductivity equation:

$$K_s = a \frac{(\phi - \theta_r)^2}{(\psi_b)^2} \frac{\lambda^2}{(\lambda + 1)(\lambda + 2)} \quad (11)$$

where

$K_s$  = saturated hydraulic conductivity, cm/sec

TABLE 1. DEFAULT LOW DENSITY SOIL CHARACTERISTICS

Soil Texture Class			Total Porosity vol/vol	Field Capacity vol/vol	Wilting Point vol/vol	Saturated Hydraulic Conductivity cm/sec
HELP	USDA	USCS				
1	CoS	SP	0.417	0.045	0.018	$1.0 \times 10^{-2}$
2	S	SW	0.437	0.062	0.024	$5.8 \times 10^{-3}$
3	FS	SW	0.457	0.083	0.033	$3.1 \times 10^{-3}$
4	LS	SM	0.437	0.105	0.047	$1.7 \times 10^{-3}$
5	LFS	SM	0.457	0.131	0.058	$1.0 \times 10^{-3}$
6	SL	SM	0.453	0.190	0.085	$7.2 \times 10^{-4}$
7	FSL	SM	0.473	0.222	0.104	$5.2 \times 10^{-4}$
8	L	ML	0.463	0.232	0.116	$3.7 \times 10^{-4}$
9	SiL	ML	0.501	0.284	0.135	$1.9 \times 10^{-4}$
10	SCL	SC	0.398	0.244	0.136	$1.2 \times 10^{-4}$
11	CL	CL	0.464	0.310	0.187	$6.4 \times 10^{-5}$
12	SiCL	CL	0.471	0.342	0.210	$4.2 \times 10^{-5}$
13	SC	SC	0.430	0.321	0.221	$3.3 \times 10^{-5}$
14	SiC	CH	0.479	0.371	0.251	$2.5 \times 10^{-5}$
15	C	CH	0.475	0.378	0.251	$2.5 \times 10^{-5}$
21	G	GP	0.397	0.032	0.013	$3.0 \times 10^{-1}$

- $a$  = constant representing the effects of various fluid constants and gravity,  $21 \text{ cm}^3/\text{sec}$
- $\phi$  = total porosity, vol/vol
- $\theta_r$  = residual volumetric water content, vol/vol
- $\psi_b$  = bubbling pressure, cm
- $\lambda$  = pore-size distribution index, dimensionless

A more detailed explanation of Equation 11 can be found in Appendix A of the HELP program Version 3 User's Guide and the cited references.

Since densification is known to decrease the saturated hydraulic conductivity of a soil layer, the total porosity, residual volumetric water content, bubbling pressure, and pore-size distribution index data reported in Rawls et al. (1982) were adjusted by a fraction of a standard deviation and substituted into Equation 11 to reflect this decrease. Examination of Equation 11 and various adjustments to Rawls' reported data indicated that a reasonable representation of moderate-density soil conditions can be obtained by a 0.5 standard deviation decrease in the total porosity and pore-size distribution index and a 0.5 standard deviation increase in the bubbling pressure and residual saturation of Rawls' compressible soils (e.g. loams and clays). These adjustments were substituted into Equations 7 and 11 to determine the total porosity, field capacity, wilting point, and hydraulic conductivity of these soils. The values obtained from these adjustments are thought to represent moderate-density soil conditions typical of compaction by vehicle traffic, static loading by the addition of soil or waste layers, etc. Default characteristics for moderate-density, compressible loams and clays are summarized in Table 2. The USDA soil textures reported in Table 2 were converted to Unified Soil Classification System (USCS) soil textures using information provided in McAneny et al. (1985). Applicable USDA and USCS soil texture abbreviations are provided in Table 3.

### ***High-Density Soil Layers***

Similar to moderate-density soil layers, densification produces a high-density, low saturated hydraulic conductivity soil layer or soil liner. Due to the geochemical and low saturated hydraulic conductivity properties of clay, soil liners are typically constructed of compacted clay. Elsbury et al. (1990) indicated that the hydraulic conductivity of clay liners can be impacted by the soil workability, gradation, and swell potential; overburden stress on the liner; liner thickness; liner foundation stability; liner desiccation and/or freeze and thawing; and degree of compaction. Compaction should destroy large soil clods and provide interlayer bonding. The process can be impacted by the lift thickness; soil water content, dry density, and degree of saturation; size of soil clods; soil preparation; compactor type and weight; number of compaction passes and coverage; and construction quality assurance. The HELP program provides default characteristics for clay soil liners with a saturated hydraulic conductivity of  $1 \times 10^{-7}$  and  $1 \times 10^{-9}$  cm/sec.

Similar to the procedure used to obtain the default moderate-density clay soil properties, Rawls et al.'s (1982) reported total porosity, pore-size distribution index, bubbling pressure, and residual saturation for clay soil layers were adjusted to determine the field capacity and wilting point of the  $1 \times 10^{-7}$  cm/sec clay liner. A hydraulic conductivity of  $6.8 \times 10^{-8}$  cm/sec was obtained by substituting a 1 standard deviation decrease in Rawls' reported total porosity and pore-size distribution index and a 1 standard deviation increase in Rawls' reported bubbling pressure and residual saturation into Equation 11. These adjustments were substituted into Equation 7 to obtain a field capacity and wilting point representative of the  $1 \times 10^{-7}$  cm/sec soil liner.

TABLE 2. MODERATE AND HIGH DENSITY DEFAULT SOILS

Soil Texture Class			Total Porosity vol/vol	Field Capacity vol/vol	Wilting Point vol/vol	Saturated Hydraulic Conductivity cm/sec
HELP	USDA	USCS				
22	L (Moderate)	ML	0.419	0.307	0.180	$1.9 \times 10^{-5}$
23	SiL (Moderate)	ML	0.461	0.360	0.203	$9.0 \times 10^{-6}$
24	SCL (Moderate)	SC	0.365	0.305	0.202	$2.7 \times 10^{-6}$
25	CL (Moderate)	CL	0.437	0.373	0.266	$3.6 \times 10^{-6}$
26	SiCL (Moderate)	CL	0.445	0.393	0.277	$1.9 \times 10^{-6}$
27	SC (Moderate)	SC	0.400	0.366	0.288	$7.8 \times 10^{-7}$
28	SiC (Moderate)	CH	0.452	0.411	0.311	$1.2 \times 10^{-6}$
29	C (Moderate)	CH	0.451	0.419	0.332	$6.8 \times 10^{-7}$
16	Liner Soil (High)		0.427	0.418	0.367	$1.0 \times 10^{-7}$
17	Bentonite (High)		0.750	0.747	0.400	$3.0 \times 10^{-9}$

### 3.5.2 Default Waste Characteristics

Table 4 provides a summary of default moisture retention values for various waste layers. Municipal waste properties provided in Tchobanoglous et al. (1977) and Equations 6 and 7 were used to determine the total porosity, field capacity, and wilting point of a well compacted municipal waste. The field capacity and wilting point were calculated using Tchobanoglous et al.'s high and low water content values, respectively. Oweis et al. (1990) provided information on the in-situ saturated hydraulic conductivity of municipal waste. Zeiss and Major (1993) described the moisture flow through

TABLE 3. DEFAULT SOIL TEXTURE ABBREVIATIONS

US Department of Agriculture	Definition
G	Gravel
S	Sand
Si	Silt
C	Clay
L	Loam (sand, silt, clay, and humus mixture)
Co	Coarse
F	Fine
Unified Soil Classification System	Definition
G	Gravel
S	Sand
M	Silt
C	Clay
P	Poorly Graded
W	Well Graded
H	High Plasticity or Compressibility
L	Low Plasticity or Compressibility

municipal waste and the effective moisture retention of municipal waste, providing information on waste with dead zones and channeling. In addition, Toth et al. (1988) provided information on compacted coal-burning electric plant ash, Poran and Ahtchi-Ali (1989) provided information on compacted municipal solid waste ash, and Das et al. (1983) provided information on fine copper slag.

The total porosities of the ash and slag wastes were determined using a phase relationship at maximum dry density. The field capacities and wilting points of the ash and slag wastes were calculated using the following empirical equations reported by Brakensiek et al. (1984):

TABLE 4. DEFAULT WASTE CHARACTERISTICS

Waste Identification		Total Porosity vol/vol	Field Capacity vol/vol	Wilting Point vol/vol	Saturated Hydraulic Conductivity cm/sec
HELP	Waste Material				
18	Municipal Waste	0.671	0.292	0.077	$1.0 \times 10^{-3}$
19	Municipal Waste with Channeling	0.168	0.073	0.019	$1.0 \times 10^{-3}$
30	High-Density Electric Plant Coal Fly Ash*	0.541	0.187	0.047	$5.0 \times 10^{-5}$
31	High-Density Electric Plant Coal Bottom Ash*	0.578	0.076	0.025	$4.1 \times 10^{-3}$
32	High-Density Municipal Solid Waste Incinerator Fly Ash**	0.450	0.116	0.049	$1.0 \times 10^{-2}$
33	High-Density Fine Copper Slag**	0.375	0.055	0.020	$4.1 \times 10^{-2}$

\* All values, except saturated hydraulic conductivity, are at maximum dry density. Saturated hydraulic conductivity was determined in-situ.

\*\* All values are at maximum dry density. Saturated hydraulic conductivity was determined by laboratory methods.

$$\begin{aligned} \text{Field Capacity} = & 0.1535 - (0.0018)(\% \text{ Sand}) + (0.0039)(\% \text{ Clay}) \\ & + (0.1943)(\text{Total Porosity}) \end{aligned} \quad (12)$$

$$\begin{aligned} \text{Wilting Point} = & 0.0370 - (0.0004)(\% \text{ Sand}) + (0.0044)(\% \text{ Clay}) \\ & + (0.0482)(\text{Total Porosity}) \end{aligned} \quad (13)$$

where  $0.05 \text{ mm} < \text{Sand Particles} < 2 \text{ mm}$  and  $\text{Clay Particles} < 0.002 \text{ mm}$  (McAneny et al. 1985). These equations were developed for natural soils having a sand content between 5 and 70 percent and a clay content between 5 and 60 percent. While the particle size distribution of some of the ash and slag wastes fell outside this range, the effects of this variation on water retention were thought to be minimal. The applicability of these equations to waste materials has not been verified.

The saturated hydraulic conductivities of the ash and slag wastes were taken directly from the references. The saturated hydraulic conductivities of the coal burning electric plant ashes at maximum dry density were determined in-situ and the maximum dry density municipal solid waste incinerator ash and fine copper slag values were determined by laboratory methods. The saturated hydraulic conductivities of various other waste materials are provided in Table 5. Similar to default soils, the HELP program uses Equation 8 to adjust the saturated hydraulic conductivities of the default wastes in the top half of the evaporative zone to account for root penetration.

A more detailed explanation of the calculation procedure used for the ash and slag wastes can be found in Appendix A of the HELP program Version 3 User's Guide. Like the soil properties, the default waste properties were determined using empirical equations developed from soil data. Therefore, these values should not be used in place of a detailed laboratory and field testing program.

TABLE 5. SATURATED HYDRAULIC CONDUCTIVITY OF WASTES

Waste Material	Saturated Hydraulic Conductivity cm/sec*	Reference
Stabilized Incinerator Fly Ash	$8.8 \times 10^{-5}$	Poran and Ahtchi-Ali (1989)
High-Density Pulverized Fly Ash	$2.5 \times 10^{-5}$	Swain (1979)
Solidified Waste	$4.0 \times 10^{-2}$	Rushbrook et al. (1989)
Electroplating Sludge	$1.6 \times 10^{-5}$	Bartos and Palermo (1977)
Nickel/Cadmium Battery Sludge	$3.5 \times 10^{-6}$	"
Inorganic Pigment Sludge	$5.0 \times 10^{-6}$	"
Brine Sludge - Chlorine Production	$8.2 \times 10^{-5}$	"
Calcium Fluoride Sludge	$3.2 \times 10^{-5}$	"
High Ash Papermill Sludge	$1.4 \times 10^{-6}$	Perry and Schultz (1977)

\* - Determined by laboratory methods.

### 3.5.3 Default Geosynthetic Material Characteristics

Table 6 provides a summary of default properties for various geosynthetic materials. The values were extracted from Geotechnical Fabrics Report--1992 Specifiers Guide (Industrial Fabrics Association International, 1991) and Giroud and Bonaparte (1985).

### 3.6 SOIL MOISTURE INITIALIZATION

The soil moisture of the layers may be initialized by the user or the program. If initialized by the program, the soil moisture is initialized near steady-state using a three step procedure. The first step sets the soil moisture of all liners to porosity or saturation and the moisture of all other layers to field capacity.

In the second step the program computes a soil moisture for each layer below the top liner system. These soil moistures are computed to yield an unsaturated hydraulic conductivity equal to 85% of the lowest effective saturated hydraulic conductivity of all

TABLE 6. DEFAULT GEOSYNTHETIC MATERIAL CHARACTERISTICS

Geosynthetic Material Description		Saturated Hydraulic Conductivity cm/sec
HELP	Geosynthetic Material	
20	Drainage Net (0.5 cm)	$1.0 \times 10^{-1}$
34	Drainage Net (0.6 cm)	$3.3 \times 10^{-1}$
35	High Density Polyethylene (HDPE) Membrane	$2.0 \times 10^{-13}$
36	Low Density Polyethylene (LDPE) Membrane	$4.0 \times 10^{-13}$
37	Polyvinyl Chloride (PVC) Membrane	$2.0 \times 10^{-11}$
38	Butyl Rubber Membrane	$1.0 \times 10^{-12}$
39	Chlorinated Polyethylene (CPE) Membrane	$4.0 \times 10^{-12}$
40	Hypalon or Chlorosulfonated Polyethylene (CSPE) Membrane	$3.0 \times 10^{-12}$
41	Ethylene-Propylene Diene Monomer (EPDM) Membrane	$2.0 \times 10^{-12}$
42	Neoprene Membrane	$3.0 \times 10^{-12}$

liner systems above the layer, including consideration for geomembrane liners. If the unsaturated hydraulic conductivity is greater than  $5 \times 10^{-7}$  cm/sec or if the computed soil moisture is less than field capacity, the soil moisture is set to equal the field capacity. In all other cases, the computed soil moistures are used.

The third step in the initialization consists of running the model for one year of simulation using the first year of climatological data and the initial soil moistures selected in step 2. At the end of the year of initialization, the soil moistures existing at that point are reported as the initial soil moistures. The simulation is then started using the first year of climatological data again.

### 3.7 DEFAULT LEAF AREA INDICES AND EVAPORATIVE ZONE DEPTHS

Recommended default values for leaf area index and evaporative depth are given in the program. Figures 3, 4 and 5 show the geographic distribution of the default values for minimum and maximum evaporative depth and maximum leaf area index. The evaporative zone depths are based on rainfall, temperature and humidity data for the climatic regions. The estimates for minimum depths are based loosely on literature values (Saxton et al., 1971) and unsaturated flow model results for bare loamy soils (Thompson and Tyler, 1984; Fleenor, 1993), while the maximum depths are for loamy soils with a very good stand of grass, assuming rooting depths will vary regionally with

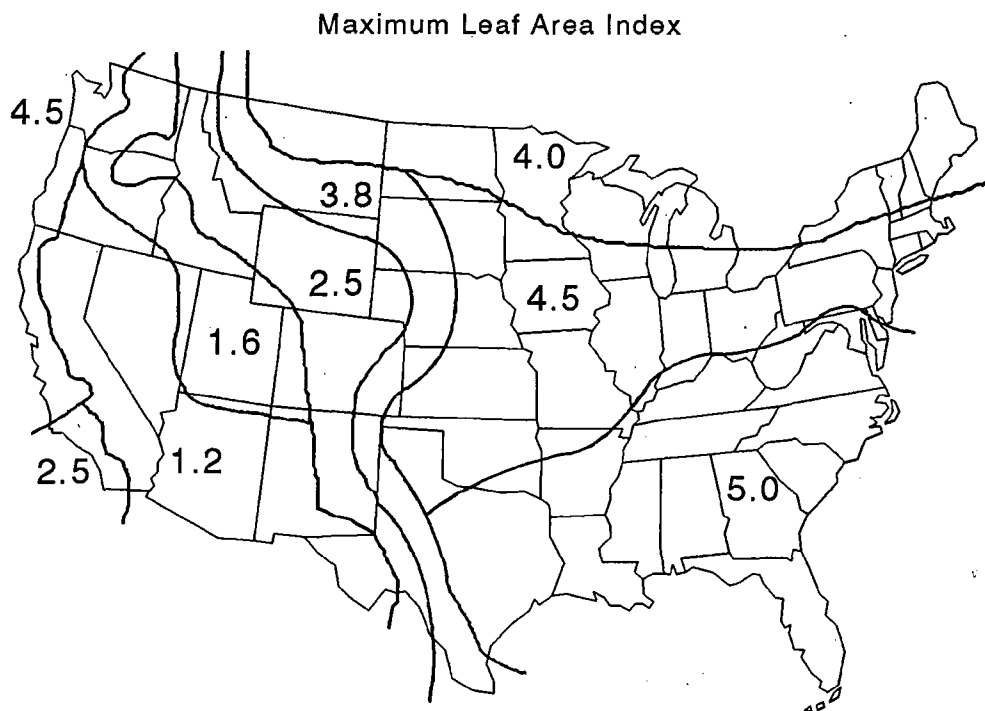


Figure 3. Geographic Distribution of Maximum Leaf Area Index

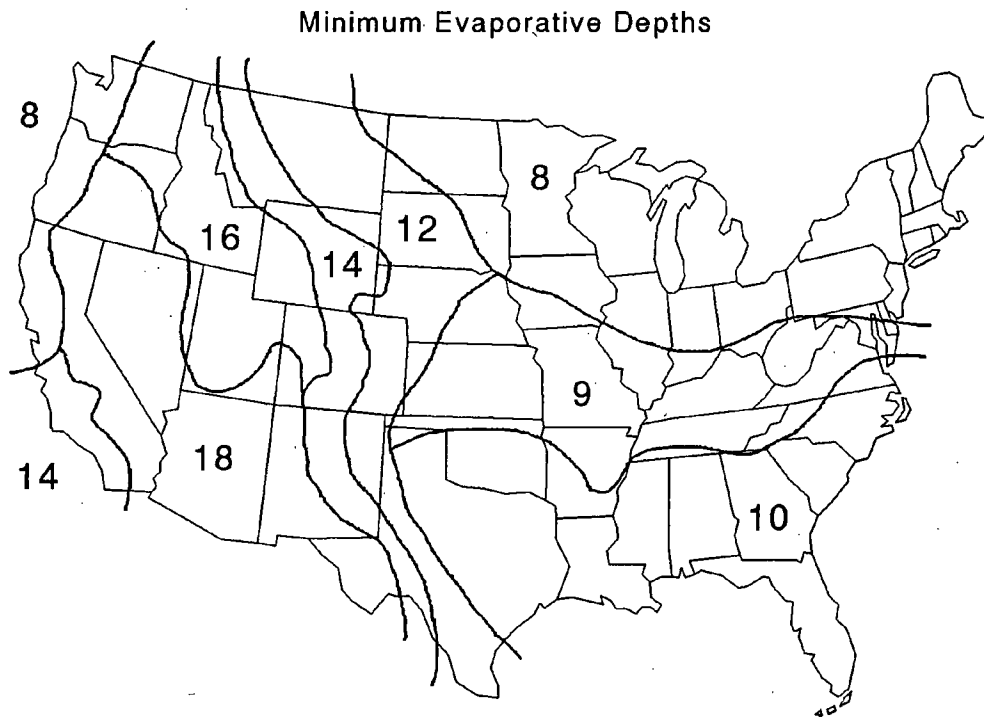


Figure 4. Geographic Distribution of Minimum Evaporative Depth

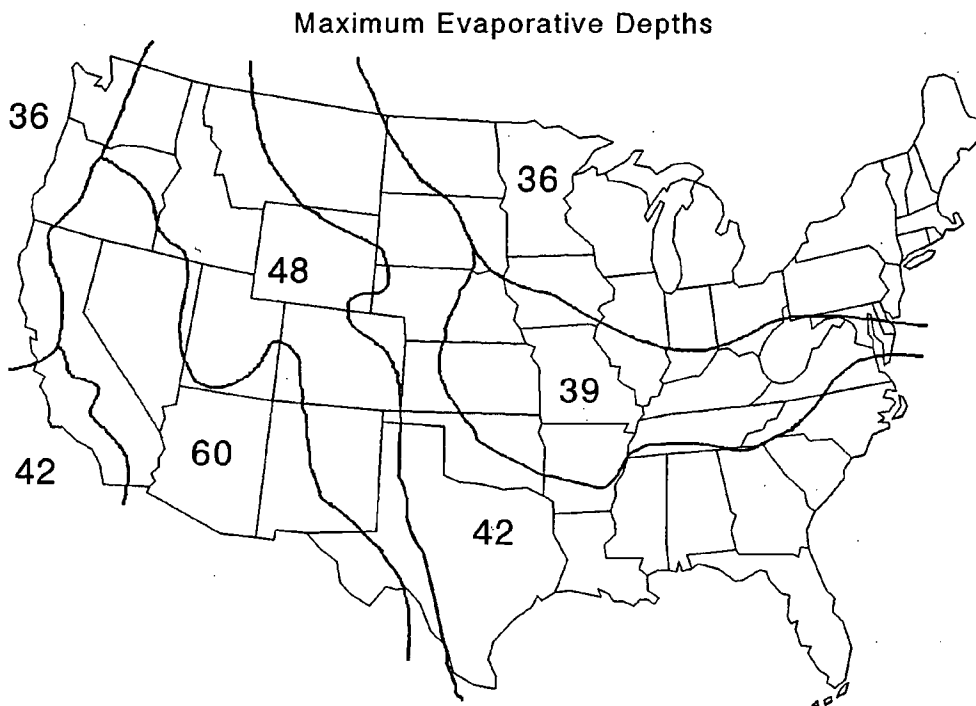


Figure 5. Geographic Distribution of Maximum Evaporative Depth

plant species and climate. The zones and values for the maximum leaf area index are based on recommendations in the documentation for the Simulator for Water Resources in Rural Basins (SWRRB) model (Arnold et al., 1989), considering both rainfall and temperature.

## SECTION 4

### METHOD OF SOLUTION

#### 4.1 OVERVIEW

The HELP program simulates daily water movement into, through and out of a landfill. In general, the hydrologic processes modeled by the program can be divided into two categories: surface processes and subsurface processes. The surface processes modeled are snowmelt, interception of rainfall by vegetation, surface runoff, and evaporation of water, interception and snow from the surface. The subsurface processes modeled are evaporation of water from the soil, plant transpiration, vertical unsaturated drainage, geomembrane liner leakage, barrier soil liner percolation and lateral saturated drainage. Vegetative growth and frozen soil models are also included in the program to aid modeling of the water routing processes.

Daily infiltration into the landfill is determined indirectly from a surface-water balance. Each day, infiltration is assumed to equal the sum of rainfall and snowmelt, minus the sum of runoff, surface storage and surface evaporation. No liquid water is held in surface storage from one day to the next, except in the snow cover. The daily surface-water accounting proceeds as follows. Snowfall and rainfall are added to the surface snow storage, if present, and then snowmelt plus excess storage of rainfall is computed. The total outflow from the snow cover is then treated as rainfall in the absence of a snow cover for the purpose of computing runoff. A rainfall-runoff relationship is used to determine the runoff. Surface evaporation is then computed. Surface evaporation is not allowed to exceed the sum of surface snow storage and intercepted rainfall. Interception is computed only for rainfall, not for outflow from the snow cover. The snowmelt and rainfall that does not run off or evaporate is assumed to infiltrate into the landfill. Computed infiltration in excess of the storage and drainage capacity of the soil is routed back to the surface and is added to the runoff or held as surface storage.

The first subsurface processes considered are evaporation from the soil and plant transpiration from the evaporative zone of the upper subprofile. These are computed on a daily basis. The evapotranspiration demand is distributed among the seven modeling segments in the evaporative zone.

The other subsurface processes are modeled one subprofile at a time, from top to bottom, using a design dependent time step, varying from 30 minutes to 6 hours. Unsaturated vertical drainage is computed for each modeling segment starting at the top of the subprofile, proceeding downward to the liner system or bottom of the subprofile. The program performs a water balance on each segment to determine the water storage and drainage for each segment, accounting for infiltration or drainage from above, subsurface inflow, leachate recirculation, moisture content and material characteristics.

If the subprofile contains a liner, water-routing or drainage from the segment directly above the liner is computed as leakage or percolation through the liner, and lateral drainage to the collection system, if present. The sum of the lateral drainage and leakage/percolation is first estimated to compute the moisture storage and head on the liner. Using the head, the leakage and lateral drainage is computed and compared to their initial guesses. If the sum of these two outflows is not sufficiently close to the initial estimate, new estimates are generated and the procedure is repeated until acceptable convergence is achieved. The moisture storage in liner systems is assumed to be constant; therefore, any drainage into a liner results in an equal drainage out of the liner. If the subprofile does not contain a liner, the lateral drainage is zero and the vertical drainage from the bottom subprofile is computed in the same manner as the upper modeling segments.

## 4.2 RUNOFF

The rainfall-runoff process is modeled using the SCS curve-number method, as presented in Section 4 of the National Engineering Handbook (USDA, SCS, 1985). This procedure was selected for four reasons: (1) it is widely accepted, (2) it is computationally efficient, (3) the required input is generally available and (4) it can conveniently handle a variety of soil types, land uses and management practices.

The SCS procedure was developed from rainfall-runoff data for large storms on small watersheds. The development is as follows (USDA, SCS, 1985). Runoff was plotted as a function of rainfall on arithmetic graph paper having equal scales, yielding a curve that becomes asymptotic to a straight line with a 1:1 slope at high rainfall as shown in Figure 6. The equation of the straight-line portion of the runoff curve, assuming no lag between the times when rainfall and runoff begin, is

$$Q = P' - S' \quad (14)$$

where

- $Q$  = actual runoff, inches
- $P'$  = maximum potential runoff (actual rainfall after runoff starts or actual rainfall when initial abstraction does not occur), inches
- $S'$  = maximum potential retention after runoff starts, inches

The following empirical equation was found to describe the relationship among precipitation, runoff and retention (the difference between the rainfall and runoff) at any point on the runoff curve:

$$\frac{F}{S'} = \frac{Q}{P'} \quad (15)$$

where

$$\begin{aligned} F &= \text{actual retention after runoff starts, inches} \\ &= P' - Q \end{aligned}$$

Substituting for  $F$ ,

$$\frac{P' - Q}{S'} = \frac{Q}{P'} \quad (16)$$

If initial abstraction is considered, the runoff curve is translated to the right, as shown in Figure 6, by the amount of precipitation that occurs before runoff begins. This amount of precipitation is termed the initial abstraction,  $I_a$ . To adjust Equation 16 for initial abstraction, this amount is subtracted from the precipitation,

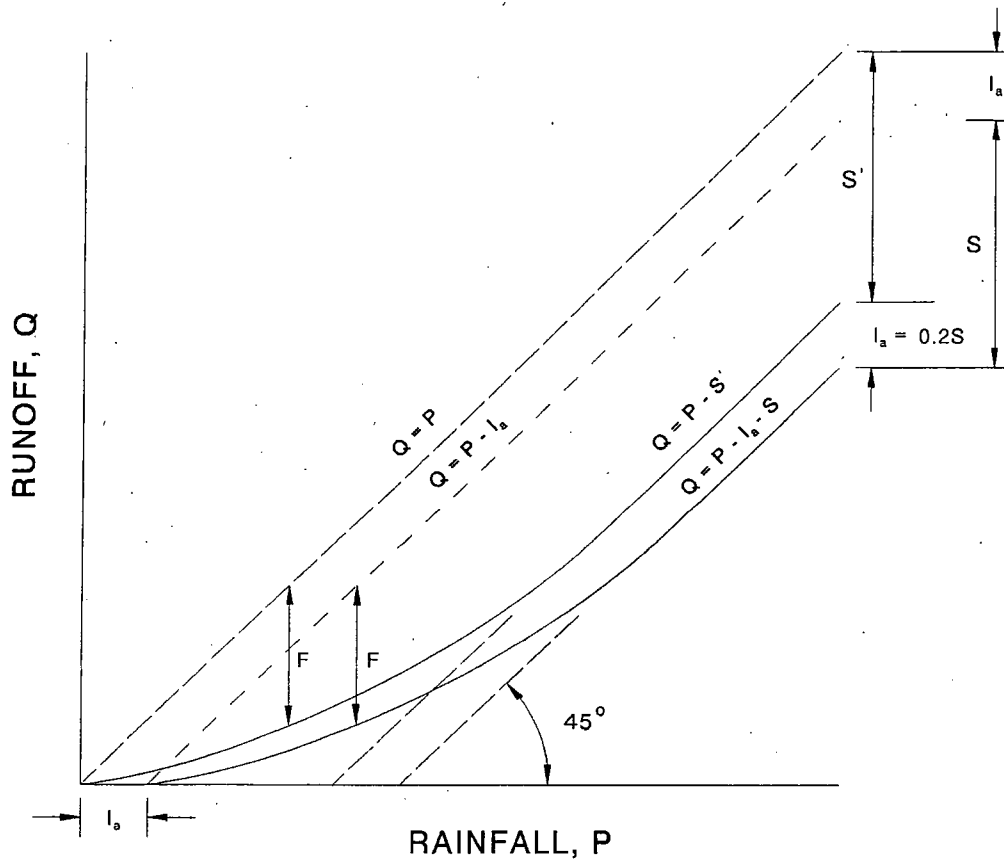


Figure 6. Relation Between Runoff, Precipitation, and Retention.

$$P' = P - I_a \quad (17)$$

Equation 16 becomes

$$\frac{P - I_a - Q}{S'} = \frac{Q}{P - I_a} \quad (18)$$

where

$P$  = actual rainfall, inches

$I_a$  = initial abstraction, inches

Figure 6 shows that the two retention parameters,  $S'$  and  $S$ , are equal:

$$S = S' \quad (19)$$

Rainfall and runoff data from a large number of small experimental watersheds indicate that, as a reasonable approximation (USDA, SCS, 1985),

$$I_a = 0.2 S \quad (20)$$

Substituting Equations 19 and 20 into Equation 18 and solving for  $Q$ ,

$$Q = \frac{(P - 0.2 S)^2}{(P + 0.8 S)} \quad (21)$$

Performing polynomial division on Equation 21 and dividing both sides of the equation by  $S$ ,

$$\frac{Q}{S} = \frac{P}{S} - 1.2 - \frac{1.0}{\frac{P}{S} + 0.8} \quad (22)$$

Equation 22 is the normalized rainfall-runoff relationship for any  $S$  and is plotted in Figure 7.

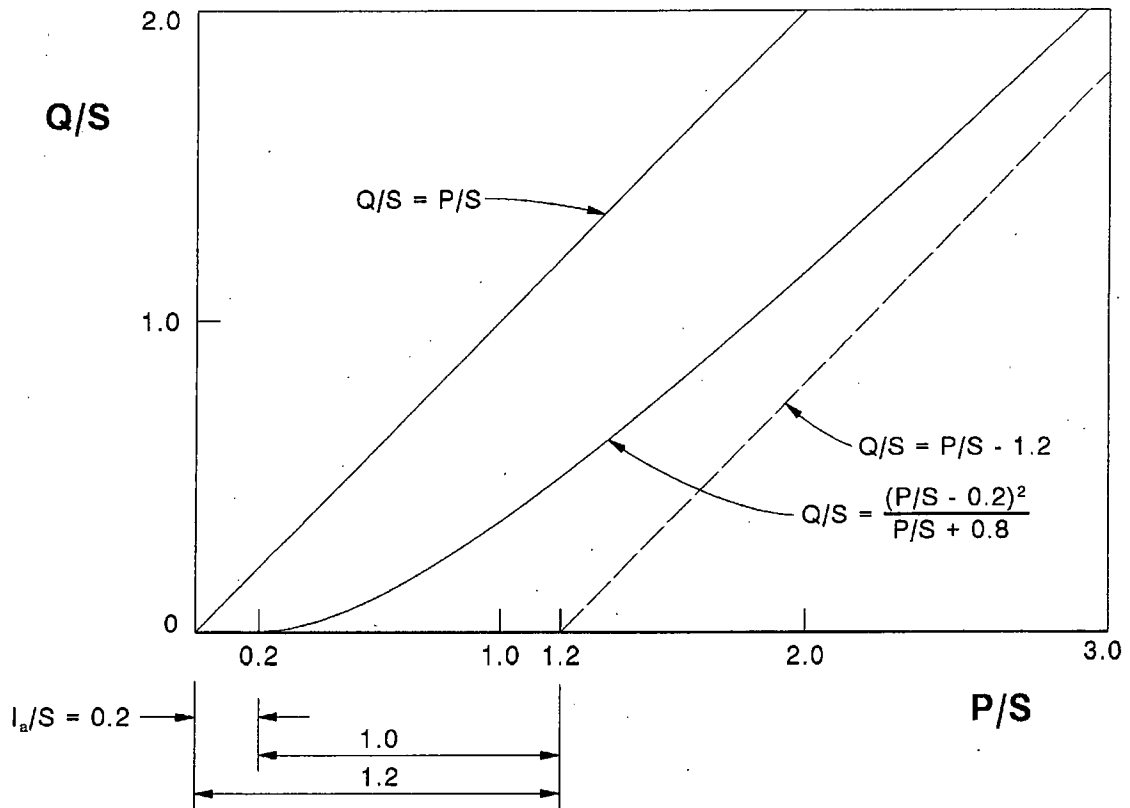


Figure 7. SCS Rainfall-Runoff Relation Normalized on Retention Parameter S

The retention parameter,  $S$ , is transformed into a so-called runoff curve number,  $CN$ , to make interpolating, averaging and weighting operations more nearly linear. The relationship between  $CN$  and  $S$  is

$$CN = \frac{1000}{S + 10} \quad (23)$$

$$S = \frac{1000}{CN} - 10 \quad (24)$$

The HELP program computes the runoff,  $Q_i$  on day  $i$ , from Equation 21 based on the net rainfall,  $P_i$ , on this day. The net rainfall is zero when the mean temperature is less than or equal to 32 °F; is equal to the precipitation when the mean temperature is above 32 °F and no snow cover is present; or is equal to the outflow from the snow cover when

a snow cover is present and the mean temperature is above 32 °F:

$$P_i = \begin{cases} 0.0 & \text{for } T_i \leq 32 \text{ }^\circ\text{F} \\ R_i & \text{for } T_i > 32 \text{ }^\circ\text{F}, \text{ } SNO_{i-1} = 0.0 \\ O_i - EMELT_i & \text{for } T_i > 32 \text{ }^\circ\text{F}, \text{ } SNO_{i-1} > 0.0 \end{cases} \quad (25)$$

where

$P_i$  = net rainfall and snowmelt available for runoff on day i, inches

$R_i$  = rainfall on day i, inches

$O_i$  = outflow from snow cover subject to runoff on day i, inches

$EMELT_i$  = evaporation of snowmelt on day i, inches

$SNO_{i-1}$  = water equivalence of snow cover at end of day i-1, inches

#### 4.2.1 Adjustment of Curve Number for Soil Moisture

The value of the retention parameter,  $S$ , for a given soil is assumed to vary with soil moisture as follows:

$$S = \begin{cases} S_{mx} \left[ 1 - \frac{SM - [(FC + WP)/2]}{UL - [(FC + WP)/2]} \right] & \text{for } SM > (FC + WP)/2 \\ S_{mx} & \text{for } SM \leq (FC + WP)/2 \end{cases} \quad (26)$$

where

$S_{mx}$  = maximum value of  $S$ , inches

$SM$  = soil water storage in the vegetative or evaporative zone, inches

$UL$  = soil water storage at saturation, inches

$FC$  = soil water storage at field capacity (the water remaining following gravity drainage in the absence of other losses), inches

$WP$  = soil water storage at wilting point (the lowest naturally occurring soil water storage), inches.

$S_{mx}$  is the retention parameter,  $S$ , for a dry condition. It is assumed that the soil water content midway between field capacity and wilting point is characteristic of being dry.

Since soil water is not distributed uniformly through the soil profile, and since the soil moisture near the surface influences infiltration more strongly than soil moisture

located elsewhere, the retention parameter is depth-weighted. The soil profile of the vegetative or evaporative zone depth is divided into seven segments. The thickness of the top segment is set at one thirty-sixth of the thickness of the vegetative or evaporative depth. The thickness of the second segment is set at five thirty-sixths of the thickness of the vegetative or evaporative zone depth. The thickness of each of the bottom five segments is set at one-sixth of the thickness of the vegetative or evaporative zone depth. The user-specified evaporative depth is the maximum depth from which moisture can be removed by evapotranspiration. This depth cannot exceed the depth to the top of the uppermost barrier soil layer. The depth-weighted retention parameter is computed using the following equation (Knisel, 1980):

$$S = \sum_{j=1}^7 W_j \cdot S_j \quad (27)$$

$$S_j = \begin{cases} S_{mx} \left[ 1 - \frac{SM_j - [(FC_j + WP_j)/2]}{UL_j - [(FC_j + WP_j)/2]} \right] & \text{for } SM_j > (FC_j + WP_j)/2 \\ S_{mx} & \text{for } SM_j \leq (FC_j + WP_j)/2 \end{cases} \quad (28)$$

where

- $W_j$  = weighting factor for segment j
- $SM_j$  = soil water storage in segment j, inches
- $UL_j$  = storage at saturation in segment j, inches
- $FC_j$  = storage at field capacity in segment j, inches
- $WP_j$  = storage at wilting point in segment j, inches

The weighting factors decrease with the depth of the segment in accordance with the following equation from the CREAMS model (Knisel, 1980):

$$W_j = 1.0159 \left[ e^{-4.16 \frac{D_j-1}{EZD}} - e^{-4.16 \frac{D_j}{EZD}} \right] \quad (29)$$

where

- $D_j$  = depth to bottom of segment j, inches

$EZD$  = vegetative or evaporative zone depth, inches

For the assumed segment thicknesses, this equation gives weighting factors of 0.111, 0.397, 0.254, 0.127, 0.063, 0.032 and 0.016 for segments 1 through 7. The top segment is the highest weighted in a relative sense since its thickness is 1/36 of the evaporative zone depth while the thickness of the second segment is 5/36 and the others are 1/6.

The runoff curve number required as input to the HELP program is that corresponding to antecedent moisture condition II (AMC-II) in the SCS method. AMC-II represents an average soil-moisture condition. The corresponding curve number is denoted  $CN_{II}$ . The HELP user can either input a value of  $CN_{II}$  directly; input a curve number and have the program adjust it for surface slope conditions; or have the program compute a value based on the vegetative cover type, the default soil type and surface slope conditions.

The value of the maximum moisture retention parameter,  $S_{mx}$ , is assumed to equal the value of  $S$  for a dry condition, antecedent moisture condition I (AMC-I) in the SCS method (USDA, SCS, 1985). It is assumed that the soil moisture content for this dry condition (a condition where the rainfall in the last five days totaled less than 0.5 inches without vegetation and 1.4 inches with vegetation) is midway between field capacity and wilting point.  $S_{mx}$  is related to the curve number for AMC-I,  $CN_I$ , as follows:

$$S_{mx} = \frac{1000}{CN_I} - 10 \quad (30)$$

$CN_I$  is related to  $CN_{II}$  by the following polynomial (Knisel, 1980):

$$CN_I = 3.751 \times 10^{-1} CN_{II} + 2.757 \times 10^{-3} CN_{II}^2 - 1.639 \times 10^{-5} CN_{II}^3 + 5.143 \times 10^{-7} CN_{II}^4 \quad (31)$$

#### 4.2.2 Computation of Default Curve Numbers

When the user requests the program to generate and use a default curve number, the program first computes the AMC-II curve number for the specified soil type and vegetation for a mild slope using the following equation:

$$CN_{II_o} = C_o + C_1 \cdot IR + C_2 \cdot IR^2 \quad (32)$$

where

- $CN_{II_0}$  = AMC-II curve number for mild slope (unadjusted for slope)
- $C_0$  = regression constant for a given level of vegetation
- $C_1$  = regression constant for a given level of vegetation
- $C_2$  = regression constant for a given level of vegetation
- $IR$  = infiltration correlation parameter for given soil type

The relationship between  $CN_{II_0}$ , the vegetative cover and default soil texture is shown graphically in Figure 8. Table 7 gives values of  $C_0$ ,  $C_1$  and  $C_2$  for the five types of vegetative cover built into the HELP program.

### 4.2.3 Adjustment of Curve Number for Surface Slope

A regression equation was developed to adjust the AMC-II curve number for surface slope conditions. The regression was developed based on kinematic wave theory where

TABLE 7. CONSTANTS FOR USE IN EQUATION 32

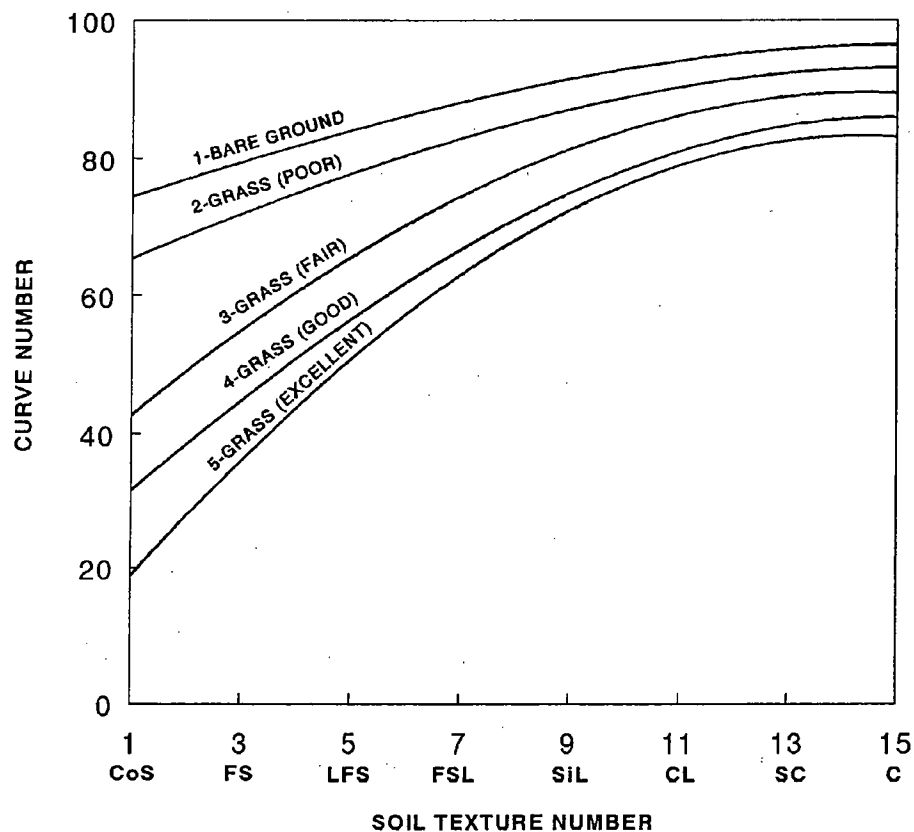


Figure 8. Relation between SCS Curve Number and Default Soil Texture Number for Various Levels of Vegetation

Vegetative Cover	$C_0$	$C_1$	$C_2$
Bare Ground	96.77	-20.80	-54.94
Poor Grass	93.51	-24.85	-71.92
Fair Grass	90.09	-23.73	-158.4
Good Grass	86.72	-43.38	-151.2
Excellent Grass	83.83	-26.91	-229.4

the travel time of runoff from the top of a slope to the bottom of the slope is computed as follows:

$$t_{run} = \frac{1.5}{(i - I)^{1/3}} \left( \frac{L^2}{S} \right)^{1/3} \left( \frac{1.49}{n} \right)^{-2/3} \quad (33)$$

where

- $t_{run}$  = runoff travel time (time of concentration), minutes
- $i$  = steady-state rainfall intensity (rate), inches/hour
- $I$  = steady-state infiltration rate, inches/hour
- $L$  = slope length, feet
- $S$  = surface slope, dimensionless
- $n$  = Manning's roughness coefficient, dimensionless

A decrease in travel time results in less infiltration because less time is available for infiltration to occur.

Using the KINEROS kinematic runoff and erosion model (Woolhiser, Smith, and Goodrich, 1990), hundreds of runoff estimates were generated using different combinations of soil texture class, level of vegetation, slope, slope length, and rainfall depth, duration and temporal distribution. Using these estimates, the curve number that would yield the estimated runoff was calculated from the rainfall depth and the runoff estimate. These curve numbers were regressed with the slope length, surface slope and the curve number that would be generated for the soil texture and level of vegetation placed at a mild slope. The four soil textures used included loamy sand, sandy loam, loam, and clayey loam as specified by saturated hydraulic conductivity, capillary drive, porosity, and maximum relative saturation. Two levels of vegetation were described--a

good stand of grass (bluegrass sod) and a poor stand of grass (clipped range). Slopes of 0.04, 0.10, 0.20, 0.35, and 0.50 ft/ft and slope lengths of 50, 100, 250, and 500 ft were used. Rainfalls of 1.1 inches, 1-hour duration and 2nd quartile Huff distribution and of 3.8 inches, 6-hour duration and balanced distribution were modeled.

The resulting regression equation used for adjusting the AMC-II curve number computed for default soils and vegetation placed at mild slopes,  $CN_{II_o}$ , is:

$$CN_{II} = 100 - (100 - CN_{II_o}) \cdot \left( \frac{L^{*2}}{S^*} \right) CN_{II_o}^{-0.81} \quad (34)$$

where

$L^*$  = standardized dimensionless length, (L/500 ft)

$S^*$  = standardized dimensionless slope, (S/0.04)

This same equation is used to adjust user-specified AMC-II curve numbers for surface slope conditions by substituting the user value for  $CN_{II_o}$  in Equation 34.

#### 4.2.4 Adjustment of Curve Number for Frozen Soil

When the HELP program predicts frozen conditions to exist, the value of  $CN_{II}$  is increased, resulting in a higher calculated runoff. Knisel et al. (1985) found that this type of curve number adjustment in the CREAMS model resulted in improved predictions of annual runoff for several test watersheds. If the  $CN_{II}$  for unfrozen soil is less than or equal to 80, the  $CN_{II}$  for frozen soil conditions is set at 95. When the unfrozen soil  $CN_{II}$  is greater than 80, the  $CN_{II}$  is reset to be 98 on days when the program has determined the soil to be frozen. This adjustment results in an increase in  $CN_I$  and consequently a decrease in  $S_{mx}$  and  $S'$  (Equations 19, 26, and 30).

From Equations 19 and 21, it is apparent that as  $S'$  approaches zero,  $Q$  approaches  $P$ . In other words, as  $S'$  decreases, the calculated runoff becomes closer to being equal to the net rainfall which is most often, when frozen soil conditions exist, predominantly snowmelt. This will result in a decrease in infiltration under frozen soil conditions, which has been observed in numerous studies.

#### 4.2.5 Summary of Daily Runoff Computation

The HELP model determines daily runoff by the following procedure:

- 1) Given  $CN_{II}$  from input or calculated by Equations 32 or 34,  $CN_I$  and  $S_{mx}$  are computed once using Equations 31 and 30, respectively.

- 2)  $S$  is computed daily using Equations 27 and 28.
- 3) The daily runoff resulting from the daily rainfall and snowmelt is computed using Equation 21.

### 4.3 PREDICTION OF FROZEN SOIL CONDITIONS

In cold regions, the effects of frozen soil on runoff and infiltration rates are significant. Because of the necessary complexity and the particular data requirements of any approach to estimating soil temperatures, the inclusion of a theoretically-based frozen soil model in the HELP program is prohibitive for the purposes of the program. However, for some regions, it is desirable to have some method for predicting the occurrence of frozen soil and the resulting increase in runoff.

Knisel et al. (1985) proposed a rather simple procedure for predicting the existence of frozen soils in the CREAMS model. A modification of that approach has been incorporated into HELP. In the HELP modification, the soil is assumed to enter a frozen state when the average temperature of the previous 30 days first drops below 32 °F. During the time in which the soil is considered to be frozen, the infiltration capacity of the soil is reduced by increasing the calculated runoff. As explained earlier, this is done by increasing the curve number. In addition, other processes are affected such as soil evaporation, vertical drainage in the evaporative zone and groundmelt of snow.

The point in which the soil is no longer considered to be frozen is determined by calculating the length of time required to thaw frozen soil; that is, the number of days in which the soil is to remain frozen after the daily mean air temperature first rises above freezing. The thaw period in days,  $DFS$ , is a constant for a particular set of climatic data. The thaw period increases with latitude and decreases with solar radiation in the winter at the site and is determined using the following relation.

$$DFS = 35.4 - 0.154 R_{S(Dec)} \quad (35)$$

where

$R_{S(Dec)}$  = estimate of the normal total solar radiation in December (June in the southern hemisphere) at the selected location, langley

$DFS$  = estimate of the number of days with mean temperatures above freezing in excess of days with mean temperatures below freezing required to thaw a frozen soil after a thaw is started

$R_{S(Dec)}$  is computed using the maximum daily potential solar radiation for the site in December,  $R_{So(Dec)}$ , (June in southern hemisphere) (Richardson and Wright, 1984) and the mean daily solar radiation for December (June in southern hemisphere) from the first year

of the user's input data file,  $R_{S(1st Dec)}$ . This estimate is used to provide consistency throughout the simulation and to limit the importance of the first year of solar radiation data.  $R_{S(Dec)}$  is computed as follows:

$$R_{S(Dec)} = 0.5 [R_{S(1st Dec)} + 0.75 \cdot R_{So(Dec)}] \quad (36)$$

where

$$R_{So(Dec)} = 711.38 DD [(H \sin |LAT| \sin SD) + (\sin H \cos |LAT| \cos SD)] \quad (37)$$

where

$R_{So(Dec)}$  = average daily potential solar radiation at site in December (June in the southern hemisphere), langley

$DD$  =  $1 + 0.0335 \sin [0.0172 (J + 88.2)]$

$J$  = Julian date, 350 for northern hemisphere and 167 for southern hemisphere

$XT$  =  $\arccos [(-\tan |LAT|) (\tan SD)]$

$LAT$  = latitude of site, radians

$SD$  =  $0.4102 \sin [0.0172 (J - 80.25)]$

In addition, a counter in the program keeps track of the number of days of below freezing (one is subtracted for each day down to a minimum of zero) or above freezing temperatures (one is added for each day up until a maximum of  $DFS$  is reached, at which point the soil becomes unfrozen) since the soil became frozen. When the soil freezes for the first time during the season, the counter is set to 0. When a thaw is completed, the counter is reset to  $(DFS + 2)/3$ , but not less than 3 unless greater than  $DFS$ . When the counter returns to 0, the soil is refrozen if the average temperature of the previous thirty days is below freezing. As such, the value of the counter also limits the occurrence of a refreeze after a thaw (i.e. the soil is prevented from refreezing immediately following a thaw when the previous 30-day average temperature may not yet have increased to above freezing) (Dozier, 1992).

#### 4.4 SNOW ACCUMULATION AND MELT

Studies have shown that the temperature at which precipitation is equally likely to be rain or snow is in the range of 32 to 36 °F. A delineation temperature of 32 °F is used in the HELP model, that is, when the daily mean temperature is below this value, the program stores precipitation on the surface as snow. Snowmelt is computed using a procedure patterned after portions of the SNOW-17 routine of the National Weather

Service River Forecast System (NWSRFS) Snow Accumulation and Ablation Model (Anderson, 1973). Using this approach, the melt process is divided into that which occurs during nonrain periods and that occurring during rainfall. Rain-on-snow melt is computed using an energy balance approach. To compute the nonrain melt, air temperature is used as an index to energy exchange across the snow-air interface. This is similar to the degree-day method of the Soil Conservation Service (used in Version 2), which uses air temperature as an index to snow cover outflow. The SNOW-17 model uses SI units in all calculations; therefore, the results are converted to English units for compatibility with other HELP routines.

#### 4.4.1 Nonrain Snowmelt

The nonrain snowmelt equation of the SNOW-17 model is computed using the following equation (Knisel, 1980):

$$M_i = \frac{1}{25.4} [ MF_i ( T_{c_i} - MBASE ) - \Delta S_i - F_{m_i} ] \quad (38)$$

where

- $M_i$  = surface melt discharged from the snow cover on day i, inches
- $MF_i$  = melt factor for day i, millimeters per °C
- $T_{c_i}$  = mean air temperature on day i, °C
- $MBASE$  = base temperature below which no melt is produced, 0 °C
- $\Delta S_i$  = change in storage of liquid water in the snow cover on day i, millimeters
- $F_{m_i}$  = portion of the surface melt refrozen during day i, millimeters

In the absence of rain,

$$O_i = M_i \quad (39)$$

where

- $O_i$  = outflow from snow cover on day i available for evaporation, runoff, and infiltration, inches

Unlike in version 2, the melt factor, MF, is not constant but varies seasonally due, in large part, to the seasonal variation in solar radiation. In most areas, the variation in the melt factor can be represented by a sine function and is expressed as:

$$MF_i = \left( \frac{MFMAX + MFMIN}{2} \right) + \left[ \left( \frac{MFMAX - MFMIN}{2} \right) \sin \left( \frac{2\pi n_i}{366} \right) \right] \quad (40)$$

where

*MFMAX* = the maximum melt factor, millimeters per day per °C.

*MFMIN* = the minimum melt factor, millimeters per day per °C.

$n_i$  = number of days since March 21 in northern hemisphere, or  
since September 21 in southern hemisphere

The maximum melt factor used in Version 3 is 5.2 mm/day-°C and is assumed to occur on June 21 in the northern hemisphere and on December 21 in the southern hemisphere. The minimum melt factor occurs on the reverse of the dates, and its value is 2.0 mm/day-°C. These melt factors are for open areas (Anderson, 1973). At latitudes greater than 50 degrees, the seasonal variation of the melt factor becomes less sinusoidal. Research has shown that at latitudes near 60 degrees the melt factor actually stays at its minimum value for most of the snow season. Therefore, for sites at latitudes above 50 degrees, an adjustment is made to  $MF_i$  to represent this gradually "flattening out" of the melt factor during the prolonged winter (Dozier, 1992).

#### 4.4.2 Rain-on-Snow Melt Condition

The rain-on-snow equation is an energy balance equation that makes use of the following assumptions:

- 1) solar (short-wave) radiation is neglected due to assumed overcast conditions.
- 2) the incoming long-wave radiation is equal to blackbody radiation at the temperature of the bottom of the cloud cover (assumed to be the mean air temperature).
- 3) a relative humidity of 90% is assumed.

The daily outflow from a snow cover available for runoff, infiltration and evaporation during a rain-on-snow occurrence may be calculated as the sum of the melt by based on air temperature, latent heat energy transfer based on vapor pressure differences, sensible heat transfer based on air temperature, and advected heat transfer from the mass of rain, less the surface melt that is refrozen by the cold snow cover or stored in the snow cover as a liquid. Taking these assumptions into account and assuming typical values for barometric pressure and wind function, the four energy transfer components and outflow from the snow cover are computed as follows:

$$O_i = \frac{1}{25.4} \left( \frac{Q_{n_i} + Q_{e_i} + Q_{h_i} + Q_{m_i}}{L_f} - F_{m_i} - \Delta S_i \right) \quad (41)$$

where

- $O_i$  = outflow from snow cover on day  $i$  available for evaporation, runoff, and infiltration, inches
- $Q_{n_i}$  = net long-wave radiation transfer on day  $i$ , langley
- $Q_{e_i}$  = latent heat energy transfer based on vapor pressure differences, langley
- $Q_{h_i}$  = latent heat energy transfer based on temperature differences, langley
- $Q_{m_i}$  = advected heat transfer from the mass of rain, langley
- $L_f$  = latent heat of fusion for water, 7.97 langley/millimeters
- $F_{m_i}$  = quantity of melt refrozen in snow cover on day  $i$ , millimeters
- $\Delta S_i$  = change in liquid storage in snow cover on day  $i$ , millimeters
- 25.4 = conversion from millimeters to inches

and

$$Q_{n_i} = 1.171 \times 10^{-7} [(T_{c_i} + 273)^4 - (T_s + 273)^4] \quad (42)$$

$$Q_{e_i} = L_s (e_a - e_s) f(u) \quad (43)$$

$$Q_{h_i} = L_s \gamma (T_{c_i} - T_s) f(u) \quad (44)$$

$$Q_{m_i} = c ROS_i T_{c_i} \quad (45)$$

$$f(u) = 0.262 + (0.0391 u) \quad (46)$$

$$e_{a_i} = 33.8639 RH [(0.00738 T_{c_i} + 0.8072)^8 - (0.000019) | 1.8 T_{c_i} + 48 | + 0.001316] \quad (47)$$

where

$T_{c_i}$  = mean air temperature on day  $i$ , °C

- $T_s$  = snow temperature,  $0^\circ\text{C}$   
 $L_s$  = latent heat of sublimation for snow, 67.7 langleys/millimeters  
 $e_a$  = vapor pressure of the atmosphere on day i, millibars (Linsley et al., 1982)  
 $e_s$  = vapor pressure of the snow cover on day i, 6.11 millibars  
 $f(u)$  = wind function, dimensionless  
 $u$  = wind speed, in kilometers/hour (average annual wind speed used in model)  
 $\gamma$  = psychometric constant, 0.68 millibars/ $^\circ\text{C}$   
 $c$  = specific heat of water, 0.1 langleys/millimeter- $^\circ\text{C}$   
 $ROS_i$  = rain on snow cover during day i, millimeters  
 $RH$  = relative humidity, 0.9

In addition to the surface melt due to heat exchange at the snow-air interface, a small amount of daily heat exchange occurs at the snow-soil interface. The soil heat exchange is not considered directly because the model does not include a soil temperature model. Therefore, this exchange is considered indirectly by the use of a constant daily groundmelt when the ground is not predicted to be frozen. This daily groundmelt,  $GM_i$ , for typical landfills with biological activity is estimated to be:

$$GM_i = \begin{cases} 0.2 \text{ inches} & \text{Nonfrozen soil conditions} \\ 0 & \text{Frozen soil conditions} \end{cases} \quad (48)$$

All groundmelt is assumed to infiltrate and is not subject to runoff or evaporation prior to infiltration. The groundmelt on day i may be limited by the quantity of snow available ( $SNO_{i-1}$  plus snowfall on day i).

#### 4.4.3 Snowmelt Summary

The SNOW-17 routine differs from the degree-day method in that it accounts for refreezing of melt water due to any heat deficit of the cover and also for the retention and transmission of liquid water in and through the cover. The liquid water in excess of that held within the snow cover becomes outflow or runoff from the snow cover. When rain-on-snow occurs, the quantity of rain is added to the surface melt, from which refreeze and retention in the snow cover may also occur. A positive value for  $\Delta S$  in Equations 38 and 41 indicates the amount of liquid water in storage within the snow

cover has increased. For further explanation concerning the calculation of  $\Delta S$  and  $F_m$  and the attenuation of excess liquid water, the user is referred to the SNOW-17 documentation (Anderson, 1973).

Naturally the amount of snowmelt is limited by the quantity of snow which is present. The order in which the HELP program determines the amount of snowmelt and remaining snow cover is as follows:

1. The amount of snow available for ablation (surface melt or evaporation) on day  $i$ ,  $AVLSNO_i$ , is determined, recognizing that surface melt occurs only at mean daily air temperatures above freezing and that groundmelt occurs only when the soil is not frozen:

$$AVLSNO_i = \begin{cases} SNO_{i-1} + PRE_i - GM_i & \text{for } T_{C_i} < 0^\circ C \\ SNO_{i-1} - GM_i & \text{for } T_{C_i} \geq 0^\circ C \end{cases} \quad (49)$$

where

$SNO_{i-1}$  = water storage in the snow cover at the end of day  $i-1$ , inches

$PRE_i$  = precipitation on day  $i$ , inches

2. The surface melt is calculated using Equations 38 or 41, but is limited to the quantity of available snow:

$$O_i = \begin{cases} 0 & \text{for } T_{F_i} < 32^\circ F \\ O_i \text{ from Equation 36} & \text{for } PRE_i = 0 \text{ and } T_{F_i} \geq 32^\circ F \\ O_i \text{ from Equation 38} & \text{for } PRE_i > 0 \text{ and } T_{F_i} \geq 32^\circ F \\ AVLSNO_i & \text{for } AVLSNO_i < O_i \text{ (Eq. 36 or 38)} \end{cases} \quad (50)$$

3. The quantity of snow remaining after considering all the types of melt is what is available for evaporation (See Surface Evaporation section).
4. The amount of water present in the snow cover at the end of day  $i$ ,  $SNO_i$ , is summed as follows:

$$SNO_i = \begin{cases} SNO_{i-1} + PRE_i - GM_i - ESNO_i & \text{for } T_{c_i} < 0^\circ\text{C} \\ SNO_{i-1} + PRE_i - GM_i - O_i - ESNO_i & \text{for } T_{c_i} \geq 0^\circ\text{C} \end{cases} \quad (51)$$

where

$ESNO_i$  = evaporation of snow in excess of surface melt,  $O_i$ , on day i, inches

#### 4.5 INTERCEPTION

Initially during a rainfall event, nearly all rainfall striking foliage is intercepted. However, the fraction of the rainfall intercepted decreases rapidly as the storage capacity of the foliage is reached. The limiting interception storage is approached only after considerable rainfall has reached the ground surface. This process is approximated by the equation:

$$INT_i = INT_{max_i} \left[ 1 - e^{-\left(\frac{R_i}{INT_{max_i}}\right)} \right] \quad (52)$$

where

$INT_i$  = interception of rainfall by vegetation on day i, inches

$INT_{max_i}$  = interception storage capacity of the vegetation on day i, inches

$R_i$  = rainfall on day i (not including rainfall on snow), inches

Although  $INT_{max}$  depends upon vegetation type, growth stage, and wind speed, the data of Horton (1919) and others indicate that 0.05 inches is a reasonable estimate of  $INT_{max}$  for a good stand of most types of non-woody vegetation. The HELP program relates  $INT_{max}$  to the above ground biomass of the vegetation,  $CV$ . This empirical relationship is:

$$INT_{max_i} = \begin{cases} 0.05 \left( \frac{CV_i}{14000} \right) & \text{for } CV_i < 14000 \\ 0.05 & \text{for } CV_i \geq 14000 \end{cases} \quad (53)$$

where  $CV_i$  is the above ground biomass on day i in kilograms per hectare.

## 4.6 POTENTIAL EVAPOTRANSPIRATION

The method used in the HELP program for computing evapotranspiration was patterned after the approach recommended by Ritchie (1972). This method uses the concept of potential evapotranspiration as the basis for prediction of the surface and soil water evaporation and the plant transpiration components. The term "potential evapotranspiration" refers to the maximum quantity of evaporation rate that the atmosphere may extract from a plot in a day. A modified Penman (1963) equation is used to calculate the energy available for evapotranspiration.

$$LE_i = PENR_i + PENA_i \quad (54)$$

where

$LE_i$  = energy available on day  $i$  for potential evapotranspiration in the absence of a snow cover, langley

$PENR_i$  = radiative component of the Penman equation on day  $i$ , langley

$PENA_i$  = aerodynamic component of the Penman equation on day  $i$ , langley

The first term of Equation 54 represents that portion of the available evaporative energy due to the radiation exchange between the sun and the earth. The second term expresses the influence of humidity and wind on  $LE$ . These two components are evaluated as follows:

$$PENR_i = \frac{\Delta_i}{(\Delta_i + \gamma)} R_{n_i} \quad (55)$$

$$PENA_i = \frac{15.36 \gamma}{(\Delta_i + \gamma)} (1 + 0.1488 u) (e_{o_i} - e_{a_i}) \quad (56)$$

where

$R_{n_i}$  = net radiation received by the surface on day  $i$ , langley

$\Delta_i$  = slope of the saturation vapor pressure curve at mean air temperature on day  $i$ , millibars per °C

$\gamma$  = constant of the wet and dry bulb psychrometer equation, assumed to be constant at 0.68 millibars per °C

- $u$  = wind speed at a height of 2 meters, in kilometers/hour (average annual wind speed used in model)
- $e_{o_i}$  = saturation vapor pressure at mean air temperature on day  $i$ , millibars (computed using Equation 47, where  $RH = 1$ )
- $e_{a_i}$  = mean vapor pressure of the atmosphere on day  $i$ , millibars (computed using Equation 47, where  $RH$  is the quarterly average dimensionless relative humidity on day  $i$  from the input data or on days with precipitation,  $RH = 1$ )

The value of  $\Delta_i$  is computed using an equation presented by Jensen (1973):

$$\Delta_i = 1.9993 [ (0.00738 T_{c_i} + 0.8072)^7 - 0.0005793 ] \quad (57)$$

where

$$T_{c_i} = \text{mean air temperature on day } i, \text{ } ^\circ\text{C}$$

The net solar radiation received by the earth's surface,  $R_{n_i}$ , is the difference between the total incoming and total outgoing radiation and is estimated as follows (Hillel, 1982; Jensen, 1973):

$$R_{n_i} = (1 - \alpha) R_{s_i} - R_{b_i} \quad (58)$$

where

- $R_{s_i}$  = incoming global (direct and sky) solar radiation on day  $i$ , langley
- $\alpha$  = albedo (reflectivity coefficient of the surface toward short-wave radiation,  $\alpha = 0.23$  when there is no snow present;  $\alpha = 0.6$  when a snow cover storing more than 5 mm of water exists)
- $R_{b_i}$  = the long-wave radiation flux from soil on day  $i$ , langley

$R_{b_i}$  decreases with increasing humidity and cloud cover and is calculated using the following equations (Jensen, 1973):

$$R_{b_i} = R_{b_{o_i}} \left[ a_i \left( \frac{R_{s_i}}{R_{s_{o_i}}} \right) - b_i \right] \quad (59)$$

where

$R_{bo_i}$  = the maximum outgoing long-wave radiation (assuming a clear day) for day i

$R_{so_i}$  = the maximum potential global solar radiation for day i

$a_i$  and  $b_i$  = coefficients which are dependent upon the humidity on day i

(for  $RH_i < 50\%$ ,  $a_i = 1.2$ ,  $b_i = 0.2$ ;

for  $50\% \leq RH_i < 75\%$ ,  $a_i = 1.1$ ,  $b_i = 0.1$ ; and

for  $RH_i \geq 75\%$ ,  $a_i = 1.0$ ,  $b_i = 0.0$ )

The outgoing long-wave radiation (heat loss) on a clear day,  $R_{bo}$ , is estimated as follows:

$$R_{bo_i} = 1.171 \times 10^{-7} (T_{c_i} + 273)^4 (0.39 - 0.05 \sqrt{e_{a_i}}) \quad (60)$$

The potential solar radiation for a given day,  $R_{so}$ , is calculated using a set of equations from the WGEN model (Richardson and Wright, 1984).

$$R_{so_i} = 711.38 DD_i [(H_i \sin |LAT| \sin SD_i) + (\sin H_i \cos |LAT| \cos SD_i)] \quad (61)$$

where

$LAT$  = latitude of the location, radians

$DD_i$  =  $1 + \{0.0335 \sin [0.0172 (J_i + 88.2)]\}$

$SD_i$  =  $0.4102 \sin [0.0172 (J_i - 80.25)]$

$H_i$  = arc cosine  $[(-\tan |LAT|) (\tan SD_i)]$

$J_i$  = the Julian date for day i in northern hemisphere and the Julian date minus 182.5 in the southern hemisphere (negative latitudes)

The potential evapotranspiration is determined by dividing the available energy, LE, by the latent heat of vaporization,  $L_v$  (or the latent heat of fusion,  $L_f$ , depending on the state of the evaporated water). The latent heat of vaporization is a function of the water temperature. In the HELP model, unless the evaporated water is snow or snowmelt, the mean daily temperature is used to estimate the water temperature and potential evapotranspiration is computed as:

where

$E_{o_i}$  = potential evapotranspiration on day i, in inches

$$E_{o_i} = \frac{LE_i}{25.4 L_v} \quad (62)$$

$$L_v = \begin{cases} 59.7 - 0.0564 T_{c_i} & \text{for water} \\ 67.67 - 0.0564 T_s & \text{for snow} \end{cases} \quad (63)$$

$L_v$  = latent heat of vaporization (for evaporating water) or latent heat of fusion (for evaporating snow), langleys per millimeters

$T_s$  = snow temperature, °C

25.4 = conversion from millimeters to inches

## 4.7 SURFACE EVAPORATION

### 4.7.1 No Snow Cover

The rate of evapotranspiration from a landfill cover is a function of solar radiation, temperature, humidity, vegetation type and growth stage, water retained on the surface, soil water content and other soil characteristics. Evapotranspiration has three components: evaporation of water or snow retained on foliage or on the landfill surface, evaporation from the soil and transpiration by plants. In the HELP program, the evapotranspiration demand is exerted first on water available at the landfill surface. This available surface water may be either rainfall intercepted by vegetation, ponded water, snowmelt or accumulated snow.

If there is no snow ( $SNO_{i-1} = 0$ ) on the surface at the start of the day and no snowfall ( $PRE_i = 0$  and  $T_{c_i} \leq 0^\circ\text{C}$ ) during the day or if there is no available snow ( $AVLSNO_i = 0$ ) and no outflow from the snow cover ( $O_i = 0$ ) on day  $i$ , the potential evapotranspiration ( $E_{o_i}$ ) is applied to any calculated interception ( $INT_i$ ) from rainfall for that day and, partially, to the ponded water. In this situation, the portion of the evaporative demand that is met by the evaporation of surface moisture on day  $i$  is given by

$$ESS_i = \begin{cases} E_{o_i} & \text{for } E_{o_i} \leq INT_i + PW_i(1 - PRF) \\ INT_i + PW_i(1 - PRF) & \text{for } E_{o_i} > INT_i + PW_i(1 - PRF) \end{cases} \quad (64)$$

where

$ESS_i$  = evaporation of surface moisture, inches

- $PW_i$  = water ponded on surface that is unable to run off and is in excess of infiltration capacity, inches
- $PRF$  = fraction of area where runoff can potentially occur

If the evaporative demand is less than the calculated interception, the amount of interception is adjusted to equal the evaporative potential.

$$INT_i = E_{o_i} \quad \text{for } E_{o_i} < INT_i \text{ from Equation 49} \quad (65)$$

#### 4.7.2 Snow Cover Present

If snow is present on the ground after calculating the melt for the day, the program computes an estimated dew-point temperature based on the mean daily temperature for the day,  $T_{c_i}$ , and the quarterly average humidity,  $RH_i$ , or the existence of precipitation; the dew-point temperature is assumed to equal to the mean daily temperature if precipitation occurred (assumes  $RH_i = 1$  if  $PRE_i > 0$ ). If the estimated dew-point temperature is greater than or equal to the temperature of the snow cover,  $T_s$ , then the evapotranspiration (evaporation of surface moisture, evaporation of soil moisture, and plant transpiration) is assigned to be zero.

$$ESS_i = 0 \quad \text{for } AVLSNO_i - O_i > 0 \text{ and } T_{d_i} \geq T_s \quad (66)$$

$$T_{d_i} = (112 - 0.9 T_{c_i}) RH_i^{1/8} + 0.1 T_{c_i} - 112 \quad (67)$$

where  $T_{d_i}$  is the estimated dew-point temperature in °C for day i.

If a snow cover existed at the start of the day after discounting the groundmelt ( $AVLSNO_i > 0$ ) and the estimated dew point is lower than the snow temperature, then evaporation of the surface melt available for outflow,  $O_i$ , from the snow cover is computed. If the potential evapotranspiration,  $E_{o_i}$ , exceeds the surface melt, then the excess evaporative demand is exerted on the snow cover. When evaporating snow or snowmelt, the estimation of the latent heat of vaporization,  $L_v$ , by Equation 63 is modified. The temperature of the water is estimated to be 0 °C instead of the mean daily air temperature,  $T_{c_i}$ . Therefore,  $L_v$  equals 59.7 langley per millimeter of snowmelt and 67.67 langley per millimeter of snow water.

Under the conditions just described ( $AVLSNO_i > 0$  and  $T_{d_i} < T_s$ ), the daily surface evaporation may consist of a portion of the available melt,  $O_i$ ; all of the melt and a portion of the snow,  $SNO_{i-1}$ ; or all of the melt and all of the snow. The following

procedure is then used for calculating surface evaporation:

1. For  $O_i > 0$ , the potential evaporative energy,  $LE_i$ , is reduced by the estimated amount of energy consumed by melting the snow. This lower potential is then exerted on the surface melt outflow. The portion of the surface melt that is evaporated is calculated as:

$$LE'_i = LE_i - 202.4 O_i \quad (68)$$

$$EMELT_i = \begin{cases} 0 & \text{for } LE'_i \leq 0 \\ \frac{LE'_i}{25.4 L_v} & \text{for } 0 < LE'_i < 25.4 L_v O_i \\ O_i & \text{for } LE'_i \geq 25.4 L_v O_i \end{cases} \quad (69)$$

where

$EMELT_i$  = surface melt that is evaporated on day i, inches

$LE'_i$  = potential evaporative energy discounted for surface melt on day i, langley

2. After allowing for the energy dissipated by the melting of snow at the surface and any evaporation of the melt, the remaining potential evaporative energy is computed as follows:

$$LE''_i = LE'_i - 25.4 L_v O_i \quad (70)$$

where

$LE''_i$  = potential evaporative energy discounted for surface melt and evaporation of surface melt on day i, langley

3. If there is energy available after any evaporation of surface melt ( $LE''_i > 0$ ), this remaining energy is applied to the snow cover. The amount of evaporated snow,  $ESNO_i$ , on day i is calculated as follows:
4. The total amount of evaporation of surface moisture,  $ESS_i$ , on day i is then calculated as the sum of the evaporated snow and evaporated outflow from the snow cover:

$$ESNO_i = \begin{cases} 0 & \text{for } LE''_i \leq 0 \\ \frac{LE''_i}{25.4 L_v} & \text{for } 0 < LE''_i < 25.4 L_v (AVLSNO_i - O_i) \\ AVLSNO_i - O_i & \text{for } LE''_i \geq 25.4 L_v (AVLSNO_i - O_i) \end{cases} \quad (71)$$

$$ESS_i = ESNO_i + EMELT_i \quad (72)$$

where  $ESS$ ,  $ESNO$ , and  $EMELT$  are water equivalent in inches.

#### 4.7.3 Remaining Evaporative Demand

The amount of energy remaining available to be applied to subsurface evapotranspiration (i.e., soil water evaporation and plant transpiration) is then the original potential evaporative energy less the energy dissipated in the melt of snow and evaporation of surface water. If snow was available for surface melt or evaporation ( $AVLSNO_i > 0$ ), the remaining energy for subsurface evapotranspiration is:

$$LE_{s_i} = LE_i - 25.4 (L_f O_i + L_v EMELT_i + L_v ESNO_i) \quad (73)$$

In the absence of a snow cover or snowfall ( $AVLSNO_i = 0$ ), the remaining energy for subsurface evapotranspiration is:

$$LE_{s_i} = LE_i - 25.4 L_v ESS_i \quad (74)$$

where  $LE_{s_i}$  is the energy available for potential evapotranspiration of soil water.

The potential evapotranspiration from the soil column in inches is a function of the energy available and the mean air temperature. The potential evapotranspiration from the soil is:

$$ETS_{o_i} = \frac{LE_{s_i}}{25.4 L_v} \quad (75)$$

where  $ETS_{o_i}$  is the potential evapotranspiration of soil water.

## 4.8 INFILTRATION

In the absence of a snow cover ( $AVLSNO_i = 0$ ), the infiltration is equal to the sum of rainfall (precipitation at temperatures  $> 0^\circ\text{C}$ ) and groundmelt less the sum of interception (evaporation of surface moisture) and runoff.

$$INF_i = PRE_i + GM_i - INT_i - Q_i \quad (76)$$

In the presence of a snow cover, the infiltration is equal to the sum of outflow from the snow cover and groundmelt less the sum of evaporation of the outflow from the snow cover and runoff.

$$INF_i = O_i + GM_i - EMELT_i - Q_i \quad (77)$$

where  $INF_i$  is the infiltration on day  $i$  in inches.

Since the runoff is computed using the total rainfall in Equation 21, it is possible for the sum of the runoff and interception to exceed rainfall. Therefore, when the sum of the runoff,  $Q_i$ , and interception,  $INT_i$ , exceeds the rainfall,  $PRE_i$ , the computed runoff is reduced by the excess and the infiltration is assigned the value of the groundmelt,  $GM_i$ . It is not possible for the sum of runoff and evaporation of the outflow from the snow cover to exceed the outflow from the snow cover because the evaporation of melt is subtracted from the outflow prior to computation of runoff by Equation 21.

#### 4.9 SOIL WATER EVAPORATION

When the soil is not frozen, any demand in excess of the available surface water is exerted on the soil column first through evaporation of soil water and then through plant transpiration. When the soil is considered frozen, the program assumes that no soil water evaporation or plant transpiration occurs.

The potential soil evaporation is estimated from the following equation based on the work of Penman (1963) when evaporation is not limited by the rate at which water can be transmitted to the surface:

$$ES_{o_i} = \frac{(PENR_i + K_{E_i} PENA_i) e^{(-0.000029 CV_i)}}{25.4 (59.7 - 0.0564 T_{c_i})} \quad (78)$$

where

- $ES_{o_i}$  = potential evaporation of soil water on day  $i$ , inches
- $PENR_i$  = radiative component of the Penman equation on day  $i$ , langley

- $PENA_i$  = aerodynamic component of the Penman equation on day i, langley  
 $CV_i$  = above ground biomass on day i, kg/ha  
 $T_{c_i}$  = mean air temperature on day i, °C  
 $K_{E_i}$  = fraction of aerodynamic component contributing to evaporation of soil water  
 =  $1 - 0.0000714 CV_i$ , but not less than 0

This equation assumes that an above ground biomass of 14,000 kg/ha or more defines a full cover canopy such that the effect of the wind and humidity term, PENA, is negligible in the potential soil evaporation equation.

As patterned after Ritchie (1972), evaporation of soil water occurs in two stages. Stage 1 evaporation demand is controlled only by the available energy, while stage 2 evaporation demand is limited by the rate at which water can be transmitted through the soil to the surface. In stage 1, the rate of evaporation is equal to the potential evaporation from the soil:

$$ESI_i = ES_{o_i} \quad (79)$$

where  $ESI_i$  is the stage 1 soil water evaporation rate on day i in inches.

Stage 1 soil water evaporation will continue to occur as long as the cumulative value of the soil water evaporation minus the infiltration is less than the upper limit for stage 1 evaporation. This limit represents the quantity of water that can be readily transmitted to the surface. Cumulative soil water depletion by soil water evaporation is computed as:

$$ESIT_i = \sum_{k=m}^i (ES_k - INF_k) \quad (80)$$

where

- $ESIT_i$  = cumulative soil water depletion on day i by soil water evaporation, inches  
 $ES_k$  = soil water evaporation on day k (computed by Equation 90), inches  
 $m$  = the last day when  $ESIT$  was equal to 0

The upper limit of stage 1 evaporation is (Knisel, 1980):

where

- $U$  = upper limit of stage 1 evaporation, inches

$$U = \frac{9}{25.4} (CON - 3)^{0.42} \quad (81)$$

$CON$  = evaporation coefficient (Equation 9), millimeters per day<sup>0.5</sup>

When  $ESIT_i$  is greater than  $U$ , stage 1 evaporation ceases and stage 2 evaporation begins. The following equation is used to compute the stage 2 evaporation rate Ritchie (1972).

$$ES2_i = \frac{1}{25.4} CON [t_i^{0.5} - (t_i - 1)^{0.5}] \quad (82)$$

where

$ES2_i$  = stage 2 soil water evaporation rate for day  $i$ , inches

$t_i$  = number of days since stage 1 evaporation ended

Since the daily total of surface and soil water evaporation cannot exceed the daily potential evaporative demand, the evaporation from the soil is limited by the amount of energy available after considering the evaporation of surface water,  $LE_{s_i}$ , (i.e., the actual evaporative demand from the soil on day  $i$ ,  $ESD_i$ , cannot exceed the potential evapotranspiration of soil water,  $ETS_{o_i}$ ). The following equation is used to determine the daily soil water evaporative demand:

$$ESD_i = \begin{cases} ES1_i & \text{for } ESIT_i < U \text{ and } ES1_i \leq ETS_{o_i} \\ ES2_i & \text{for } ESIT_i \geq U \text{ and } ES2_i \leq ETS_{o_i} \\ ETS_{o_i} & \text{for } ESIT_i < U \text{ and } ES1_i > ETS_{o_i} \\ ETS_{o_i} & \text{for } ESIT_i \geq U \text{ and } ES2_i > ETS_{o_i} \end{cases} \quad (83)$$

The soil water evaporative demand is then distributed to the soils near the surface, down to a maximum depth for soil water evaporation but not exceeding the evaporative zone depth. The maximum depth is a function of the capillarity of the material, increasing with smaller pore size. Pore size is related to the saturated hydraulic conductivity of a soil. Therefore, the following correlation was developed to estimate the maximum depth of soil water evaporation based on empirical observations:

where

$$SEDMX = 4.6068 \times 1.5952^{-\log_{10} K} \quad (84)$$

$K$  = saturated hydraulic conductivity in the evaporative zone, cm/sec

$SEDMX$  = estimated maximum depth of soil water evaporation, inches

Limits are placed on the depth of soil water evaporation as follows to confine the capillary rise to the zone where a significant upward moisture flux is likely to occur (in top 18 inches for sands and in the top 48 inches for clays):

$$SED = \begin{cases} EZD & \text{for } EZD \leq SEDMX \text{ and } EZD \leq 48 \\ 48 & \text{for } EZD \leq SEDMX \text{ and } EZD > 48 \\ SEDMX & \text{for } EZD > SEDMX \text{ and } 18 \leq SEDMX \leq 48 \\ 18 & \text{for } EZD > SEDMX \text{ and } SEDMX < 18 \\ 48 & \text{for } EZD > SEDMX \text{ and } SEDMX > 48 \end{cases} \quad (85)$$

where

$SED$  = depth of soil water evaporation, inches

$EZD$  = evaporative zone depth, inches

The soil water evaporation demand is distributed throughout the seven segments in the soil water evaporative depth,  $SED$ , by the following equation (Knisel, 1980):

$$ESD_i(j) = ESD_i \cdot W(j) \quad (86)$$

where

$ESD_i(j)$  = soil water evaporative demand on segment  $j$  on day  $i$ , inches

$W(j)$  = weighting factor for segment  $j$ , for  $j = 1$  to  $7$

$$W(j) = 1.0159 \left[ e^{-4.16 \frac{D_{j-1}}{SED}} - e^{-4.16 \frac{D_j}{SED}} \right] \quad \text{for } D \leq SED \quad (87)$$

where

$D_j$  = depth to bottom of segment  $j$ , inches; if  $D$  is greater than  $SED$ , then  $SED$  is substituted for  $D$  in Equation 87

#### 4.10 PLANT TRANSPIRATION

The potential plant transpiration,  $EP_o$ , is computed as follows when the mean daily temperature is above 32 °F and the soil is not frozen:

$$EP_{o_i} = \frac{LAI_i}{3} E_{o_i} \quad (88)$$

The actual plant transpiration demand equals the potential plant transpiration except when the daily total of the soil water evaporative demand and potential plant transpiration demand exceeds the potential evapotranspirative demand on the soil water for the day:

$$EPD_i = \begin{cases} EP_{o_i} & \text{for } EP_{o_i} + ES_i \leq ETS_{o_i} \\ ETS_{o_i} - ES_i & \text{for } EP_{o_i} + ES_i > ETS_{o_i} \end{cases} \quad (89)$$

where  $EPD_i$  is the actual plant transpiration demand in inches on day i.

The plant transpiration demand is distributed throughout the seven segments in the evaporative zone,  $EZD$ , by the following equation (Knisel, 1980):

$$EPD_i(j) = EPD_i \cdot W(j) \quad (90)$$

where

$EPD_i(j)$  = soil water evaporative demand on segment j on day i, inches

$W(j)$  = weighting factor for segment j, for j = 1 to 7

$$W_j = 1.0159 \left[ e^{-4.16 \frac{D_{j-1}}{EZD}} - e^{-4.16 \frac{D_j}{EZD}} \right] \quad \text{for } j = 1 \text{ to } 7 \quad (91)$$

where

$D_j$  = depth to bottom of segment j, inches

#### 4.11 EVAPOTRANSPIRATION

The actual subsurface evapotranspiration on day  $i$ ,  $ETS_i$ , is often less than the sum of the soil water evaporative demand on day  $i$ ,  $ESD_i$ , and the plant transpiration demand on day  $i$ ,  $EPD_i$ , due to a shortage of soil water. The segment demands are then exerted on the soil profile from the surface down. If there is inadequate water storage above the wilting point in the segment to meet the demand, the soil water evapotranspiration from the segment is limited to that storage and the excess (unsatisfied) demand is added to the demand on the next lower segment within the evaporative zone.

The soil water evaporation demand is exerted first from the surface down. The actual soil water evaporation from a segment is equal to the demand,  $ESD_i(j)$ , plus any excess demand,  $ESX(j)$ , but not greater than the available water,  $SM_j - WP_j$ . The soil water evaporation is

$$ES_i(j) = \begin{cases} ESD_i(j) + ESX(j) & \text{for } ESD_i + ESX(j) \leq SM(j) - WP(j) \\ SM(j) - WP(j) & \text{for } ESD_i + ESX(j) > SM(j) - WP(j) \end{cases} \quad (92)$$

$$ESX(j+1) = ESD_i(j) + ESX(j) - ES_i(j) \quad (93)$$

where

$ES_i(j)$  = soil water evaporation from segment  $j$  on day  $i$ , inches

The plant transpiration demand is exerted next from the surface down. The actual transpiration from a segment is equal to the demand,  $EPD_i(j)$ , plus any excess demand,  $EPX(j)$ , but not greater than the available water,  $AW_i(j)$ , after extracting the soil water evaporation. The plant transpiration from a segment is also limited to one quarter of the plant available water capacity plus the available drainable water.

$$EP_i(j) = \begin{cases} EPD_i(j) + EPX(j) & \text{for } EPD_i(j) + EPX(j) \leq AW_i(j) \\ & \& EPD_i(j) + EPX(j) \leq EPL_i(j) \\ AW_i(j) & \text{for } EPD_i(j) + EPX(j) > AW_i(j) \\ & \& AW_i(j) \leq EPL_i(j) \\ EPL_i(j) & \text{for } EPD_i(j) + EPX(j) > AW_i(j) \\ & \& AW_i(j) > EPL_i(j) \end{cases} \quad (94)$$

$$EPX(j+1) = EPD_i(j) + EPX(j) - EP_i(j) \quad (95)$$

$$AW_i(j) = SM_i(j) - [ES_i(j) + WP(j)] \quad (96)$$

$$EPL_i(j) = \begin{cases} 0.25 [FC(j) - WP(j)] & \text{for } SM_i(j) - ES_i(j) < FC(j) \\ \text{else} & \\ SM_i(j) - [ES_i(j) + FC(j)] + 0.25 [FC(j) - WP(j)] & \end{cases} \quad (97)$$

where

$EP_i(j)$  = plant transpiration from segment j on day i, inches

$EPL_i(j)$  = plant transpiration limit from segment j on day i, inches

$WP(j)$  = wilting point of segment j, inches

$FC(j)$  = field capacity of segment j, inches

The actual evapotranspiration from segment j on day i,  $ET_i(j)$ , is the sum of the soil water evaporation and the plant transpiration.

$$ET_i(j) = ES_i(j) + EP_i(j) \quad (98)$$

The water extraction profile agrees very well with profiles for permanent grasses measured by Saxton et al. (1971).

The total subsurface evapotranspiration on day i,  $ETS_i$ , is the sum of the evapotranspiration from the top seven segments, the evaporative zone.

$$ETS_i = \sum_{j=1}^7 ET(j) \quad (99)$$

The total evapotranspiration on day i,  $ET_i$ , is the sum of the subsurface evapotranspiration and the surface evaporation.

$$ET_i = ETS_i + ESS_i \quad (100)$$

## 4.12 VEGETATIVE GROWTH

The HELP program accounts for seasonal variation in leaf area index through a general vegetative growth model. This model was extracted from the SWRRB program (Simulator for Water Resources in Rural Basins) developed by the USDA Agricultural Research Service (Arnold et al., 1989). The vegetative growth model computes daily values of total and active above ground biomass based on the maximum leaf area index value input by the user, daily temperature and solar radiation data, mean monthly temperatures and the beginning and ending dates of the growing season. The maximum value of leaf area index depends on the type of vegetation and the quality of the vegetative stand. The program supplies typical values for selected covers; these range from 0 for bare ground to 5.0 for an excellent stand of grass. The default weather data files contain normal mean monthly temperatures and beginning and ending dates of the growing season for 183 locations in the United States.

The vegetative growth model assumes that the vegetative species are perennial and that the vegetation is not harvested. Phenological development of the vegetation is based on the cumulative heat units during the growing season. Vegetative growth starts at the beginning of the growing season and continues during the first 75 percent of the growing season. Growth occurs only when the daily temperature is above the base temperature, assumed to be 0 °C for winter tolerant crops and mixtures of perennial grasses. The heat units for a day is computed as follows.

$$HU_i = T_{c_i} - T_b \quad (101)$$

where

$HU_i$  = heat units on day i, °C-days

$T_b$  = base temperature for plants, 5 °C

The fraction of the growing season that has occurred by day i is equal to the heat unit index on day i. It is computed as follows.

$$HUI_i = \sum_{k=m}^i \frac{HU_k}{PHU} \quad \text{for } m \leq i \leq n, \text{ else } HUI_i = 0 \quad (102)$$

$$PHU = \sum_{k=m}^n HU_k \quad (103)$$

where

$HUI_i$  = heat unit index or fraction of the growing season on day i,  
dimensionless

- $PHU$  = potential heat units in normal growing season, °C-days  
 $m$  = Julian date of start of growing season  
 $n$  = Julian date of end of growing season

The daily mean temperature is assumed to vary harmonically as follows for computing  $PHU$ :

$$T_{c_k} = \overline{TM} + 0.5 (TM_{max} - TM_{min}) \cos \left( 2\pi \frac{k - 200}{365} \right) \quad (104)$$

where

- $T_{c_k}$  = estimate of normal mean daily temperature on day k, °C  
 $\overline{TM}$  = mean of the 12 normal mean monthly temperatures, °C  
 $TM_{max}$  = maximum of the 12 normal mean monthly temperatures, °C  
 $TM_{min}$  = minimum of the 12 normal mean monthly temperatures, °C

The potential increase in biomass for a day is a function of the interception of radiation energy. The photosynthetic active radiation is estimated as follows.

$$PAR_i = 0.02092 R_{s_i} \{ 1 - \exp[-0.65(LAI_{i-1} + 0.05)] \} \quad (105)$$

where

- $PAR_i$  = photosynthetic active radiation, MJ/m<sup>2</sup>  
 $R_{s_i}$  = global solar radiation, langley  
 $LAI_{i-1}$  = leaf area index of active biomass at end of day i-1, dimensionless

The leaf area index on day i,  $LAI_i$ , is given by the equation

$$LAI_i = \begin{cases} 0 & HUI_i = 0 \\ \frac{(LAI_{mx})(WLV_i)}{WLV_i + 13360 \exp(-0.000608 WLV_i)} & 0 < HUI_i \leq 0.75 \\ 16 (LAI_{0.75}) (1 - HUI_i)^2 & HUI_i > 0.75 \end{cases} \quad (106)$$

where

$LAI_{mx}$  = maximum leaf area index from input, dimensionless

$WLV_i$  = active above-ground biomass on day i, kg/ha

$LAI_d$  = LAI value on day d, (# is the day when vegetation starts declining as estimated as the day when  $HUI_i = 0.75$ ), dimensionless

The potential increase in biomass during the growing season is

$$DDM_{o_i} = BE \cdot PAR_i \quad (107)$$

where

$DDM_{o_i}$  = potential increase in total biomass on day i, kg/ha

$BE$  = conversion from energy to biomass, 35 kg m<sup>2</sup>/ha MJ

The actual increase in biomass may be regulated by water or temperature stress.

$$DDM_i = REG_i \cdot DDM_{o_i} \quad (108)$$

$$REG_i = \min(WS_i, TS_i) \quad (109)$$

where

$DDM_i$  = actual daily increase in total biomass (dry matter) on day i during first 75% of growing season, kg/ha

$REG$  = minimum stress factor for growth regulation (smaller of water stress factor,  $WS_i$ , and temperature stress factors,  $TS_i$ ), dimensionless

The water stress factor,  $WS_i$ , is the ratio of the actual transpiration to plant transpiration demand.

$$WS_i = \frac{\sum_{j=1}^7 EP_i(j)}{\sum_{j=1}^7 EPD_i(j)} \quad (110)$$

The temperature stress factor,  $TS_i$ , is given by the equation

$$TS_i = \begin{cases} 0 & \text{for } T_{c_i} \leq Tb \\ \exp \left[ \delta \left( \frac{To - T_{c_i}}{T_{c_i} - Tb} \right)^2 \right] & \text{for } Tb < T_{c_i} < To \\ \exp \left[ \delta \left( \frac{To - T_{c_i}}{2To - (Tb + T_{c_i})} \right)^2 \right] & \text{for } T_{c_i} \geq To \end{cases} \quad (111)$$

$$\delta = \frac{\ln(0.9)}{\left\{ \frac{To - [(To + Tb)/2]}{(To + Tb)/2} \right\}^2} \quad (112)$$

where

$Tb$  = base temperature for mixture of perennial winter and summer grasses, 5 °C

$To$  = optimal temperature for mixture of perennial winter and summer grasses, 25 °C

As an additional constraint, the temperature stress factor is set equal to zero (and therefore growth ceases) when the daily mean temperature is more than 10 °C below the average annual temperature.

$$TS_i = 0 \quad \text{when } T_{c_i} < (\overline{TM} - 10 \text{ °C}) \quad (113)$$

The active live biomass is

$$DM_i = \begin{cases} 0 & \text{for } HUI_i = 0 \\ \sum_{k=m}^i DDM_k & \text{for } 0 < HUI_i \leq 0.75 \\ 8 DM_d (1 - HUI_i)^2 & \text{for } HUI_i > 0.75 \end{cases} \quad (114)$$

where

$DM_i$  = total active live biomass (dry matter) on day  $i$ , kg/ha

$DM_d$  = total active live biomass (dry matter) on day d (when  $HUI_i = 0.75$ ),  
kg/ha

The root mass fraction of the total active biomass is a function of the heat unit index where the fraction is greatest at the start of the growing season and decreases throughout the season.

$$RF_i = (0.4 - 0.2 HUI_i) \quad (115)$$

where

$RF_i$  = fraction of total active biomass partitioned to root system on day i,  
dimensionless

The above ground photosynthetic active biomass is computed as follows:

$$WLV_i = DM_i (1.0 - RF_i) \quad (116)$$

where

$WLV_i$  = active above-ground biomass on day i, kg/ha

The program also accounts for plant residue (inactive biomass) in addition to active biomass because inactive biomass also provides shading of the surface and reduces evaporation of soil water. Plant residue is predicted to decay throughout the year as a function of temperature and soil moisture. Plant residue is formed as the active plants go into decline and at the end of the growing season. The decrease in active biomass during the last quarter of the growing season is added to the plant residue. Similarly, at the end of the growing season the active biomass is also added to the plant residue or photosynthetic inactive biomass.

$$RSD_i = \begin{cases} RSD_{i-1} (1.0 - DECR_i) & \text{for } i \leq d \text{ or } i > n+1 \\ (RSD_{i-1} + DM_{i-1} - DM_i) (1.0 - DECR_i) & \text{for } d < i \leq n \\ (RSD_{i-1} + DM_{i-1}) (1.0 - DECR_i) & \text{for } i = n+1 \end{cases} \quad (117)$$

where

$RSD_n$  = plant biomass residue on day i, kg/ha

$DECR_i$  = biomass residue decay rate on day i, dimensionless

The plant residue decay rate decreases with moisture contents below field capacity in the evaporative zone, becoming zero at the wilting point. Similarly, the decay rate decreases as the soil temperature at the bottom of the evaporative zone falls below 35 °C and becomes very slow at temperatures below 10 °C, approaching a rate of 0.005. The maximum rate is 0.05. The decay rate is

$$DEC R_i = 0.05 [\min (CDG_i, SUT_i)] \quad (118)$$

where

$SUT_i$  = soil moisture factor on plant residue decay, dimensionless

$CDG_i$  = soil temperature factor on plant residue decay, dimensionless

The soil moisture factor on plant residue decay is computed as follows:

$$SUT_i = \begin{cases} 1.0 & \text{for } \sum_{j=1}^7 SM_i(j) \geq \sum_{j=1}^7 FC(j) \\ \frac{\sum_{j=1}^7 [SM_i(j) - WP(j)]}{\sum_{j=1}^7 [FC(j) - WP(j)]} & \text{for } \sum_{j=1}^7 SM_i(j) < \sum_{j=1}^7 FC(j) \end{cases} \quad (119)$$

The soil temperature factor on plant residue decay is computed as follows:

$$CDG_i = 0.1 + \frac{0.9 ST_i(7)}{ST_i(7) + \exp [9.93 - 0.312 ST_i(7)]} \quad (120)$$

where

$TS_i(7)$  = soil temperature at bottom of evaporative zone (segment 7), °C

The soil temperature is computed in the manner presented in the SWRRB model (Arnold et al., 1989). The long-term average surface soil temperature is the same as the long-term average air temperature. Changes in temperatures below the surface are dampened by the depth below the surface. The average annual soil temperature is constant throughout the depth, but the difference between the maximum soil temperature and the minimum soil temperature in a year decreases with increasing depth. In addition, the change in the surface soil temperature from day to day is reduced by total above ground biomass (active and inactive) and snow cover.

The total above ground biomass is the sum of the above ground active biomass and the plant residue. This total is used to compute soil temperature for plant decay rate, evaporation of soil water, and interception.

$$CV_i = WLVI_i + RSD_i \quad (121)$$

where

$$CV_i = \text{total above ground biomass on day } i, \text{ kg/ha}$$

When the normal daily mean temperature is greater than 10 °C all year round, the model assumes that grasses can grow all year. As such, there is no longer a winter dormant period when the active biomass decreases to zero. Therefore, the model assumes that biomass also decays all year in proportion to the quantity of biomass present. Assuming that 20 percent of the biomass is in the root system, the above ground active biomass is computed as follows:

$$WLVI_i = 0.8 BE \cdot PAR_i \cdot REG_i + WLVI_{i-1} (1.0 - DECR_i) \quad (122)$$

The growth and decay terms are computed the same as given in Equations 105, 107, 109, 116, and 118. The leaf area index is computed using  $WLVI_i$  from Equation 122 in Equation 106.

#### 4.13 SUBSURFACE WATER ROUTING

The subsurface water routing proceeds one subprofile at a time, from top to bottom. Water is routed downward from one segment to the next using a storage routing procedure, with storage evaluated at the mid-point of each time step. Mid-point routing provides an accurate and efficient simulation of simultaneous incoming and outgoing drainage processes, where the drainage is a function of the average storage during the time step. Mid-point routing tends to produce relatively smooth, gradual changes in flow conditions, avoiding the more abrupt changes that result from applying the full amount of moisture to a segment at the beginning of the time step. The process is smoothed further by using time steps that are shorter than the period of interest.

Mid-point routing is based on the following equation of continuity for a segment:

$$\begin{aligned} \Delta \text{ Storage} &= \text{Drainage In} - \text{Drainage Out} - \text{Evapotranspiration} \\ &+ \text{Leachate Recirculation} + \text{Subsurface Inflow} \end{aligned} \quad (123)$$

$$\begin{aligned} \Delta SM(j) = 0.5 \{ [DR_i(j) + DR_{i-1}(j)] - [DR_i(j+1) + DR_{i-1}(j+1)] \\ - [ET_i(j) + ET_{i-1}(j)] + [RC_i(j) + RC_{i-1}(j)] \\ + [SI_i(j) + SI_{i-1}(j)] \} \end{aligned} \quad (124)$$

$$\Delta SM(j) = SM_i(j) - SM_{i-1}(j) \quad (125)$$

where

$\Delta SM(j)$  = change in storage in segment j, inches

$DR_i(j)$  = drainage into segment j from above during time step i, inches

$SM_i(j)$  = soil water storage of segment j at the mid-point of time step i, inches

$ET_i(j)$  = evapotranspiration from segment j during time step i, inches

$RC_i(j)$  = lateral drainage recirculated into segment j during time step i, inches

$SI_i(j)$  = subsurface inflow into segment j during time step i, inches

Note that segments are numbered from top to bottom and therefore the drainage into segment j+1 from above equals the drainage out of segment j through its lower boundary. This routing is applied to all segments except liners and the segment directly above liners. Drainage into the top segment of the top subprofile is equal to the infiltration from the surface; drainage into the top segment of other subprofiles is equal to the leakage through the liner directly above the subprofile. Water is routed for a whole day in a subprofile before routing water in the next subprofile. The leakage from a subprofile for each time step during the day is totalled and then uniformly distributed throughout the day as inflow into the next subprofile.

The only unknown terms in the water routing equation are  $SM_i(j)$  and  $DR_i(j+1)$ ; all other terms have been computed previously or assigned during input. Subsurface inflow is specified during input. Infiltration and evapotranspiration are computed for the day before performing subsurface water routing for the day. Leachate recirculation is known from the calculated lateral drainage for the previous day. The drainage into a segment is known from the calculation of drainage out of the previous segment or from the computation of leakage from the previous subprofile. The two unknowns are solved simultaneously using the continuity and unsaturated drainage equations.

The number of time steps in a day can vary from subprofile to subprofile. A minimum of 4 time steps per day and a maximum of 48 time steps per day can be used. The number of time steps for each subprofile is computed as a function of the design of

the lateral drainage layer in the subprofile and the potential impingement into the lateral drainage layer. The time step is sized to insure that the lateral drainage layer, when initially wetted to field capacity, cannot be saturated in a single time step even in the absence of drainage from the layer.

$$\Delta t = \frac{T(k) [POR(k) - FC(k)]}{IR_{max}} \quad (126)$$

$$N = \begin{cases} 4 & \text{for } \Delta t > 0.25 \text{ days} \\ \text{int} \left( \frac{1}{\Delta t} + 1 \right) & \text{for } 0.021 \text{ days} \leq \Delta t \leq 0.25 \text{ days} \\ 48 & \text{for } \Delta t < 0.021 \text{ days} \end{cases} \quad (127)$$

where

$\Delta t$  = maximum size of time step, days

$T(k)$  = thickness of lateral drainage layer k, inches

$POR(k)$  = porosity of layer k, vol/vol

$FC(k)$  = field capacity of layer k, vol/vol

$IR_{max}$  = maximum impingement rate into lateral drainage layer, inches/day

$N$  = number of time steps per day, dimensionless

The maximum impingement rate is the lowest saturated hydraulic conductivity of the subprofile layers above the liner, but not greater than maximum daily infiltration (estimated to be about 10 inches/day).

Drainage out of the bottom segment above the liner of a subprofile is the sum of lateral drainage, if a lateral drainage layer, and the leakage or percolation from the segment or the liner of the subprofile. Drainage from this segment is also a function of the soil moisture content of the segment. The soil moisture content, lateral drainage and leakage are solved simultaneously using continuity, lateral drainage and percolation/leakage equations.

The water routing routine does not consider the storage capacity of the lower segments when computing the drainage out of a segment. Therefore, the routine may route more water down than the lower segments can hold and drain. Any water in excess of the storage capacity of a segment (porosity) is routed back up the profile into the segment above the saturated segment. In this way, the water contents of segments are corrected by backing water up from the bottom to the top, saturating segments as the corrections are made. If the entire top subprofile becomes saturated or if water is routed

back to the surface, the excess water is added to the runoff for the day. If runoff is restricted, the excess water is ponded on the surface and subjected to evaporation and infiltration during the next time step.

#### 4.14 VERTICAL DRAINAGE

The rate at which water moves through a porous medium as a saturated flow governed by gravity forces is given by Darcy's law:

$$q = K i = K \frac{dh}{dl} \quad (128)$$

where

- $q$  = rate of flow (discharge per unit time per unit area normal to the direction of flow), inches/day
- $K$  = hydraulic conductivity, inches/day
- $i$  = hydraulic head gradient, dimensionless
- $h$  = piezometric head (elevation plus pressure head), inches
- $l$  = length in the direction of flow, inches

This equation is also applicable to unsaturated conditions provided that the hydraulic conductivity is considered a function of soil moisture and that the piezometric head includes suction head.

The HELP program assumes pressure head (including suction) to be constant within each segment of vertical percolation and lateral drainage layers. This assumption is reasonable at moisture contents above field capacity (moisture contents where drainage principally occurs). In circumstances where a layer restricts vertical drainage and head builds up on top of the surface of the layer, as with barrier soil liners and some low permeability vertical percolation layers, the program assumes the pressure head is uniformly dissipated in the low permeability segment. For a given time step these assumptions yield a constant head gradient throughout the thickness of the segment. For vertical percolation layers with constant pressure, the piezometric head gradient in the direction of flow is unity, and the rate of flow equals the hydraulic conductivity:

$$i = \frac{dh}{dl} = 1 \quad (129)$$

$$q = K \quad (130)$$

For low permeability vertical percolation layers and soil liners, the hydraulic head gradient is

$$i = \frac{dh}{dl} = \frac{h_w + l}{l} \quad (131)$$

where

$$h_w = \text{pressure head on top of layer, inches}$$

The unsaturated hydraulic conductivity is estimated by Campbell's equation (Equation 5). Multiplying the water content terms ( $\theta$ ,  $\theta_r$ , and  $\phi$ ) in Equation 5 by the segment thickness yields an equivalent equation with the water content terms expressed in terms of length:

$$K = K_s \left( \frac{SM - RS}{UL - RS} \right)^{3 + \frac{2}{\lambda}} \quad (132)$$

Here,  $SM$ ,  $RS$ , and  $UL$  represent the soil water content ( $\theta$ ), residual soil water content ( $\theta_r$ ), and saturated soil water content ( $\phi$ ) of the segment, each expressed as a depth of water in inches. The HELP program uses Equation 132 to compute unsaturated hydraulic conductivity.

Based on Equations 130 and 132, the drainage from segment  $j$  during the time step  $i$ ,  $DR_i(j+1)$ , is as follows:

$$DR_i(j+1) = K_s(j) \cdot i \cdot DT \left[ \frac{SM_i(j) - RS(j)}{UL(j) - RS(j)} \right]^{3 + \frac{2}{\lambda(j)}} \quad (133)$$

where

$$K_s(j) = \text{saturated hydraulic conductivity of segment } j, \text{ inches/day}$$

$$DT = \text{the time step size, days}$$

$$= 1 / N$$

Rearranging Equation 133 to solve for  $SM_i(j)$  and substituting it into Equation 124 for  $SM_i(j)$  yields the following non-linear equation for the remaining unknown,  $DR_i(j+1)$ :

$$\begin{aligned}
DR_i(j+1) = & - 2 [UL(j) - RS(j)] \left[ \frac{DR_i(j+1)}{K_s(j) i DT} \right]^{\frac{\lambda_j}{3\lambda_j+2}} \\
& + 2 [SM_{i-1}(j) - RS(j)] + DR_{i-1}(j) + DR_i(j) - DR_{i-1}(j+1) \\
& - ET_{i-1}(j) - ET_i(j) + RC_{i-1}(j) + RC_i(j) + SI_{i-1}(j) + SI_i(j)
\end{aligned} \tag{134}$$

The HELP program solves this equation for  $DR_i(j+1)$  iteratively using  $DR_{i-1}(j+1)$  as its initial guess in the right hand side of Equation 134. If the computed value of  $DR_i(j+1)$  is within 0.3 percent of the guess or 0.1 percent of the storage capacity of segment  $j$ , the computed value is accepted; else, a new guess is made and the process is repeated until the convergence criteria are satisfied. After  $DR_i(j+1)$  is computed, the program computes  $SM_i(j)$  using Equation 124. Constraints are placed on the solution of  $DR_i(j+1)$  and  $SM_i(j)$  so as to maintain these parameters within their physical ranges; 0 to  $K_s DT$  for  $DR_i(j+1)$ , and  $WP(j)$  to  $UL(j)$  for  $SM_i(j)$ .

#### 4.15 SOIL LINER PERCOLATION

The rate of percolation through soil liners depend on the thickness of the saturated material directly above it. The depth of this saturated zone is termed the hydraulic (pressure) head on the soil liner. The average head on the liner is a function of the thicknesses of all segments that are saturated directly above the liner and the moisture content of first unsaturated segment above the liner. The average head on the entire surface of the liner is computed using the following equation:

$$h_w(k)_i = \begin{cases} TS(m) \cdot \frac{SM_i(m) - FC(m)}{UL(m) - FC(m)} + \sum_{j=m+1}^n TS(j) \\ \text{for } SM_i(m) > FC(m) \text{ else} \\ \sum_{j=m+1}^n TS(j) \end{cases} \tag{135}$$

where

- $h_w(k)_i$  = average hydraulic head on liner  $k$  during time step  $i$ , inches
- $TS(j)$  = thickness of segment  $j$ , inches
- $m$  = number of the lowest unsaturated segment in subprofile  $k$
- $n$  = number of the segment directly above the soil liner in subprofile  $k$

The percolation rate through a liner soil layer is computed using Darcy's law, as given in Equation 128. As presented in Equation 131, the vertical hydraulic gradient through the soil liner, segment  $n+1$ , is

$$\frac{dh}{dl} = \frac{h_w(k) + TS(n+1)}{TS(n+1)} \quad (136)$$

The HELP program assumes that soil liner remains saturated at all times. Percolation is predicted to occur only when there is a positive hydraulic head on top of the liner; therefore, the percolation rate through a soil liner is

$$q_p(k)_i = \begin{cases} 0 & \text{for } h_w(k)_i = 0 \\ K_s(n+1) \frac{h_w(k)_i + TS(n+1)}{TS(n+1)} & \text{for } h_w(k)_i > 0 \end{cases} \quad (137)$$

where

$q_p(k)_i$  = percolation rate from subprofile  $k$  during time step  $i$ , inches/day

#### 4.16 GEOMEMBRANE LINER LEAKAGE

In Version 3 of the HELP program geomembrane liners are identified as individual layers in the landfill profile. The geomembranes can be used alone as a liner or in conjunction with low permeability soil to form a composite liner. The soil would be defined as a soil liner in a separate layer. The program permits the membrane to be above, below or between high, medium or low permeability soils. Leakage is calculated for intact sections of geomembrane and for sections with pinholes or installation defects.

Giroud and Bonaparte (1989) defined composite liners as a low permeability soil liner covered with a geomembrane. However, composite liner design schemes can include various combinations of geomembranes, geotextiles, and soil layers. Therefore, in this section a composite liner is defined to be a liner system composed of one or more geomembranes and a low permeability soil, possibly separated by a geotextile. The HELP program defines a geomembrane as a thin "impervious" sheet of plastic or rubber used as a liquid barrier. Geotextiles are defined as flexible, porous fabrics of synthetic fibers used for cushioning, separation, reinforcement, and filtration.

The geomembrane component of a composite liner virtually eliminates leakage except in the area of defects, punctures, tears, cracks and bad seams. The low permeability soil component increases the breakthrough time and provides physical strength. In contact with a geomembrane the low permeability soil decreases the rate of leakage through the

hole in the geomembrane. As such, the two components of a composite liner complement each other. Geomembrane and soil liners also have complimentary physical and chemical endurance properties.

Giroud and Bonaparte (1989) provided a detailed summary of procedures for calculating leakage through composite liners. Methods described in this section were derived from Giroud and Bonaparte's work, summarizing also the work of Brown et al. (1987), Jayawickrama et al. (1988) and Fukuoka (1985, 1986). In these procedures Giroud and Bonaparte (1989) assumed that the hydraulic head acting on the landfill liners and the depth of liquid on these liners are equivalent since the effects of velocity head are relatively small for landfill liners.

#### 4.16.1 Vapor Diffusion Through Intact Geomembranes

Intact geomembranes are liners or sections of liners without any manufacturing or installation defects, that is without any holes. Since the voids between the molecular chains of geomembrane polymers are extremely narrow, leakage through intact geomembranes is likely only at the molecular level, regardless of whether transport is caused by liquid or vapor pressure differences. Therefore, transport of liquids through intact sections of composite liners is controlled by the rate of water vapor transport through the geomembrane. The hydraulic conductivities of the adjacent soil layers are much higher than the permeability of the geomembrane and therefore do not affect the leakage through intact sections of geomembranes.

A combination of Fick's and Darcy's laws results in a relationship between geomembrane water vapor diffusion coefficient, obtained from water vapor transmission tests, and "equivalent geomembrane hydraulic conductivity". Giroud and Bonaparte (1989) recommended using the term "equivalent hydraulic conductivity" since water transport through intact geomembranes is not described truly by Darcy's law for transport through porous media. The following equation for water transport through intact geomembranes was developed by substituting this relationship into Fick's law:

$$WVT = \text{diffusivity} \cdot \Delta p = \frac{\text{permeability} \cdot \Delta p}{T_g} \quad \text{Fick's law} \quad (138)$$

$$q_L = \frac{WVT}{\rho} = K_s \frac{\Delta h}{T_g} \quad \text{Darcy's law} \quad (139)$$

where

$WVT$  = water vapor transmission, g/cm<sup>2</sup>-sec

$\Delta p$  = vapor pressure difference, mm Hg

- $T_g$  = thickness of geomembrane, cm  
 $q_L$  = geomembrane leakage rate, cm/sec  
 $\rho$  = density of water, g/cm<sup>3</sup>  
 $K_g$  = equivalent saturated hydraulic conductivity of geomembrane, cm/sec  
 $\Delta h$  = hydraulic head difference, cm H<sub>2</sub>O

Expressing  $\Delta p$  in terms of hydraulic head,  $\Delta h$ , diffusivity (also known as permeance or coefficient of diffusion) and hydraulic conductivity are related as follows:

$$K_g = \frac{\text{diffusivity} \cdot T_g}{\rho} \quad (140)$$

Equation 139 applies to the diffusion of water through the geomembrane induced by hydraulic head or vapor pressure differences. The program applies Darcy's law to geomembrane liners in the same manner as for soil liners (Equation 137). Diffusivity is expressed in the program as equivalent hydraulic conductivity. Table 8 provides default "equivalent hydraulic conductivities" for geomembranes of various polymer types. Leakage through intact sections of geomembranes is computed as follows:

$$q_{L_1}(k)_i = \begin{cases} 0 & \text{for } h_g(k)_i = 0 \\ K_g(k) \frac{h_g(k)_i + T_g(k)}{T_g(k)} & \text{for } h_g(k)_i > 0 \end{cases} \quad (141)$$

where

- $q_{L_1}(k)_i$  = geomembrane leakage rate by diffusion during time step i, inches/day  
 $K_g(k)$  = equivalent saturated hydraulic conductivity of geomembrane in subprofile k, inches/day  
 $h_g(k)_i$  = average hydraulic head on geomembrane liner in subprofile k during time step i, inches  
 $T_g(k)$  = thickness of geomembrane in subprofile k, inches

#### 4.16.2 Leakage Through Holes in Geomembranes

Properly designed and constructed geomembrane liners are seldom installed completely free of flaws as evident from leakage flows and post installation leak tests.

TABLE 8. GEOMEMBRANE DIFFUSIVITY PROPERTIES\*

Geomembrane Material	Coefficient of Migration, cm <sup>2</sup> /sec	Equivalent Hydraulic Conductivity, cm/sec
Butyl Rubber	2x10 <sup>-11</sup>	1x10 <sup>-12</sup>
Chlorinated Polyethylene (CPE)	6x10 <sup>-11</sup>	4x10 <sup>-12</sup>
Chlorosulfonated Polyethylene (CSPE) or Hypalon	5x10 <sup>-11</sup>	3x10 <sup>-12</sup>
Epichlorohydrin Rubber (CO)	3x10 <sup>-9</sup>	2x10 <sup>-10</sup>
Elasticized Polyolefin	1x10 <sup>-11</sup>	8x10 <sup>-13</sup>
Ethylene-Propylene Diene Monomer (EPDM)	2x10 <sup>-11</sup>	2x10 <sup>-12</sup>
Neoprene	4x10 <sup>-11</sup>	3x10 <sup>-12</sup>
Nitrile Rubber	5x10 <sup>-10</sup>	3x10 <sup>-11</sup>
Polybutylene	7x10 <sup>-12</sup>	5x10 <sup>-13</sup>
Polyester Elastomer	2x10 <sup>-10</sup>	2x10 <sup>-11</sup>
Low-Density Polyethylene (LDPE)	5x10 <sup>-12</sup>	4x10 <sup>-13</sup>
High-Density Polyethylene (HDPE)	3x10 <sup>-12</sup>	2x10 <sup>-13</sup>
Polyvinyl Chloride (PVC)	2x10 <sup>-10</sup>	2x10 <sup>-11</sup>
Saran Film	9x10 <sup>-13</sup>	6x10 <sup>-14</sup>

\* From Giroud and Bonaparte (1985)

Geomembrane flaws can range in size from pinholes that are generally a result of manufacturing flaws such as polymerization deficiencies to larger defects resulting from seaming errors, abrasion, and punctures occurring during installation. Giroud and Bonaparte (1989) defines pinhole-sized flaws to be smaller than the thickness of the geomembrane. Since geomembrane liner thicknesses are typically 40 mils or greater, the HELP program assigns the diameter of pinholes to be 40 mils or 0.001 m (defect area = 7.84x10<sup>-7</sup> m<sup>2</sup>). Giroud and Bonaparte (1989) indicates that pinhole flaws are more commonly associated with the original, less sophisticated, geomembrane manufacturing

techniques. Current manufacturing and polymerization techniques have made pinhole flaws less common. Giroud and Bonaparte (1989) defined installation defect flaws to be of a size equal to or larger than the thickness of the geomembrane. Based on 6 case studies that produced consistent results, Giroud and Bonaparte (1989) recommended using a defect area of  $1 \text{ cm}^2$  (20 x 5 mm) for conservatively high predictions of liner leakage on projects with intensive quality assurance/quality control monitoring during liner construction. Therefore, the HELP program uses a defect area of  $1 \text{ cm}^2$ . Finally, the HELP program user must define the flaw density or frequency (pinholes or defects/acre) for each geomembrane liner. Giroud and Bonaparte (1989) recommended using a flaw density of 1 flaw/acre for intensively monitored projects. A flaw density of 10 flaws/acre or more is possible when quality assurance is limited to spot checks or when environmental difficulties are encountered during construction. Greater frequency of defects may also result from poor selection of materials, poor foundation preparation and inappropriate equipment as well as other design flaws and poor construction practices.

Geosyntec (1993) indicated that geomembranes may undergo deterioration due to aging or external elements such as chemicals, oxygen, micro-organisms, temperature, high-energy radiation, and mechanical action (i.e., foundation settlement, slope failure, etc.). Although geomembrane deterioration can create geomembrane flaws or increase the size of existing flaws, the HELP program does not account for this time-dependent deterioration in the liner.

The liquid that passes through a geomembrane hole will flow laterally between the geomembrane and the flow limiting (controlling) layer of material adjacent to the geomembrane, unless there is perfect contact between the geomembrane and the controlling soil or free flow from the hole. The space between the geomembrane and the soil is assumed to be uniform. The size of this space depends on the roughness of the soil surface, the soil particle size, the rugosity and stiffness of the geomembrane, and the magnitude of the normal stress (overburden pressure) that tends to press the geomembrane against the soil. The HELP program ranks the contact between a geomembrane and soil as perfect, excellent, good, poor, and worst case (free flow). The HELP program also permits designs where a geomembrane is separated from a low permeability soil by a geotextile. The leakage is controlled by the hydraulic transmissivity of the gap or geotextile between the geomembrane and the soil. This interfacial flow between the geomembrane and soil layer covers an area called the wetted area. The hole in the geomembrane is assumed to be circular and the interfacial flow is assumed to be radial; therefore, the wetted area is circular. Giroud and Bonaparte (1989); Bonaparte et al. (1989); and Giroud et al. (1992) examined steady-state leakage through a geomembrane liner for all of these qualitative levels of contact and provided either theoretical or empirical solutions for the leakage rate and the radius of interfacial flow. Leakage and wetted area are dependent on the static hydraulic head on the liner; the hydraulic conductivity and thickness of the surrounding soil, waste, or geotextile layers; the size of the flaw; and the contact (interface thickness) between the geomembrane and the controlling soil layer.

The HELP program designates the controlling soil layer as either high, medium or low permeability. High is a saturated hydraulic conductivity greater than or equal to  $1 \times 10^{-1}$  cm/sec; medium is greater than or equal to  $1 \times 10^{-4}$  cm/sec and less than  $1 \times 10^{-1}$  cm/sec; and low is less than  $1 \times 10^{-4}$  cm/sec. The low permeability layers are assumed to remain saturated in the wetted area throughout the simulation. As mentioned earlier, geomembranes are geosynthetics with a very low cross-plane hydraulic conductivity (See Table 8). On the other hand, geotextiles are geosynthetics with a high cross-plane hydraulic conductivity and high in-plane transmissivity (See Table 9). The fabrics can help minimize damage to the membrane by the surrounding soil or waste layers. The in-plane transmissivity of geotextiles used as geomembrane cushions is used to compute the radius of interfacial flow and leakage through a geomembrane separated from the controlling soil by a geotextile.

### ***Worst Case (Free Flow) Leakage***

Giroud and Bonaparte (1989) theoretically examined free flow through a geomembrane surrounded by infinitely pervious media such as air or high permeability soil or waste layers (Brown et al., 1987). However, Giroud and Bonaparte (1989) cautioned that if the leachate head on the geomembrane liner is very small, surface tensions in the surrounding high permeability layers could prevent free flow through the geomembrane flow. With time, leachate-entrained, fine-grained particles can clog the high permeability layers, greatly reducing the permeability of these layers and possibly preventing free flow. Free flow is assumed whenever the layers above and below the geomembrane have high permeability.

TABLE 9. NEEDLE-PUNCHED, NON-WOVEN GEOTEXTILE PROPERTIES \*

Applied Compressive Stress, kPa	Resulting Geotextile Thickness, cm	In-Plane Flow		Cross-Plane Flow
		Geotextile Transmissivity, $\text{cm}^2/\text{sec}$ **	Horizontal Hydraulic Conductivity, cm/sec	Vertical Hydraulic Conductivity, cm/sec
1 to 8	0.41	0.3	0.7	0.4
100	0.19	0.04	0.2	---
200	0.17	0.02	0.1	---

\* Geotechnical Fabrics Report--1992 Specifiers Guide (Industrial Fabrics Association International, 1991), and Giroud and Bonaparte (1985).

\*\* Transmissivity = horizontal hydraulic conductivity x thickness.

Pinholes. Giroud and Bonaparte (1989) concluded that percolation through pinholes surrounded by high permeability layers can be considered as flow through a pipe and recommended using Poiseuille's equation. Therefore, the HELP program uses the following form of Poiseuille's equation to predict free flow leakage through geomembrane pinholes:

$$q_{L_2}(k)_i = \frac{(86,400) \pi n_2(k) \rho_{15} g h_g(k)_i d_2^4}{(4,046.9) (128) \eta_{15} T_g(k)} \quad (142)$$

$$q_{L_2}(k)_i = \frac{1.775 \times 10^{-4} n_2(k) h_g(k)_i}{T_g(k)} \quad (143)$$

where

$q_{L_2}(k)_i$  = leakage rate through pinholes in subprofile k during time step i, inches/day

86,400 = units conversion, 86,400 seconds per day

$n_2(k)$  = pinhole density in subprofile k, #/acre

$\rho_{15}$  = density of water at 15°C = 999 kg/m<sup>3</sup>

$g$  = gravitational constant, 386.1 inches/sec<sup>2</sup>

$d_2$  = diameter of a pinhole, 0.001 meters

4,046.9 = units conversion, 4,046.9 m<sup>2</sup>/acre

$\eta_{15}$  = dynamic viscosity of water at 15°C = 0.00114 kg/m sec

$T_g(k)$  = thickness of geomembrane in subprofile k, inches

$1.775 \times 10^{-4}$  = constant,  $1.775 \times 10^{-4}$  inches acre/day

Installation Defects. Giroud and Bonaparte (1989) also concluded that leakage through defects in geomembranes surrounded by high permeability layers can be considered as flow through an orifice and recommended using Bernoulli's equation. Therefore, the HELP program uses the following form of Bernoulli's equation to predict free flow leakage through geomembrane defects:

$$q_{L_3}(k)_i = \frac{86,400 C_B n_3(k) a_3 \sqrt{2 g h_g(k)_i}}{4046.9} \quad (144)$$

$$q_{L_3}(k)_i = 0.0356 n_3(k) \sqrt{h_g(k)_i} \quad (145)$$

where

$q_{L_3}(k)_i$  = leakage rate through defects in subprofile k during time step i,  
inches/day

$C_B$  = head loss coefficient for sharp edged orifices, 0.6

$n_3(k)$  = installation defect density for subprofile k, #/acre

$a_3$  = defect area, 0.0001 m<sup>2</sup>

$h_g(k)_i$  = average hydraulic head on geomembrane liner in subprofile k  
during time step i, inches

0.0356 = constant, 0.0356 inches<sup>0.5</sup> acre/day

### ***Perfect Liner Contact***

Perfect geomembrane liner contact means that there is no gap or interface between the geomembrane liner and controlling soil or waste layer. Perfect contact is not common but can be achieved if the geomembrane is sprayed directly onto a compacted, fine-grained soil or waste layer or if the geomembrane and controlling layers are manufactured together. Problems associated with the installation of spray-on liners (e.g. application, polymerization, etc.) has limited their use. Perfect liner contact results in only vertical percolation through the controlling layer below the liner flaw; however, both vertical and horizontal flow can occur in the layer opposite the controlling soil or waste layer.

Giroud and Bonaparte (1989) indicated that a lower bound estimate of leakage for perfect contact conditions can be estimated using Darcy's law assuming vertical flow through the controlling layer only in the area below the hole. An upper bound prediction can be obtained by assuming radial flow in the controlling layer and integrating Darcy's law in spherical coordinates to obtain the following equation:

$$Q_h = \frac{\pi K_s h_g d_o}{1 - \frac{0.5 d_o}{T_s}} \quad (146)$$

where

$Q_h$  = leakage rate through pinholes and installation defects, m<sup>3</sup>/sec

$K_s$  = saturated hydraulic conductivity of soil layer, m/sec

- $h_g$  = hydraulic head on geomembrane, m  
 $d_o$  = diameter of the geomembrane flaw, m  
 $T_s$  = thickness of soil layer, m

A geomembrane flaw diameter of 0.1 cm is used for pinhole flaws. Considering the density of pinholes, converting units and assuming  $d/T_s \approx 0$ , the leakage rate for pinholes in geomembrane with perfect contact is

$$q_{L_2}(k)_i = \frac{\pi n_2(k) K_s(k) h_g(k)_i 0.04}{6,272,640} \quad (147)$$

where

- $q_{L_2}(k)_i$  = leakage rate through pinholes in subprofile k during time step i, inches/day  
 $n_2(k)$  = pinhole density in subprofile k, #/acre  
 $K_s(k)$  = saturated hydraulic conductivity of soil layer at the base of subprofile k, inches/day  
 $h_g(k)_i$  = average hydraulic head on liner in subprofile k during time step i, inches  
 0.04 = diameter of a pinhole, 0.04 inches  
 6,272,640 = units conversion, 6,272,640 square inches per acre

Since the area of defect flaws was identified to be 1 cm<sup>2</sup>, an equivalent defect diameter was calculated to be 1.13 cm. Considering the density of installation defects and converting units, the leakage rate for installation defects in geomembrane with perfect contact is

$$q_{L_3}(k)_i = \frac{\pi n_3(k) K_s(k) h_g(k)_i 0.445}{6,272,640 \left[ 1 - \frac{(0.5)(0.445)}{T_s(k)} \right]} \quad (148)$$

where

- $q_{L_3}(k)_i$  = leakage rate through installation defects in subprofile k during time step i, inches/day  
 $n_3(k)$  = installation defect density in subprofile k, #/acre  
 0.445 = diameter of an installation defect, 0.445 inches

$T_s(k)$  = thickness of soil layer at base of subprofile k, inches

### **Interfacial Flow**

Problems associated with the installation of geomembrane liners typically causes an interface or gap to develop between the installed geomembrane liner and the adjacent materials. Even with a large overburden pressure on the geomembrane liner, gaps exist due to geomembrane wrinkles from installation; clods, large particle size and irregularities in the subsoil; and the stiffness of the geomembrane preventing the liner from filling the small voids between soil particles. However, the thickness of the interface is dependent on the effective stress on the liner. Percolation through geomembrane flaws typically involves radial flow through the interface and vertical flow through the controlling layer (See Figure 9). This flow also occurs in reverse when the controlling layer is placed over the geomembrane (See Figure 10). Layer erosion and consolidation can increase the interface thickness over time; however, such increases are not considered in the HELP program.

The head acting on the geomembrane liner decreases from a maximum at the edge of the geomembrane flaw to zero at the edge of the wetted area. Flow through the interface and controlling layer completely dissipates the leachate head or, as with intact liners, the total head on the liner. The leachate is assumed to flow radially until this head is dissipated; this radial distance is called the wetted area.

Giroud and Bonaparte (1989) indicated that the interfacial flow is dependent on the hydraulic transmissivity (thickness) of the air or geotextile cushion occupying the interface, the hydraulic head on the geomembrane, the hydraulic conductivity of the controlling soil layer, and the size of the geomembrane flaw. Vertical flow through the controlling layer is dependent on the hydraulic conductivity of the layer, the hydraulic gradient on the layer at various locations in the wetted area, and the area of the wetted area.

Giroud and Bonaparte (1989) and Giroud et al. (1992) used Darcy's law for flow through a porous media, considering both radial and interfacial flow, and developed the following equation, modified for flow per unit area and temperature corrected, for estimating leakage through circular flaws in geomembranes with interfacial flow.

$$q_h = K_s i_{avg} n \pi R^2 \left( \frac{\eta_{20}}{\eta_{15}} \right) \quad (149)$$

where

$q_h$  = interfacial flow leakage rate through flawed geomembrane, m/sec

$K_s$  = saturated hydraulic conductivity of controlling soil layer, m/sec

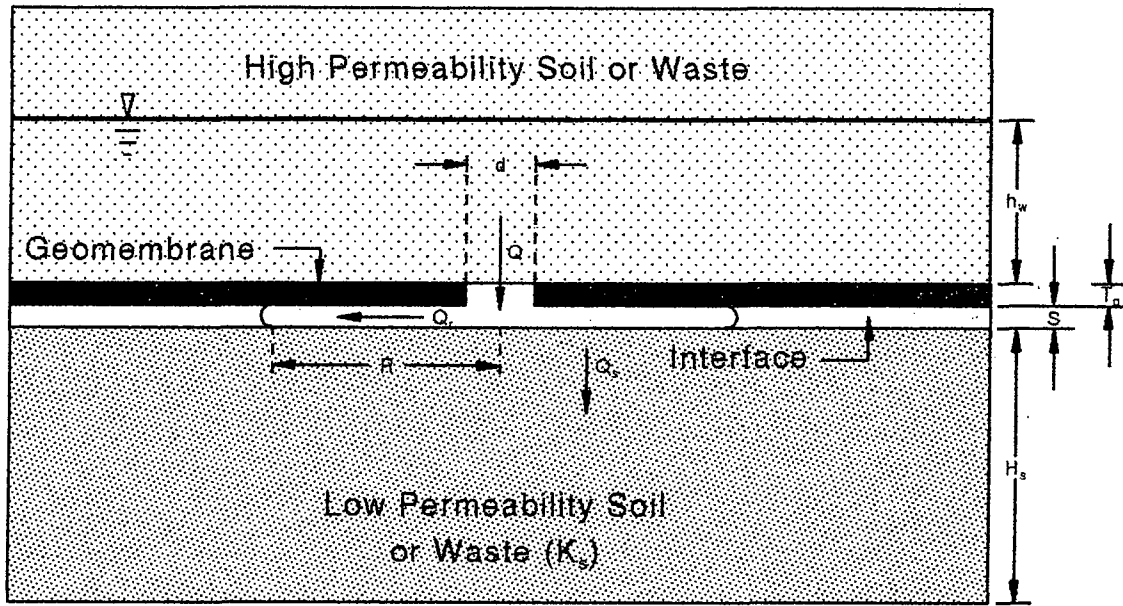


Figure 9. Leakage with Interfacial Flow Below Flawed Geomembrane

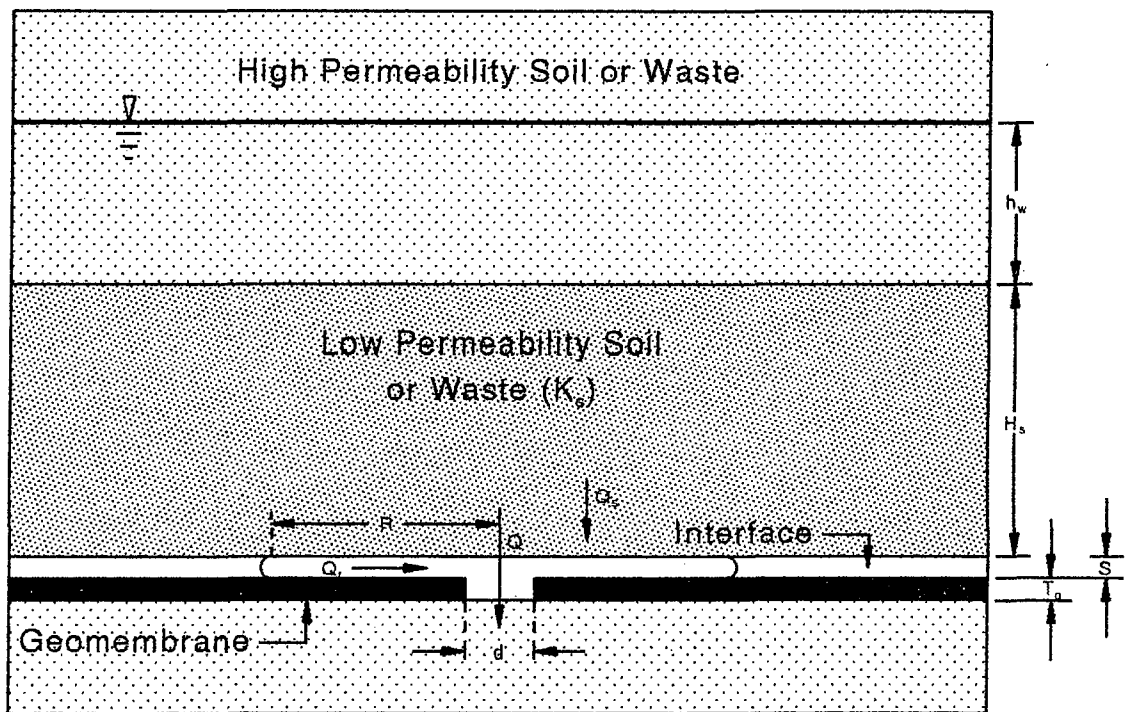


Figure 10. Leakage with Interfacial Flow Above Flawed Geomembrane

- $i_{avg}$  = average hydraulic gradient on wetted area of controlling soil layer, dimensionless  
 $n$  = density of flaws, # per m<sup>2</sup>  
 $R$  = radius of wetted area or interfacial flow around a flaw, m  
 $\eta_{20}$  = absolute viscosity of water at 20°C, 0.00100 kg/m-sec  
 $\eta_{15}$  = absolute viscosity of water at 15°C, 0.00114 kg/m-sec

Since the U.S. Geological Survey defined hydraulic conductivity, in Meinzer units, as the number of gallons per day of water passing through 1 ft<sup>2</sup> of medium under a unit hydraulic gradient (1 ft/1 ft) at a temperature of 60°F (15°C) (Viessman et al., 1977; Linsley et al., 1982), Equation 149 was corrected to reflect an absolute water viscosity at 15°C (Giroud and Bonaparte, 1989).

Giroud et al. (1992) developed the following equation to describe the average hydraulic gradient on the geomembrane; a description of the development is presented in the following paragraphs.

$$i_{avg} = 1 + \left[ \frac{h_g}{2 T_s \ln \left( \frac{R}{r_o} \right)} \right] \quad (150)$$

where

- $h_g$  = total hydraulic head on geomembrane, m  
 $T_s$  = thickness of controlling soil layer, m  
 $r_o$  = radius of a geomembrane flaw, m

Methods for calculating the wetted area radius for various liner contact conditions and design cases are presented in the following sections.

The HELP program applies Equations 149 and 150 as follows:

$$q_{L_{2,3}}(k)_i = \left( \frac{0.00100}{0.00114} \right) \left[ \frac{K_s(k) i_{avg_{2,3}}(k)_i n_{2,3}(k) \pi R_{2,3}(k)_i^2}{6,276,640} \right] \quad (151)$$

$$i_{avg_{2,3}}(k)_i = 1 + \left[ \frac{h_g(k)_i}{2 T_s(k) \ln \left( \frac{R_{2,3}(k)_i}{r_{o_{2,3}}} \right)} \right] \quad (152)$$

where

$q_{L_{2,3}}(k)_i$  = leakage rate through pinholes (2) or installation defects (3) with interfacial flow in subprofile k during time step i, inches/day

$K_s(k)$  = saturated hydraulic conductivity of controlling soil layer in subprofile k, inches/day

$i_{avg_{2,3}}(k)_i$  = average hydraulic gradient on wetted area of controlling soil layer from pinholes (2) or installation defects (3) in subprofile k during time step i, dimensionless

$n_{2,3}(k)$  = density of pinholes (2) or defects (3) in subprofile k, #/acre

$R_{2,3}(k)_i$  = radius of wetted area or interfacial flow around a pinhole (2) or an installation defect (3) in subprofile k during time step i, inches

6,272,640 = units conversion, 6,272,640 square inches per acre

$r_{o_{2,3}}$  = radius of flaw; pinhole  $r_{o_2} = 0.02$  inches; defect  $r_{o_3} = 0.22$  inches

$h_g(k)_i$  = average hydraulic head on liner in subprofile k during time step i, inches

$T_s(k)$  = thickness of soil layer at base of subprofile k, inches

### ***Geotextile Interface***

Giroud and Bonaparte (1989) assumed a unit hydraulic gradient for vertical flow through the controlling layer (i.e., Equation 149 without the  $i_{avg}$  term) and applied the principle of conservation of mass to the radial and vertical flow through the geomembrane. They integrated the resulting equation and developed the following equation for estimating the radius of the wetted area:

$$R = \left[ \frac{4 h_g \theta_{int}}{K_s \left[ 2 \ln \left( \frac{R}{r_o} \right) + \left( \frac{r_o}{R} \right)^2 - 1 \right]} \right]^{\frac{1}{2}} \quad (153)$$

where

$\theta_{int}$  = hydraulic transmissivity of the interface or geotextile, m<sup>2</sup>/sec

However, assuming a unit hydraulic gradient indicates that the depth of saturated material on the geomembrane is substantially smaller than the thickness of the controlling layer. This was a limitation of Giroud and Bonaparte's (1989) method for estimating geomembrane liner leakage. However, Giroud et al. (1992) used a simplified and conservative form of Equation 153, the principle of conservation of mass for flow through the two layers, and integrated the resulting equation to obtain an equation similar in form to Darcy's law ( $Q = Kia$ ). The hydraulic gradient term in the resulting equation was identified as the average hydraulic gradient on the geomembrane liner and is provided in Equation 150.

Equation 153 is solved iteratively by using  $(h_g + r_o)$  as the initial guess and then substituting the computed  $R$  into the right hand side until it converges. Equation 151 is also limited by the fact that the thickness between the installed geomembrane liner and the controlling layer is not easily determined, especially for multiple design cases. However, Giroud and Bonaparte (1989) provided information on the hydraulic transmissivity (loaded thickness times in-plane hydraulic conductivity) of geotextile cushion under a variety of effective stresses (See Table 9). Therefore, the HELP program only uses Equation 153 to estimate the leakage through flaws in geomembrane liners installed with geotextile cushions. The cushion is assumed to completely fill the interface between the liner and controlling layer. For other liner design cases, Giroud and Bonaparte (1989); Bonaparte et al. (1989); and Giroud et al. (1992) used laboratory and field data and theoretically based equations to develop semi-empirical and empirical equations for estimating the wetted area radius for excellent, good, and poor contact between the geomembrane liner and controlling layer.

Pinholes. The HELP program applies Equation 153 for computing the radius of the wetted area of leakage from pinholes and through a geotextile interface and a controlling soil layer as given in Equation 154 for each time step and each subprofile. The radius is then used in Equation 152 to compute the average hydraulic gradient. The radius and average hydraulic gradient is then used in Equation 151 to compute the leakage rate for pinholes.

$$R_2(k)_i = \left[ \frac{4 h_g(k)_i \theta_{int}(k)}{K_s(k) \left\{ \left[ 2 \ln \left( \frac{R_2(k)_i}{0.02} \right) \right] + \left( \frac{0.02}{R_2(k)_i} \right)^2 - 1 \right\}} \right]^{\frac{1}{2}} \quad (154)$$

where

$\theta_{int}(k)$  = hydraulic in-plane transmissivity of the geotextile in subprofile k,  
inches<sup>2</sup>/day

Installation Defects. The HELP program applies Equation 153 for computing radius of leakage from installation defects and through a geotextile interface and a controlling soil layer as follows:

$$R_3(k)_i = \left[ \frac{4 h_g(k)_i \theta_{int}(k)}{K_s(k) \left\{ \left[ 2 \ln \left( \frac{R_3(k)_i}{0.22} \right) \right] + \left( \frac{0.22}{R_3(k)_i} \right)^2 - 1 \right\}} \right]^{\frac{1}{2}} \quad (155)$$

This radius is then used in Equation 152 to compute the average hydraulic gradient. The radius and average hydraulic gradient is then used in Equation 151 to compute the leakage rate for installation defects.

### ***Excellent Liner Contact***

Excellent liner contact is achieved under three circumstances. Medium permeability soils and materials are typically cohesionless and therefore generally are able to conform to the geomembrane, providing excellent contact. The second circumstance is for very well prepared low permeability soil layer with exceptional geomembrane placement typically achievable in the laboratory, small lysimeters or small test plots. The third circumstance is by the use of a geosynthetic clay liner (GCL) adjacent to the geomembrane with a good foundation. The GCL, upon wetting, will swell to fill the gap between the geomembrane and the foundation, providing excellent contact.

Medium Permeability Controlling Soil. Giroud and Bonaparte (1989) indicated that if a geomembrane liner is installed with a medium permeability material (saturated hydraulic conductivity greater than or equal to  $1 \times 10^{-4}$  cm/sec and less than  $1 \times 10^{-1}$  cm/sec) above the geomembrane as the controlling soil layer, the flow to the geomembrane flaw will be impeded by the medium permeability layer and the leakage through the flaw will be less than free flow leakage. Similarly, if medium permeability material below the geomembrane acts as the controlling soil layer, the flow from the flaw will be impeded by the medium permeability layer and leakage will also be less than free flow. Whenever a medium permeability soil acts as the controlling soil layer, the contact is modeled as excellent. However, even with excellent contact, there will be some level of flow between the geomembrane and medium permeability layer. Bonaparte et al. (1989) used a theoretical examination of the flow in the interface between the medium permeability soil and the geomembrane liner to develop several empirical approaches that averaged the logarithms of the perfect contact leakage and free flow leakage predictions to obtain the following equation for the radius of convergence of leakage to a flaw in a geomembrane placed on high permeability material and overlain by medium permeability material:

$$R = 0.97 a_o^{0.38} h_g^{0.38} K_s^{-0.25} \quad (156)$$

where

- $R$  = radius of interfacial flow around a geomembrane flaw, m
- $a_o$  = geomembrane flaw area,  $7.84 \times 10^{-7} \text{ m}^2$  for pinholes and  $0.0001 \text{ m}^2$  for installation defects
- $h_g$  = total hydraulic head on geomembrane, m
- $K_s$  = saturated hydraulic conductivity of controlling soil layer, m/sec

This equation is also used to calculate the wetted radius of interfacial flow for geomembranes overlain by high permeability soil and underlain by medium permeability soil. This radius, as it is actually computed below in Equations 157 or 155, is then used in Equation 152 to compute the average hydraulic gradient. The radius and average hydraulic gradient are then used in Equation 151 to compute the leakage rate for geomembrane flaws.

*Pinholes.* By inserting the pinhole area, converting units and simplifying, Equation 156 is converted to the following equation for radius of interfacial flow from pinholes in geomembranes with medium permeability controlling soil layers.

$$R_2(k)_i = 0.0494 h_g(k)_i^{0.38} K_s(k)^{-0.25} \quad (157)$$

where

- $R_2(k)_i$  = radius of wetted area or interfacial flow around a pinhole in subprofile k during time step i, inches
- $K_s(k)$  = saturated hydraulic conductivity of controlling soil layer in subprofile k, inches/day
- $h_g(k)_i$  = average hydraulic head on liner in subprofile k during time-step i, inches

*Installation Defects.* By inserting the installation defect area, converting units and simplifying, Equation 156 is converted to the following equation for radius of interfacial flow from installation defects in geomembranes with medium permeability controlling soil layers.

$$R_3(k)_i = 0.312 h_g(k)_i^{0.38} K_s(k)^{-0.25} \quad (158)$$

where

$R_3(k)_i$  = radius of wetted area or interfacial flow around a pinhole in subprofile k during time step i, inches

Low Permeability Controlling Soil. Giroud and Bonaparte (1989) indicated that, when a geomembrane liner is installed on or under a low-permeability soil or waste layer, excellent geomembrane liner contact can be obtained if the liner is flexible and without wrinkles and the controlling layer is well compacted, flat, and smooth; has not been deformed by rutting due to construction equipment; and has no clods or cracks. Excellent contact is also possible when using a GCL with a good foundation as the low permeability soil layer. Using the theoretical techniques previously mentioned and laboratory data, Brown et al. (1987) developed charts for estimating the leakage rate through circular flaws in geomembrane liners for what Giroud and Bonaparte (1989) defined to be excellent liner contact. Leakage rates predicted using these charts are dependent on the flaw surface area, the saturated hydraulic conductivity of the controlling soil or waste layer, and the total leachate head on the geomembrane. Giroud and Bonaparte (1989) summarized and extrapolated or interpolated the data in these charts and developed the following equation for the wetted area radius with excellent liner contact with low permeability soil (saturated hydraulic conductivity less than  $1 \times 10^{-4}$  cm/sec); units are as in Equation 156:

$$R = 0.5 a_o^{0.05} h_g^{0.5} K_s^{-0.06} \quad (159)$$

This radius, as it is actually computed below in Equations 160 or 161, is then used in Equation 152 to compute the average hydraulic gradient. The radius and average hydraulic gradient are then used in Equation 151 to compute the leakage rate for geomembrane flaws.

*Pinholes.* By inserting the pinhole area, converting units and simplifying, Equation 159 is converted to the following equation for radius of leakage from pinholes in geomembranes with excellent contact with low permeability controlling soil layers.

$$R_2(k)_i = 0.0973 h_g(k)_i^{0.5} K_s(k)^{-0.06} \quad (160)$$

*Installation Defects.* By inserting the installation defect area, converting units and simplifying, Equation 159 is converted to the following equation for radius of leakage from installation defects in geomembranes with excellent contact with low permeability controlling soil layers.

$$R_3(k)_i = 0.124 h_g(k)_i^{0.5} K_s(k)^{-0.06} \quad (161)$$

### ***Good Liner Contact***

Using the equations for perfect and excellent liner contact and free-flow percolation through geomembrane liners, Giroud and Bonaparte (1989) developed leakage rate curves for a variety of conditions (i.e., leachate head, saturated hydraulic conductivity, etc.). The worst case field leakage was arbitrarily defined to be midway between free-flow and excellent contact leakage estimates. The area between worst case field leakage and excellent contact leakage was arbitrarily divided into thirds and defined as good and poor field leakage. However, due to the lengthy calculations required to estimate good and poor liner leakage, Giroud and Bonaparte (1989) developed empirical equations to predict leakage through geomembrane liners under good and poor field conditions. These equations are discussed in the following paragraphs.

Giroud and Bonaparte (1989) indicated that good geomembrane liner contact can be defined as a geomembrane, installed with as few wrinkles as possible, on an adequately compacted, low-permeability layer with a smooth surface. Similar to Equations 156 and 159, Giroud and Bonaparte (1989) observed families of approximately parallel linear curves when plotting the leakage rate as a function of total head on the geomembrane liner, geomembrane flaw area, and saturated hydraulic conductivity of the controlling soil or waste layer. Giroud and Bonaparte (1989) concluded that the leakage rate through damaged geomembranes is approximately proportional to equations of the form  $a_o^y h_g^x K_s^z$ . Therefore, Giroud and Bonaparte (1989) proposed the following equation for determining the wetted area radius for good liner contact:

$$R = 0.26 a_o^{0.05} h_g^{0.45} K_s^{-0.13} \quad (162)$$

This radius, as it is actually computed below in Equations 163 or 164, is then used in Equation 152 to compute the average hydraulic gradient. The radius and average hydraulic gradient are then used in Equation 151 to compute the leakage rate for geomembrane flaws. Similar to Equation 159, Equation 162 has the limitation that the saturated hydraulic conductivity of the controlling soil layer must be less than  $1 \times 10^{-4}$  cm/sec. Equation 162 is valid only in units of meters and seconds.

Pinholes. Inserting pinhole area, performing units conversion and simplifying, Equation 162 is converted for radius of leakage from pinholes in geomembranes with good contact with low permeability controlling soil layers as follows:

$$R_2(k)_i = 0.174 h_g(k)_i^{0.45} K_s(k)^{-0.13} \quad (163)$$

Installation Defects. By inserting the installation defect area, converting units and simplifying, Equation 162 is converted to the following equation for radius of leakage from installation defects in geomembranes with good contact with low permeability controlling soil layers.

$$R_3(k)_i = 0.222 h_g(k)_i^{0.45} K_s(k)^{-0.13} \quad (164)$$

### ***Poor Liner Contact***

Giroud and Bonaparte (1989) indicated that poor geomembrane liner contact can be defined as a geomembrane, installed with a certain number of wrinkles, on a poorly compacted, low-permeability soil or waste layer, with a surface that does not appear smooth. Similar to Equation 162, Giroud and Bonaparte (1989) proposed the following equation for determining the radius of leakage through a geomembrane for poor contact with a low permeability controlling soil layer:

$$R = 0.61 a_o^{0.05} h_g^{0.45} K_s^{-0.13} \quad (165)$$

This radius, as it is actually computed below in Equations 166 or 167, is then used in Equation 152 to compute the average hydraulic gradient. The radius and average hydraulic gradient are then used in Equation 151 to compute the leakage rate for geomembrane flaws. Similar to Equations 159 and 162, Equation 165 has the limitation that the saturated hydraulic conductivity of the controlling soil layer must be less than  $1 \times 10^{-4}$  cm/sec. Equation 165 is valid using units of meters and seconds.

Pinholes. By inserting pinhole area, performing units conversion and simplifying, Equation 165 is converted to the following equation for radius of leakage from pinholes in geomembranes with poor contact with low permeability controlling soil layers.

$$R_2(k)_i = 0.174 h_g(k)_i^{0.45} K_s(k)^{-0.13} \quad (166)$$

Installation Defects. By inserting the installation defect area, converting units and simplifying, Equation 165 is converted to the following equation for radius of leakage

from installation defects in geomembranes with poor contact with low permeability controlling soil layers.

$$R_3(k)_i = 0.521 h_g(k)_i^{0.45} K_s(k)^{-0.13} \quad (167)$$

#### 4.17 GEOMEMBRANE AND SOIL LINER DESIGN CASES

As previously mentioned, the HELP program simulates leakage through both the intact and damaged portions of geomembrane liners. Leakage through geomembrane flaws (pinholes and defects) is modeled for various liner contact conditions. The minimum level of leakage will occur through an intact geomembrane liner. The total leakage is the sum of leakage through (1) intact geomembrane sections and (2) pinhole-size and (3) defect-size geomembrane flaws.

$$q_{L_T} = q_{L_1} + q_{L_2} + q_{L_3} \quad (168)$$

The HELP program insures that the total leakage through the geomembrane and controlling layers is not greater than the volume of drainable water. The program also checks to insure that the leakage rate is not greater than the product of the hydraulic gradient and the saturated hydraulic conductivity of the controlling layer.

Giroud and Bonaparte (1989) and Giroud et al. (1992) developed their equations for intact geomembranes, geomembranes surrounded by highly-pervious materials, and composite liners; defined as a geomembrane installed over a low-permeable soil liner and covered by a drainage layer. However, various other liner design cases are possible and, although the equations were not specifically designed to address these designs, similar physical conditions indicated that these equations would be applicable to other liner design cases. However, the applicability of these equations to other liner designs has not been fully verified.

Geomembrane liners are frequently installed with various defects that increase as design and installation monitoring efforts decrease. Therefore, the HELP program user must identify the liner contact condition (perfect, excellent, good, poor, or worst case) for each damaged geomembrane liner. The user must also identify the hydraulic conductivity of the controlling layer and the geomembrane flaw type (pinhole or defect) and density. The user must also identify the thickness and equivalent hydraulic conductivity of the geomembrane for the intact portions of the liner. In some cases, the user will have to identify the geotextile cushion thickness and in-plane hydraulic transmissivity.

Based on the design of the geomembrane liner system (layer type, saturated hydraulic conductivity, and location of controlling soil layer), the HELP program can compute leakage for 6 different geomembrane liner design cases (See Figures 11 through 16).

These design cases are discussed in the following sections.

**Design Case 1.** Geomembrane liner Design Case 1 consists of a geomembrane installed between two highly permeable soil or waste layers (See Figure 11). The program uses the free flow equations (Equation 143 for pinholes and Equation 145 for installation defects) to calculate the leakage rate through flaws. The vapor diffusion equation (Equation 141) is used to calculate the leakage rate through the intact portion of the geomembrane liner. The damaged and intact leakage estimates are then added together to predict the total leakage through the geomembrane liner.

**Design Case 2.** Geomembrane liner Design Case 2 consists of three design scenarios: 1) a geomembrane liner installed on top of a highly permeable layer and overlaid by a medium permeability layer; 2) a geomembrane liner installed on top of a medium permeability layer and overlaid by a highly permeable layer; and 3) a geomembrane liner installed between two medium permeability layers (See Figure 12). Three levels of contact (perfect, excellent, or worst case) between the geomembrane and medium permeability layer are allowed for this design case. The program uses Equations 147 and 148 to calculate the perfect contact leakage rate through pinholes and installation defects, respectively. Equations 151, 152, 157 (for pinholes) and 158 (for installation defects) are used to calculate the excellent contact leakage rate. As in Design Case 1, free flow equations (Equation 143 for pinholes and Equation 145 for installation defects) are used to calculate the worst case contact leakage rate. Finally, the vapor diffusion equation (Equation 141) is used to calculate the leakage rate through the intact portion of the geomembrane liner for all three scenarios and levels of contact. The damaged and intact leakage estimates are subsequently added together to predict the total leakage through the geomembrane liner.

**Design Case 3.** Geomembrane liner Design Case 3 consists of a geomembrane overlying a low permeability layer (either a soil liner or vertical percolation layer), which is the controlling soil layer (See Figure 13). The geomembrane may be covered with either a high permeability, medium permeability, or low permeability soil or waste layer

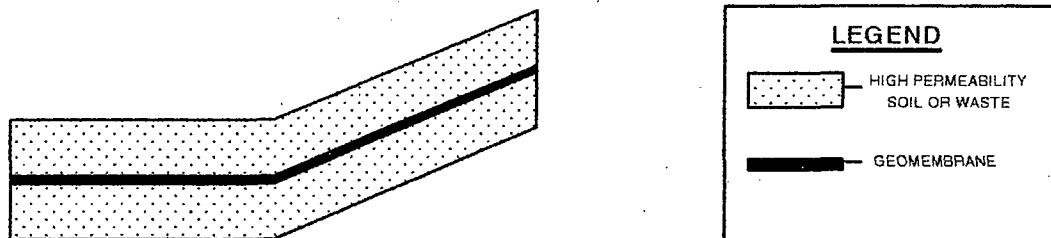


Figure 11. Geomembrane Liner Design Case 1

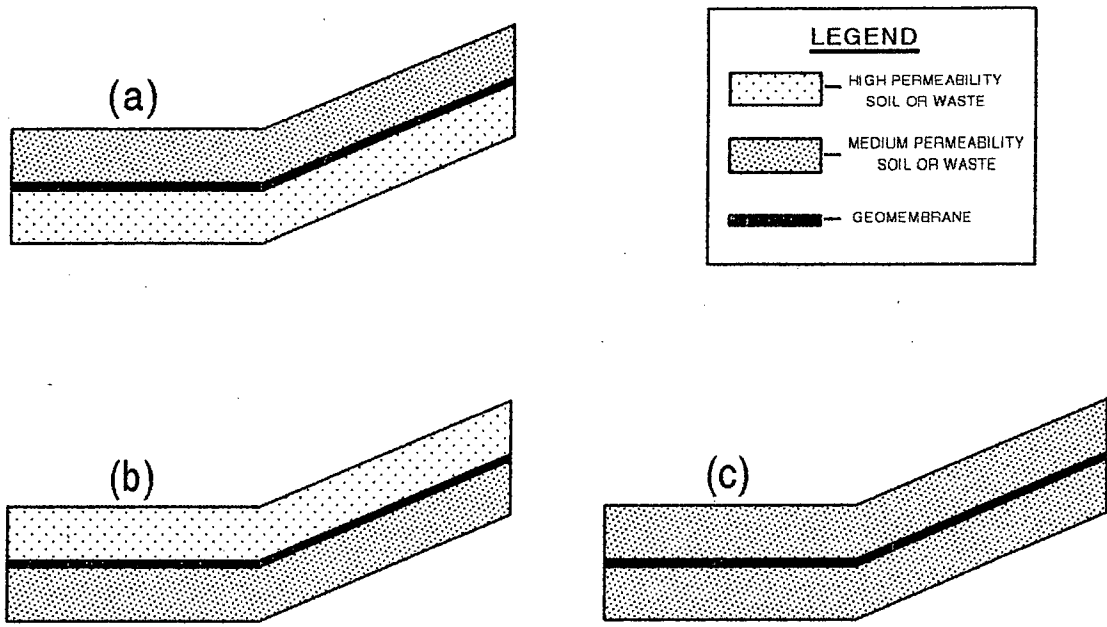


Figure 12. Geomembrane Liner Design Case 2

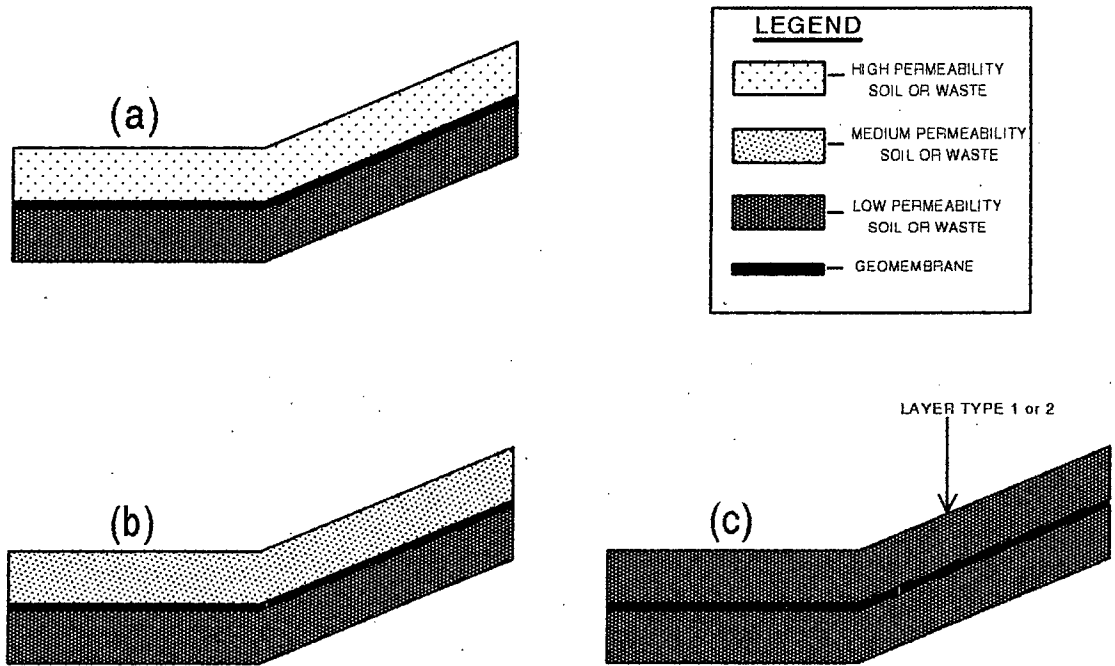


Figure 13. Geomembrane Liner Design Case 3

designated as either a vertical percolation or lateral drainage layer. The level of contact between the geomembrane and low permeability controlling soil layer may be defined as perfect, excellent, good, poor, or worst case. The program uses Equations 147 and 148 to calculate the perfect contact leakage rate through pinholes and installation defects, respectively. Equations 151 and 152 are used to calculate the interfacial flow leakage rate and hydraulic head gradient for excellent, good and poor levels of contact. Equations 160, 163 and 166 are used to calculate the radius of interfacial flow from pinholes respectively for excellent, good and poor levels of contact. Equations 161, 164 and 167 are used to calculate the radius of interfacial flow from installation defects respectively for excellent, good and poor levels of contact. As in Design Case 1, free flow equations (Equation 143 for pinholes and Equation 145 for installation defects) are used to calculate the worst case contact leakage rate. Finally, the vapor diffusion equation (Equation 141) is used to calculate the leakage rate through the intact portion of the geomembrane liner for all levels of contact. The damaged and intact leakage estimates are subsequently added together to predict the total leakage through the geomembrane liner.

**Design Case 4.** Geomembrane liner Design Case 4 is simply the inverse of Design Case 3 (See Figure 14); the low permeability controlling soil layer overlies the geomembrane. The same soil and layer types and levels of contacts may be used. The same equations as described for Design Case 3 are used to calculate leakage for the various contacts and flaw sizes. This geomembrane liner design case is the exact inverse of that considered

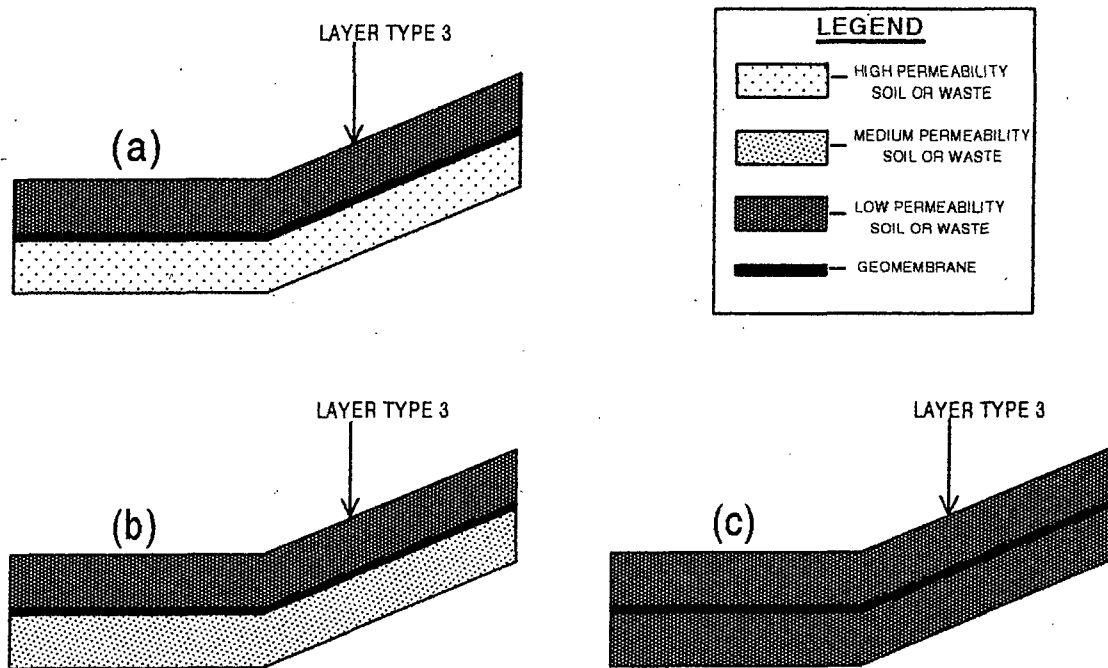


Figure 14. Geomembrane Liner Design Case 4

by Giroud and Bonaparte (1989). However, since the total head loss for leakage through damaged geomembrane liners is assumed to occur through the interface and controlling layer, the equations proposed by Giroud and Bonaparte (1989) should apply as well for the inverted case. However, the total head on the geomembrane for this design case and Design Case 6 is equal to the sum of the leachate depth in the layer above the liner system and the thickness of saturated soil liner above the geomembrane as shown in Figure 10; the hydraulic head is the total thickness of continuously saturated soil or waste above the geomembrane. In Design Cases 1, 2, 3 and 5, the total head is just the depth of saturated material above the liner system as shown in Figure 9.

**Design Case 5.** As shown in Figure 15, geomembrane liner Design Case 5 consists of eight scenarios that have a geotextile cushion placed between the geomembrane liner and the controlling soil layer. The controlling soil layer may be composed of medium or low permeability soil. The controlling soil layer may be above or below the geomembrane, but, if above, the controlling soil layer cannot be a soil liner. The geotextile is not connected to the leachate collect system, which would cause them to act as a drainage layer. The geotextile functions solely as a liner cushion and defines the interfacial flow between the geomembrane and controlling soil layer. Assuming the cushion completely fills the interface, Equations 151, 152, 154 (for pinholes) and 155 (for installation defects) are used to estimate the leakage rate as a function of the hydraulic in-plane transmissivity of the geotextile. Table 9 provides hydraulic transmissivity values, at several compressive stresses, for needle-punched, non-woven geotextiles. Recall that the hydraulic transmissivity of geotextiles is greatly affected by the applied compressive stress and the degree of clogging.

**Design Case 6.** Geomembrane liner Design Case 6 consists of a geomembrane liner installed on a high, medium, or low permeability soil or waste layer with a geotextile cushion separating the geomembrane and an overlying soil liner (layer type 3). (See Figure 16). Similar to Design Case 5, the program uses Equations 151, 152, 154 (for pinholes) and 155 (for installation defects) to estimate the leakage rate as a function of the hydraulic in-plane transmissivity of the geotextile. However, as in Design Case 4, the total head on the geomembrane is equal to the sum of the continuously saturated material above the liner system and the thickness of the soil liner above the geomembrane.

Flow through the geotextile cushion in either Design Case 5 or 6 can increase the geomembrane liner leakage due to an increase in the wetted area and possibly creating a connection between the geomembrane flaw and controlling layer macropores. On the other hand, laboratory tests have shown that a needlepunched, nonwoven geotextile cushion installed between a geomembrane liner and controlling layer can decrease leakage if the effective stress on the liner or controlling layer is adequate to push the geotextile into irregularities in the controlling layer (worst case and possibly poor contact cases). This prevents free lateral flow between the liner and controlling layer. However, the beneficial effects of geotextile cushions may be limited to cases of poor design and

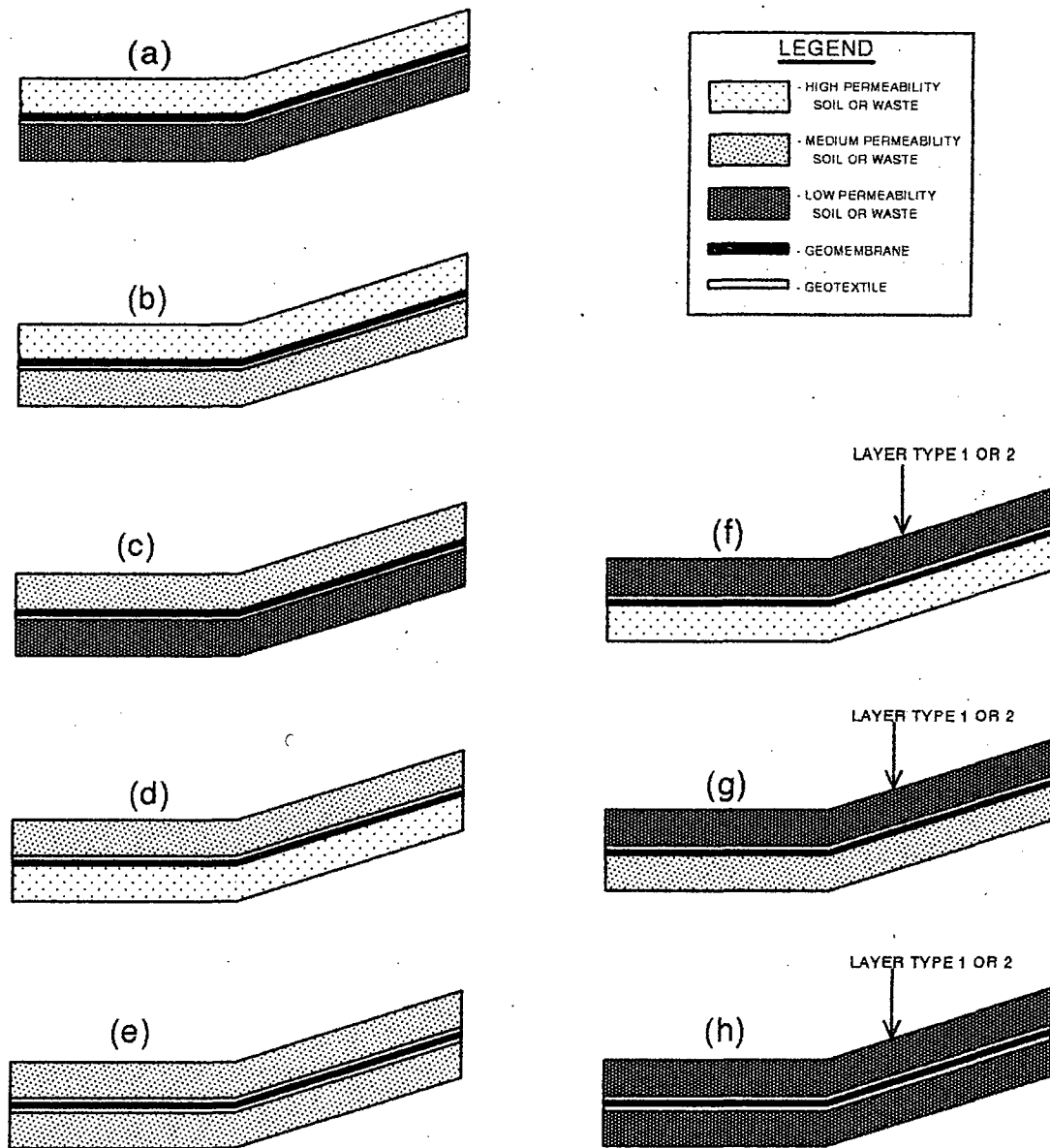


Figure 15. Geomembrane Liner Design Case 5

installation.

#### 4.18 LATERAL DRAINAGE

Unconfined lateral drainage from porous media is modeled by the Boussinesq equation (Darcy's law coupled with the continuity equation), employing the Dupuit-Forcheimer (D-F) assumptions. The D-F assumptions are that, for gravity flow to a shallow sink, the flow is parallel to the liner and that the velocity is in proportion to the

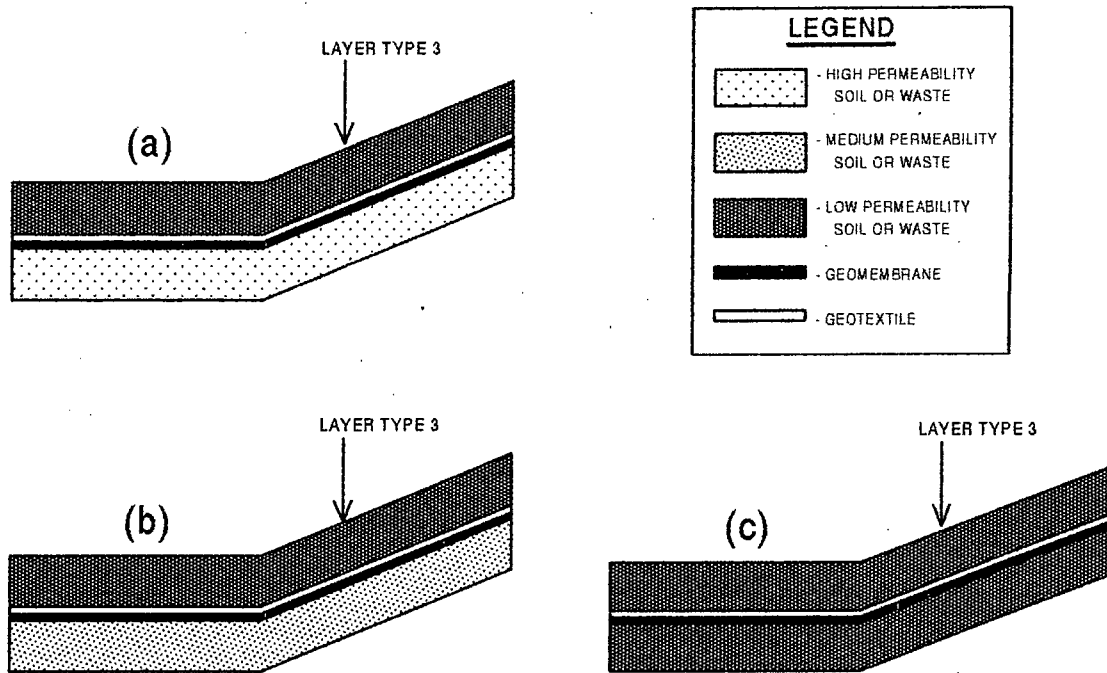


Figure 16. Geomembrane Liner Design Case 6

slope of the water table surface and independent of depth of flow (Forcheimer, 1930). These assumptions imply the head loss due to flow normal to the liner is negligible, which is valid for drain layers with high hydraulic conductivity and for shallow depths of flow, depths much shorter than the length of the drainage path. The Boussinesq equation may be written as follows (See Figure 17 for definition sketch):

$$f \frac{\partial h}{\partial t} = K_D \frac{\partial}{\partial l} \left[ (h - l \sin \alpha) \frac{\partial h}{\partial l} \right] + R \quad (169)$$

where

- $f$  = drainable porosity (porosity minus field capacity), dimensionless
- $h$  = elevation of phreatic surface above liner at edge of drain, cm
- $t$  = time, sec
- $K_D$  = saturated hydraulic conductivity of drain layer, cm/sec
- $l$  = distance along liner surface in the direction of drainage, cm
- $\alpha$  = inclination angle of liner surface
- $R$  = net recharge (impingement minus leakage), cm/sec

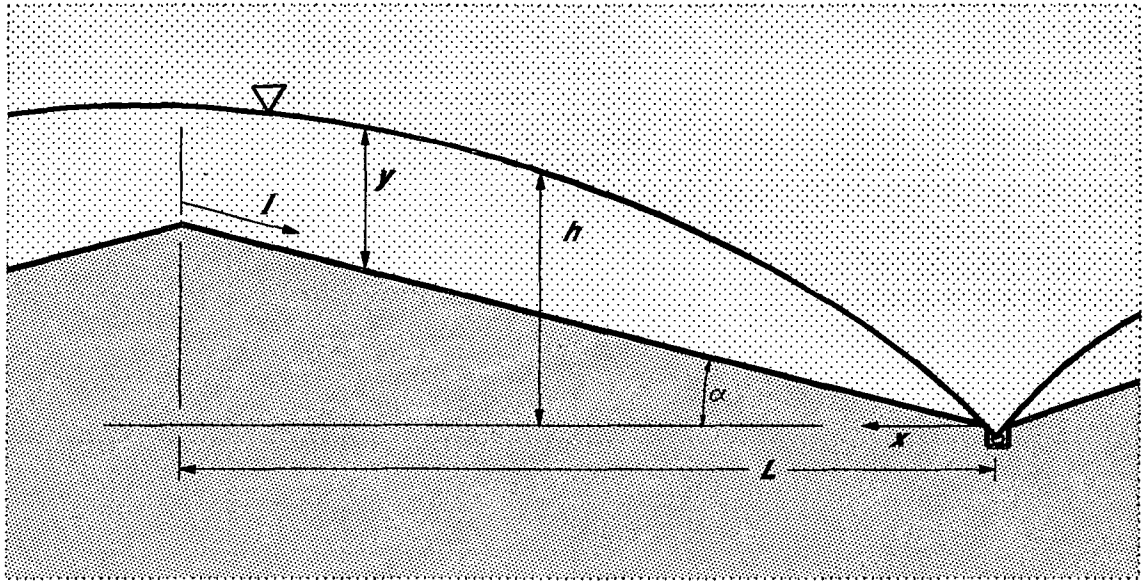


Figure 17. Lateral Drainage Definition Sketch

Where the saturated zone directly above the liner extends into more than one modeling segment, the saturated hydraulic conductivity,  $K_D$ , is assigned the weight-averaged saturated hydraulic conductivity of the saturated zone.

$$K_D = \frac{\sum_{j=n}^m K_s(j) \cdot d(j)}{y} \quad \text{where } y = \sum_{j=n}^m d(j) \quad (170)$$

where

- $K_s(j)$  = saturated hydraulic conductivity of segment  $j$ , cm/sec
- $d(j)$  = thickness of saturated soil in segment  $j$ , cm
- $m$  = number of the lowest unsaturated segment in subprofile
- $n$  = number of the segment directly above the liner in subprofile
- $y$  = depth of saturated lateral drainage ( $h - x \tan \alpha$ ), cm
- $x$  = horizontal distance from drain, cm

The lateral drainage submodel assumes that the relationship between lateral drainage rate and average saturated depth for steady flow approximates the overall relationship for an unsteady drainage event. For steady flow, the lateral drainage rate is equal to the net recharge.

$$\frac{\partial h}{\partial t} = 0 \quad \frac{dQ_D}{dx} = R \quad Q_{D_0} = R \cdot L \quad q_D = \frac{Q_{D_0}}{L} \quad (171)$$

where

- $Q_D$  = lateral drainage rate per unit width of drain at any  $x$ , cm<sup>2</sup>/sec  
 $Q_{D_0}$  = lateral drainage rate into collector pipe at drain,  $x = 0$ , (flow rate per unit length of collector), cm<sup>2</sup>/sec  
 $L$  = length of the horizontal projection of the liner surface (maximum drainage distance) cm  
 $q_D$  = lateral drainage rate at drain in flow per unit area of landfill, cm/sec

Translating the axis from  $l$  (parallel to the liner) to  $x$  (horizontal) and substituting for  $R$ , the steady lateral drainage equation is described as follows:

$$R = \frac{Q_{D_0}}{L} = q_D = K_D \cos^2 \alpha \frac{d}{dx} \left( y \frac{dh}{dx} \right) \quad (172)$$

After expressing  $h$  in terms of  $y$  and expanding, Equation 171 can be rewritten as follows:

$$y \frac{d^2 y}{dx^2} + \left( \frac{dy}{dx} \right)^2 + (\tan \alpha) \frac{dy}{dx} = \frac{q_D}{K_D \cos^2 \alpha} \quad (173)$$

Nondimensionally, it can be rewritten as follows:

$$y^* \frac{d^2 y^*}{dx^{*2}} + \left( \frac{dy^*}{dx^*} \right)^2 + (\tan \alpha) \frac{dy^*}{dx^*} = \frac{q_D^*}{\cos^2 \alpha} \quad (174)$$

where

$x^*$  =  $x / L$ , nondimensional horizontal distance

$y^*$  =  $y / L$ , nondimensional depth of saturation above liner

$$q_D^* = q_D / K_D, \text{ nondimensional lateral drainage rate}$$

Assuming a unit hydraulic gradient in the direction of flow at the drain, the boundary conditions for Equation 174 are

$$\frac{dy^*}{dx^*} = \frac{1}{\cos \alpha} - \tan \alpha \quad \text{at } x^* = 0 \quad (175)$$

$$y^* \left( \frac{dy^*}{dx^*} + \tan \alpha \right) = 0 \quad \text{at } x^* = 1 \quad (176)$$

An alternative boundary condition is used for shallow saturated depths and small lateral drainage rates [ $q_D^* \leq 0.4(\sin^2 \alpha)$ ]. For values of  $q_D^* > 0.4(\sin^2 \alpha)$ , the depth of saturated drainage media at the upper end of the liner is greater than 0.

$$y^* = \frac{q_D^*}{\cos^2 \alpha} \quad (177)$$

Equation 177 can be solved analytically for the two limiting cases by simplifying, employing the boundary conditions and integrating from  $x^* = 0$  to  $x^* = 1$ . For small drain rates or shallow saturated depths, such that  $q_D^* < 0.4(\sin^2 \alpha)$  or  $\bar{y}^* < 0.2 \tan \alpha$  ( $\bar{y}^*$  = average depth of saturation above the entire liner),

$$\bar{y}^* = \frac{q_D^*}{2 (\sin \alpha) (\cos \alpha)} \quad \text{for } q_D^* < 0.4 \sin^2 \alpha \quad (178)$$

or

$$q_D^* = 2 (\sin \alpha) (\cos \alpha) \bar{y}^* \quad \text{for } \bar{y}^* < 0.2 \tan \alpha$$

For large drainage rates, such that  $q_D^* > 0.4(\sin^2 \alpha)$  or  $\bar{y}^* > 0.2 \tan \alpha$ ,

Equation 174 was solved numerically for a wide range of values of the parameters,  $q_D^*$  and  $\alpha$ . The nondimensional average depth of saturation on top of the liner ( $\bar{y}^*$ ) was computed numerically for each solution. Analysis of these solutions showed that the

$$\bar{y}^* = \frac{\pi \sqrt{q_D^*}}{4 \cos \alpha} \quad \text{for } q_D^* > 0.4 \sin^2 \alpha$$

or

(179)

$$q_D^* = \left( \frac{4 \bar{y}^* \cos \alpha}{\pi} \right)^2 \quad \text{for } \bar{y}^* > 0.2 \tan \alpha$$

relationship among  $q_D$ ,  $y$ ,  $L$ ,  $K$ , and  $\alpha$  is closely approximated by the following equation which converges to the analytical solutions for small drainage rates (Equation 178) and large drainage rates (Equation 179).

$$\bar{y}^* = \frac{\pi \sqrt{q_D^*}}{4 \cos \alpha} \left( \frac{2 \sqrt{0.4}}{\pi} \right) \left( \frac{q_D^*}{0.4 \sin^2 \alpha} \right)^{\left[ \frac{1}{2 \ln \left( \frac{2 \sqrt{0.4}}{\pi} \right)} \right]} \quad \text{for } q_D^* \geq 0.4 \sin^2 \alpha$$
(180)

This two-part function (Equations 179 and 180) is continuous and smooth and matches the closed-form, asymptotic solutions for the cases where  $\bar{y}^* < \tan \alpha$  and  $\bar{y}^* > \tan \alpha$ . The estimate of  $q_D^*$  given by Equations 178 and 180 is within one percent of the value obtained by solving Equation 174 numerically. Equations 178 and 180 are used to compute  $q_D$  in the lateral drainage submodel. The equations are applied iteratively along with the liner leakage or percolation equations and storage equation to solve concurrently for the average depth of saturation, the liner leakage or percolation and the average depth of saturation above the liner during each time period. The process is repeated for each subprofile with a lateral drainage layer for every time step.

#### 4.19 LATERAL DRAINAGE RECIRCULATION

The lateral drainage from any subprofile may be collected or recirculated. If collected, that fraction of the drainage is removed from the landfill and the quantity is reported as a volume collected. If recirculated, that fraction of the drainage from the subprofile is stored during the day and then uniformly distributed the next day throughout the specified layer. The recirculation is then applied in the vertical water routing procedure using Equations 124 and 134. Recirculation can be distributed to any layer that is not a liner.

where

$$RC_i(j) = \text{recirculation into segment } j \text{ during a timestep on day } i, \text{ inches}$$

$$RC_i(j) = \frac{1}{N(k_j)} \sum_{k=1}^{nk} \sum_{n=1}^{N(k)} \frac{FRC(k,j) q_D(k)_{i-1,n}}{N(k)} \quad (181)$$

$N(k_j)$  = number of timesteps in a day for subprofile k containing segment j

$k$  = number of the subprofile

$nk$  = total number of subprofiles in the landfill

$n$  = number of the timestep in day i-1

$N(k)$  = total number of timesteps in a day for subprofile k, day<sup>-1</sup>

$FRC(k,j)$  = fraction of the lateral drainage from subprofile k that is recirculated to segment j

$q_d(k)_{i-1,n}$  = lateral drainage rate from subprofile k during timestep n on day i-1, inches/day

#### 4.20 SUBSURFACE INFLOW

Subsurface inflow is treated as steady, uniform seepage into a layer. Inflow may be specified for any layer. If the inflow for a liner is specified, the inflow is added to the inflow into the next lower layer that is not a liner. If inflow is specified for a liner system that is on the bottom of the landfill profile, the inflow is added to the inflow of the first layer above the liner system. The subsurface inflow is then applied in the vertical water routing procedure using Equations 124 and 134. The inflow is specified for each layer in the input. The inflow is specified as the volume per year per unit area, which is then simply converted by the program to a volume per time step based on a unit area. Volume per unit area is used throughout the program for storage and flows.

#### 4.21 LINKAGE OF SUBSURFACE FLOW PROCESSES

The drainage rate out of a subprofile must equal the sum of lateral drainage rate and the leakage rate through the liner system. The subsurface water routing, liner leakage and lateral drainage calculations are linked as follows:

1. Water is routed through the subprofile from top to bottom by unsaturated vertical drainage using Equation 134.
2. The total drainage rate out of the segment directly above the liner system is initially assumed to be the same as in the previous time step. Excess water is backed up through the subprofile as necessary.

3. The average depth of saturation above the liner system and the effective lateral hydraulic conductivity of the saturated zone are computed using Equation 135. The depth or head is only an estimate since it is based on estimated drainage out of the subprofile.
4. Lateral drainage and liner leakage or percolation are computed using Equation 178 or 180 for lateral drainage, Equation 137 for soil liner percolation, and Equations 141, 143, 145, 147, 148, 151, 152, 154, 155, 157, 158, 160, 161, 163, 164, 166, 167 or 168 for geomembrane liner leakage. The estimated saturated depth is used in these computations.
5. A new estimate of the average depth of saturation is generated by updating the water storage using the computed lateral drainage and percolation/leakage. If the new estimate is within the larger of 5 percent or 0.01 inches of the original estimate, then the updated water storage and the computed rates are accepted. If not, the original and new estimate are averaged to generate a new estimate and steps 4 and 5 are repeated until the convergence criterion is met. If the estimated and computed total drainage are greater than the available gravity water (storage in excess of field capacity), then the total drainage is assigned the value of the gravity water. Then, the leakage and lateral drainage volumes are proportional to the relative rates, and the depth of saturation is computed by Equation 178 using the assigned lateral drainage rate.
6. The procedure is repeated for each time step in a day, and the lateral drainage volumes are summed as are the liner leakage/percolation volumes for the subprofile before beginning computations for the next subprofile. The daily lateral drainage is then partitioned to removal and recirculation as specified in the input. The liner leakage/percolation is assigned as drainage into the next subprofile or out of the landfill. The depths of saturation for time steps during the day are averaged and reported as average daily head.

## SECTION 5

### ASSUMPTIONS AND LIMITATIONS

#### 5.1 METHODS OF SOLUTION

The modeling procedures documented in the previous section are necessarily based on many simplifying assumptions. Most of these are stated in the sections documenting the individual procedures. Generally, these assumptions are reasonable and consistent with the objectives of the program when applied to standard landfill designs. However, some of these assumptions may not be reasonable for unusual designs. The major assumptions and limitations of the program are summarized below.

Precipitation on days when the mean air temperature is below freezing is assumed to occur as snow. Snowmelt is assumed to be a function of energy from air temperature, solar radiation and rainfall. Solar radiation effects are included in an empirical melt factor. In addition, groundmelt is assumed to occur at a constant rate of 0.5 mm/day as long as the ground is not frozen. Snow and snowmelt are subject to evaporation prior to runoff and infiltration. The program does not consider the effects of aspect angle or drifting in its accounting of snow behavior.

Prediction of frozen soil conditions is a simple, empirical routine based on antecedent air temperatures. Thaws are based on air temperatures and climate data. Soils while frozen are assumed to be sufficiently wet so as to impede infiltration and to promote runoff. Similarly, no evapotranspiration and drainage are permitted from the evaporative zone while frozen.

Runoff is computed using the SCS method based on daily amounts of rainfall and snowmelt. The program assumes that areas adjacent to the landfill do not drain onto the landfill. The time distribution of rainfall intensity is not considered. The program cannot be expected to give accurate estimates of runoff volumes for individual storm events on the basis of daily rainfall data. However, because the SCS rainfall-runoff relationship is based on considerable daily field data, long-term estimates of runoff should be reasonable. One would expect the SCS method to underestimate runoff from short duration, high intensity storms; larger curve numbers could be used to compensate if most of the precipitation is from short duration, high intensity storms. The SCS method does not explicitly consider the length and slope of the surface over which overland flow occurs; however, a routine based on a kinematic wave model was developed to account for surface slope and length.

Potential evapotranspiration is modeled by an energy-based Penman method. As applied, the program uses average quarterly relative humidity and average annual wind speed. It is assumed that these data yield representative monthly results. Similarly, the program assumes that the relative humidity is 100% on days when precipitation occurs.

The program uses an albedo of 0.23 for soils and vegetation and 0.60 for snow. The actual evapotranspiration is a function of other data, also. The solar radiation and temperature data are often synthetically generated. The vegetation data is generated by a vegetative growth model. The evaporative zone depth is assumed to be constant throughout the simulation period. However, outside of the growing season, the actual depth of evapotranspiration is limited to the maximum depth of evaporation of soil water, which is a function of the soil saturated hydraulic conductivity.

Vegetative growth is based on a crop growth model. Growth is assumed to occur during the first 75% of the growing season based on heating units. Recommendations for the growing season are based primarily for summer grasses and assume that the growing season is that portion of the year when the temperature is above 50 to 55 °F. However, the user may specify a more appropriate growing season for different vegetation. The optimal growth temperature and the base temperature are based on a mixture of winter and summer perennial grasses. It is assumed that other vegetation have similar growth constraints and conditions. It is further assumed that the vegetation is not harvested.

The HELP program assumes Darcian flow for vertical drainage through homogeneous, temporally uniform soil and waste layers. It does not consider preferential flow through channels such as cracks, root holes or animal burrows. As such, the program will tend to overestimate the storage of water during the early part of the simulation and overestimate the time required for leachate to be generated. The effects of these limitations can be minimized by specifying a larger effective saturated hydraulic conductivity and a smaller field capacity. The program does increase the effective saturated hydraulic conductivity of default soils for vegetation effects.

Vertical drainage is assumed to be driven by gravity alone and is limited only by the saturated hydraulic conductivity and available storage of lower segments. If unrestricted, the vertical drainage rate out of a segment is assumed to equal the unsaturated hydraulic conductivity of the segment corresponding to its moisture content, provided that moisture content is greater than the field capacity or the soil suction of the segment is less than the suction of the segment directly below. The unsaturated hydraulic conductivity is computed by Campbell hydraulic equation using Brooks-Corey parameters. It is assumed that all materials conducting unsaturated vertical drainage have moisture retention characteristics that can be well represented by Brooks-Corey parameters and the Campbell equation. The pressure or soil suction gradient is ignored when applying the Campbell equation; therefore, the unsaturated drainage and velocity of the wetting front may be underestimated. This is more limiting for dry conditions in the lower portion of the landfill; the effects of this limitation can be reduced by specifying a larger saturated hydraulic conductivity. For steady-state conditions, this limitation has little or no effect.

The vertical drainage routine does not permit capillary rise of water from below the evaporative zone depth. Evapotranspiration is not modeled as capillary rise, but rather as a distributed extraction that emulates capillary rise. This is limiting for dry conditions where the storage of water to satisfy evaporative demand is critical and for designs where

the depth to the liner is shallow. This limitation can be reduced by increasing the field capacity in the evaporative zone and the evaporative zone depth.

Percolation through soil liners is modeled by Darcy's law, assuming free drainage from the bottom of the liner. The liners are assumed to be saturated at all times, but leakage occurs only when the soil moisture of the layer above the liner is greater than the field capacity. The program assumes that an average hydraulic head can be computed from the soil moisture and that this head is applied over the entire surface of the liner. As such, when the liner is leaking, the entire liner is leaking at the same rate. The liners are assumed to be homogeneous and temporally uniform.

Leakage through geomembrane is modeled by a family of theoretical and empirical equations. In all cases, leakage is a function of hydraulic head. The program assumes that holes in the geomembrane are dispersed uniformly and that the average hydraulic head is representative of the head at the holes. The program further assumes that the holes are predominantly circular and consist of two sizes. Pinholes are assumed to be 1 mm in diameter while installation defects are assumed to have an cross-sectional area of 1 cm<sup>2</sup>. It is assumed that holes of other shapes and sizes could be represented as some quantity of these characteristic defects. Leakage through holes in geomembranes is often restricted by an adjacent layer or soil or material termed the controlling soil layer. Materials having a saturated hydraulic conductivity greater than or equal to  $1 \times 10^{-1}$  cm/sec are considered to be a high permeability material; materials having a saturated hydraulic conductivity greater than or equal to  $1 \times 10^{-4}$  cm/sec but less than  $1 \times 10^{-1}$  cm/sec are considered to be a medium permeability material; and materials having a saturated hydraulic conductivity less than  $1 \times 10^{-4}$  cm/sec are considered to be a low permeability material. The program assumes that no aging of the liner occurs during a simulation.

The lateral drainage model is based on the assumption that the lateral drainage rate and average saturated depth relationship that exists for steady-state drainage also holds for unsteady drainage. This assumption is reasonable for leachate collection, particularly for closed landfills where drainage conditions should be fairly steady. Where drainage conditions are more variable, such as in the cover drainage system, the lateral drainage rate is underestimated when the saturated depth is building and overestimated when the depth is falling. Overall, this assumption causes the maximum depth to be slightly overestimated and the maximum drainage rate to be slightly underestimated. The long-term effect on the magnitude of the water balance components should be small. As with leakage or percolation through liners, the average saturated depth is computed from the gravity water and moisture retention properties of the drain layer and other layers when the drain layer is saturated. The program assumes that horizontal and vertical saturated hydraulic conductivity to be of similar magnitude and that the horizontal value is specified for lateral drainage layer.

Subsurface inflow is assumed to occur at a constant rate and to be uniformly distributed spatially throughout the layer, despite entering the side. This assumption causes a delay in its appearance in the leachate collection and more rapid achievement of steady-state moisture conditions. This limitation can be minimized by dividing the

landfill into sections where inflow occurs and sections without inflow.

Leachate recirculation is assumed to be uniformly distributed throughout the layer by a manifold or distribution system. Leachate collected on one day for recirculation is distributed steadily throughout the following day.

## 5.2 LIMITS OF APPLICATION

The model can simulate water routing through or storage in up to twenty layers of soil, waste, geosynthetics or other materials for a period of 1 to 100 years. As many as five liner systems, either barrier soil, geomembrane or composite liners, can be used. The model has limits on the order that layers can be arranged in the landfill profile. Each layer must be described as being one of four operational types: vertical percolation, lateral drainage, barrier soil liner or geomembrane liner. The model does not permit a vertical percolation layer to be placed directly below a lateral drainage layer. A barrier soil liner may not be placed directly below another barrier soil liner. A geomembrane liner may not be placed directly below another geomembrane liner. Three or more liners, barrier soil or geomembrane, cannot be placed adjacent to each other. The top layer may not be a barrier soil or geomembrane liner. If a liner is not placed directly below the lowest lateral drainage layer, the lateral drainage layers in the lowest subprofile are treated by the model as vertical percolation layers. If a geomembrane liner is specified as the bottom layer, the soil or material above the liner is assumed to be the controlling soil layer. No other restrictions are placed on the order of the layers.

The lateral drainage equation was developed and tested for the expected range of hazardous waste landfill design specifications. The ranges examined for slope and maximum drainage length of the drainage layer were 0 or 30 percent and 25 to 2000 feet; however, the formulation of the equations indicates that the range of the slope could be extended readily to 50 percent and the length could be extended indefinitely.

Several relations must exist between the moisture retention properties of a material. The porosity, field capacity and wilting point can theoretically range from 0 to 1 in units of volume per volume, but the porosity must be greater than the field capacity, and the field capacity must be greater than the wilting point. The general relation between soil texture class and moisture retention properties is shown in Figure 2.

The initial soil moisture content cannot be greater than the porosity or less than the wilting point. If the initial moisture contents are initialized by the program, the moisture contents are set near the steady-state values. However, the moisture contents of layers below the top liner system or cover system are specified too high for arid and semi-arid locations and too low for very wet locations, particularly when thick profiles are being modeled.

Values for the maximum leaf area index may range from 0 for bare ground to 5.0 for

an excellent stand of grass. Greater leaf area indices may be used but have little impact on the results. Detailed recommendations for leaf area indices and evaporative depths are given in the program. For numerical stability, the minimum evaporative zone depth should be at least 3 inches.

The program computes the evaporation coefficient for the cover soils based on their soil properties. The default values for the evaporation coefficient are based on experimental results reported by Ritchie (1972) and others. The model imposes upper and lower limits of 5.50 and 3.30 for the evaporation coefficient so as not to exceed the range of experimental data.

The program performs water balance analysis for a minimum period of one year. All simulations start on the January 1 and end on December 31. The condition of the landfill, soil properties, thicknesses, geomembrane hole density, maximum level of vegetation, etc., are assumed to be constant throughout the simulation period. The program cannot simulate the actual filling operation of an active landfill. Active landfills are modeled a year at a time, adding a yearly lift of material and updating the initial moisture of each layer for each year of simulation.

## REFERENCES

- Anderson, E. (1973). "National Weather Service river forecast system--snow accumulation and ablation model," Hydrologic Research Laboratory, National Oceanic and Atmospheric Administration, Silver Spring, MD.
- Arnold, J. G., Williams, J. R., Nicks, A. D., and Sammons, N. B. (1989). "SWRRB, a simulator for water resources in rural basins," Agricultural Research Service, USDA, Texas A&M University Press, College Station, TX.
- Bartos, M. J., and Palermo, M. R. (1977). "Physical and engineering properties of hazardous industrial wastes and sludges," Technical Resource Document EPA-600/2-77-139, US Army Engineer Waterways Experiment Station, Vicksburg, MS.
- Bonaparte, R., Giroud, J. P., and Gross, B. A. (1989). "Rates of leakage through landfill liners," *Proceedings of geosynthetics 1989 conference*, GeoServices Inc., San Diego, CA.
- Brakensiek, D. L., Engleman, R. L., and Rawls, W. J. (1981). "Variation within texture classes of soil water parameters," *Transactions of the American Society of Agricultural Engineers* 24(2), 335-339.
- Brakensiek, D. L., Rawls, W. J., and Stephenson, G. R. (1984). "Modifying SCS hydrologic soil groups and curve numbers for rangeland soils," *American Society of Agricultural Engineers* Paper No. PNR-84-203.
- Brooks, R. H. and Corey, A. T. (1964). "Hydraulic properties of porous media," *Hydrology Paper No. 3*, Colorado State University, Fort Collins, CO. 27 pp.
- Brown, K. W., Thomas, J. C., Lytton, R. L., Jayawikrama, P., and Bahrt, S. C. (1987). "Quantification of leak rates through holes in landfill liners," Technical Resource Document EPA/600/S2-87-062, US Environmental Protection Agency, Cincinnati, OH.
- Brutsaert, W. (1967). "Some methods of calculating unsaturated permeability," *Transactions of the American Society of Agricultural Engineers* 10(3), 400-404.
- Campbell, G. S. (1974). "A simple method for determining unsaturated hydraulic conductivity from moisture retention data," *Soil Science* 117(6), 311-314.
- Darcy, H. (1856). *Les fontaines publique de la ville de Dijon*. Dalmont, Paris. As cited by Hillel, D. (1982). *Introduction to soil physics*. Academic Press, New York.

Das, B. M., Tarquin, A. J., and Jones, A. D. (1983). "Geotechnical properties of a copper slag," Transportation Research Record 941, Transportation Research Board, National Academy of Sciences, Washington, D.C.

Dozier, T. S. (1992). "Examination and modification of three surface hydrologic processes in the HELP model," M.S. thesis, Mississippi State University, Mississippi State, MS.

Elsbury, B. R., Daniel, D. E., Sraders, G. A., and Anderson, D. C. (1990). "Lessons learned from compacted clay liner," *Journal of Geotechnical Engineering* 116(11).

Fleenor, B. (1993). "Examination of vertical water movement HELP Beta Version 3 versus RMA42," M.S. thesis, University of California, Davis, CA.

Forchheimer, P. (1930). *Hydraulik*. 3rd ed., Teuber, Leipzig and Berlin. As cited by Hillel, D. (1982). *Introduction to soil physics*. Academic Press, New York.

Freeze, R. A., and Cherry, J. A. (1979). *Groundwater*. Prentice-Hall, Englewood Cliffs, NJ.

Fukuoka, M. (1985). "Outline of large scale model test on waterproof membrane," Unpublished Report, Japan.

Fukuoka, M. (1986). "Large scale permeability tests for geomembrane-subgrade system," *Proceedings of the third international conference on geotextiles, volume 3*," Balkema Publishers, Rotterdam, The Netherlands.

Geosyntec Consultants. (1993). "Long-term performance of high density polyethylene cap at Chem-Nuclear's proposed Illinois low-level radioactive waste disposal facility - original and revision," Boynton Beach, FL.

Giroud, J. P., Badu-Tweneboah, K., and Bonaparte, R. (1992). "Rate of leakage through a composite liner due to geomembrane defects," *Geotextiles and Geomembranes* 11(1), 1-28.

Giroud, J. P., and Bonaparte, R. (1985). "Waterproofing and drainage: Geomembranes and synthetic drainage layers." *Geotextiles and geomembranes-- definitions, properties, and design - selected papers, revisions, and comments*, 2nd ed., Industrial Fabrics Association International, St. Paul, MN.

Giroud, J. P., and Bonaparte, R. (1989). "Leakage through liners constructed with geomembrane liners--parts I and II and technical note," *Geotextiles and Geomembranes* 8(1), 27-67, 8(2), 71-111, 8(4), 337-340.

Giroud, J. P., Khatami, A., and Badu-Tweneboah, K. (1989). "Evaluation of the rate of leakage through composite liners," *Geotextiles and Geomembranes* 8(4), 337-340.

Hillel, D. (1982). *Introduction to soil physics*. Academic Press, New York.

Horton, R. E. (1919). "Rainfall interception," *Monthly Weather Review* 47(9), 603-623.

Industrial Fabrics Association International. (1991). "Geotextile fabrics report-- 1992 specifiers guide," Volume 9, Number 9, St. Paul, MN.

Jayawickrama, P. W., Brown, K. W., Thomas, J. C., and Lytton, R. L. (1988). "Leakage rates through flaws in membrane liners," *Journal of Environmental Engineering* 114(6).

Jensen, M. E., ed. (1973). *Consumptive use of water and irrigation water requirements*. American Society of Civil Engineers, New York.

Knisel, W. G., ed. (1980). "CREAMS, a field scale model for chemical runoff and erosion from agricultural management systems. Vols. I, II, and III" Conservation Report 26, USDA-SEA. 643 pp.

Knisel, W. G., Moffitt, D. C., and Dumper, T. A. (1985). "Representing seasonally frozen soil with the CREAMS model," *American Society of Agricultural Engineering* 28 (September - October), 1487-1492.

Linsley, R. K., Kohler, M. A., and Paulhus, J. L. H. (1982). *Hydrology for engineers*. 3rd ed., McGraw-Hill, New York. 508 pp.

McAneny, C. C., Tucker, P. G., Morgan, J. M., Lee, C. R., Kelley, M. F., and Horz, R. C. (1985). "Covers for uncontrolled hazardous waste sites," Technical Resource Document EPA/540/2-85/002, US Army Engineer Waterways Experiment Station, Vicksburg, MS.

National Oceanic and Atmospheric Administration. (1974). *Climatic atlas of the United States*. US Department of Commerce, Environmental Science Services Administration, National Climatic Center, Ashville, NC. 80 pp.

Oweis, I. S., Smith, D. A., Ellwood, R. B., and Greene, D. S. (1990). "Hydraulic characteristics of municipal refuse," *Journal of Geotechnical Engineering* 116(4), 539-553.

Penman, H. L. (1963). "Vegetation and hydrology," Technical Comment No. 53, Commonwealth Bureau of Soils, Harpenden, England.

Perrier, E. R., and Gibson, A. C. (1980). "Hydrologic simulation on solid waste disposal sites," Technical Resource Document EPA-SW-868, US Environmental Protection

Agency, Cincinnati, OH. 111 pp.

Perry, J. S., and Schultz, D. I. (1977). "Disposal and alternate uses of high ash paper-mill sludge." *Proceedings of the 1977 national conference on treatment and disposal of industrial wastewaters and residues*, University of Houston, Houston, TX.

Poran, C. J., and Ahtchi-Ali, F. (1989). "Properties of solid waste incinerator fly ash," *Journal of Geotechnical Engineering* 115(8), 1118-1133.

Rawls, W. J., Brakensiek, D. L., and Saxton, K. E. (1982). "Estimation of soil water properties," *Transactions of the American Society of Civil Engineers*. pp. 1316-1320.

Richardson, C. W. (1981). "Stochastic simulation of daily precipitation, temperature, and solar radiation," *Water Resources Research* 17(1), 182-190.

Richardson, C. W., and Wright, D. A. (1984). "WGEN: A model for generating daily weather variables," ARS-8, Agricultural Research Service, USDA. 83 pp.

Ritchie, J. T. (1972). "A model for predicting evaporation from a row crop with incomplete cover," *Water Resources Research* 8(5), 1204-1213.

Ruffner, J. A. (1985). *Climates of the states, National Oceanic and Atmospheric Administration narrative summaries, tables, and maps for each state, volume 1 Alabama - New Mexico and volume 2 New York - Wyoming and territories*. Gale Research Company, Detroit, MI. 758 pp. and 1572 pp.

Rushbrook, P. E., Baldwin, G., and Dent, C. B. (1989). "A quality-assurance procedure for use at treatment plants to predict the long-term suitability of cement-based solidified hazardous wastes deposited in landfill sites." *Environmental Aspects of Stabilization and Solidification of Hazardous and Radioactive Wastes*, ASTM STP 1033, P. L. Cote' and T. M. Gilliam, eds., American Society for Testing and Materials, Philadelphia, PA.

Saxton, K. E., Johnson, H. P., and Shaw, R. H. (1971). "Modeling evapotranspiration and soil moisture." *Proceedings of american society of agricultural engineers 1971 winter meeting*, St. Joseph, MI. No. 71-7636.

Schroeder, P. R., and Gibson, A. C. (1982). "Supporting documentation for the hydrologic simulation model for estimating percolation at solid waste disposal sites (HSSWDS)," Draft Report, US Environmental Protection Agency, Cincinnati, OH. 153 pp.

Schroeder, P. R., Morgan, J. M., Walski, T. M., and Gibson, A. C. (1984a). "The hydrologic evaluation of landfill performance (HELP) model, volume I, user's guide for

version 1," Technical Resource Document EPA/530-SW-84-009, US Environmental Protection Agency, Cincinnati, OH. 120 pp.

Schroeder, P. R., Gibson, A. C., and Smolen, M. D. (1984b). "The hydrologic evaluation of landfill performance (HELP) model, volume II, documentation for version 1," Technical Resource Document EPA/530-SW-84-010, US Environmental Protection Agency, Cincinnati, OH. 256 pp.

Schroeder, P. R., and Peyton, R. L. (1987a). "Verification of the hydrologic evaluation of landfill performance (HELP) model using field data," Technical Resource Document, EPA 600/2-87-050, US Environmental Protection Agency, Cincinnati, OH. 163 pp.

Schroeder, P. R., and Peyton, R. L. (1987b). "Verification of the lateral drainage component of the HELP model using physical models," Technical Resource Document, EPA 600/2-87-049, US Environmental Protection Agency, Cincinnati, OH. 117 pp.

Schroeder, P. R., Peyton, R. L., McEnroe, B. M., and Sjostrom, J. W. (1988a). "The hydrologic evaluation of landfill performance (HELP) model: Volume III. User's guide for version 2," Internal Working Document EL-92-1, Report 1, US Army Engineer Waterways Experiment Station, Vicksburg, MS. 87 pp.

Schroeder, P. R., McEnroe, B. M., Peyton, R. L., and Sjostrom, J. W. (1988b). "The hydrologic evaluation of landfill performance (HELP) model: Volume IV. Documentation for version 2," Internal Working Document EL-92-1, Report 2, US Army Engineer Waterways Experiment Station, Vicksburg, MS. 72 pp.

Swain, A. (1979). "Field studies of pulverized fuel ash in partially submerged conditions." *Proceedings of the symposium of the engineering behavior of industrial and urban fill*, The Midland Geotechnical Society, University of Birmingham, Birmingham, England, pp. D49-D61.

Tchobanoglous, G., Theisen, H., and Eliassen, R. (1977). *Solid wastes: engineering principles and management issues*. McGraw-Hill, New York.

Thompson, F. L., and Tyler, S. W. (1984). "Comparison of Two Groundwater Flow Models--UNSAT1D and HELP," EPRI CS-3695, Topical Report, October, Prepared by Battelle, Pacific Northwest Laboratories, for Electric Power Research Institute, Palo Alto, CA, 71 pp.

Toth, P. S., Chan, H. T., and Cragg, C. B. (1988). "Coal ash as a structural fill, with special reference to the Ontario experience," *Canadian Geotechnical Journal* 25, 694-704.

USDA, Soil Conservation Service. (1985). *National engineering handbook, section 4*,

*hydrology*. US Government Printing Office, Washington, D.C.

Viessman, W. Jr., Knapp, J. W., Lewis, G. L., and Harbaugh, T. E. (1977). *Introduction to hydrology*. 2nd ed., Harper and Row Publishers, New York.

Woolhiser, D. A., Smith, R. E., and Goodrich, D. C. (1990). "KINEROS, a kinematic runoff and erosion model: Documentation and user manual," ARS-77, US Department of Agriculture, Agricultural Research Service, 130 pp.

Zeiss, C., and Major, W. (1993). "Moisture flow through municipal solid waste: patterns and characteristics," *Journal of Environmental Systems* 22(3), 211-232.